Thesis entitled

Role of tumor suppressor *MTUS1*/ATIP1 in gliomagenesis: association with epigenetics and DNA repair

Submitted to the University of Hyderabad

For the degree of

Doctor of Philosophy

by

Nikhil Ranjan

Reg. No. 15LTPH08

Under the supervision of

Prof. P. Prakash Babu

Department of Biotechnology and Bioinformatics

School of Life Sciences

University of Hyderabad, Hyderabad

Telangana- 500046

December 2021

University of Hyderabad
Hyderabad- 500 046, India

Declaration

Department of Biotechnology and Bioinformatics

School of Life Sciences

University of Hyderabad, Hyderabad

India

I hereby declare that I have produced the work entitled "Role of tumor suppressor *MTUS1*/ATIP1 in gliomagenesis: association with epigenetics and DNA repair" submitted for the award of a doctorate, on my own, in the Department of Biotechnology and Bioinformatics, School of Life Sciences, University of Hyderabad, Hyderabad, under the supervision of Prof. P. Prakash Babu. I hereby declare that this work is original, free from plagiarism and not been submitted in part or full for any other degree or diploma of any other University or Institution.

I swear upon oath that these statements are true and that I have not concealed anything.

Nikhil Ranjan

Place: Hyderabad

Name: Nikhil Ranjan

Date: 31/12/2021

Reg. No. 15LTPH08

University of Hyderabad
Hyderabad- 500 046, India

Certificate

This is to certify that the thesis entitled **"Role of tumor suppressor *MTUS1*/ATIP1 in gliomagenesis: association with epigenetics and DNA repair"** submitted by **Mr. Nikhil Ranjan** bearing registration number 15LTPH08 in partial fulfillment of the requirements for the award of Doctor of Philosophy in the Department of Biotechnology and Bioinformatics, School of Life Sciences is a bonafide work carried out by him under my supervision and guidance.

This thesis is free from plagiarism and has not been submitted previously in part or in full to this or any other University or Institution for the award of any degree or diploma. Parts of this thesis have been:

A. Published in the Cancers journal:

> **Ranjan, N.**; Pandey, V.; Panigrahi, M.K.; Klumpp, L.; Naumann, U.; Babu, P.P. The Tumor Suppressor MTUS1/ATIP1 Modulates Tumor Promotion in Glioma: Association with Epigenetics and DNA Repair. **Cancers**, March 12, 2021, 13, 1245. https://doi.org/10.3390/ cancers13061245.

B. Presented in the following conferences:

Apr 2021

> Oral award paper presentation, 12th Annual Conference of Indian Society of Neuro-Oncology (ISNOCON 2021), Christian Medical College, Vellore, India

Dec 2020

Oral presentation, Society for Neurochemistry India (SNCI) on "Brain Diseases, Injuries and Infections: Emerging challenges and treatment strategies", University of Hyderabad, India

Nov 2019

Oral presentation, Hertie Institute für Klinische Hirnforschung Lunch Seminar, HIH, Tübingen, Germany

Oct 2019

Oral presentation, Neurowissenschaftliche Nachwuchskonferenz, NeNa, Tübingen Neurocampus, Schamberg, Germany

May 2019

Poster presentation, Mildred Scheel Cancer Conference (MSCC), Deutsche Krebshilfe, Bonn, Germany

Further, Mr. Nikhil Ranjan has passed the following examination in the respective courses towards the fulfilment of the coursework requirement for Ph.D.

S. No.	Course Code	Name	Credits	Pass/Fail
1	BT 801	Analytical Techniques	4	**Pass**
2	BT 802	Research Ethics, Data Analysis and Biostatistics	3	**Pass**
3	BT 803	Lab work and Seminar	5	**Pass**

31/12/2021

Prof. P. Prakash Babu
(Research supervisor)

Prof. P. Prakash Babu
Department of Biotechnology & Bioinformatics
School of Life Sciences
University of Hyderabad
Hyderabad-500 046. (T.S.)

31/12/2021

Head
(Dept. of Biotechnology and Bioinformatics)

HEAD
Dept. of Biotechnology & Bioinformatics
University of Hyderabad
Hyderabad.

Dean
(School of Life Sciences)

DEAN
School of Life Sciences
University of Hyderabad
Hyderabad-500 046.

University of Hyderabad
Hyderabad- 500 046, India

PLAGIARISM FREE CERTIFICATE

This is to certify that the similarity index of this thesis as checked by the Library of University of Hyderabad excluding bibliographic content 39%. Out of this 32% similarity is identified from the candidate's own publication (Nikhil Ranjan) which has been certified by Indira Gandhi Memorial Library (IGML), University of Hyderabad and forms the adequate part of the thesis. The details of the student's publication are as follows:

Ranjan, N., Pandey, V., Panigrahi, M.K., Klumpp, L., Naumann, U., Babu, P.P., *The Tumor Suppressor MTUS1/ATIP1 Modulates Tumor Promotion in Glioma: Association with Epigenetics and DNA Repair.* **Cancers**, March 2021, 13, 1245. DOI: https://doi.org/10.3390/ cancers13061245

Similarity index – 32%

About 7% similarity was identified from external sources in the present thesis which is according to prescribed regulations of the University. All the publications related to this thesis have been appended at the end of the thesis. Hence the present thesis is considered to be plagiarism-free.

31/12/2021

Prof. P. Prakash Babu

Supervisor

Prof. P. Prakash Babu
Department of Biotechnology & Bioinformatics
School of Life Sciences
University of Hyderabad
Hyderabad-500 046. (T.S.)

Acknowledgements

I would like to express my profound gratitude to my supervisor **Prof. P. Prakash Babu** for the freedom, guidance, constant encouragement and suggestions throughout my Ph.D.

I will be always grateful to **Prof. Dr. Ulrike Naumann** for allowing me to work under her guidance and especially for all the critical comments, support and encouragement she provided.

I thank my Doctoral Committee members **Dr. Sunanda Bhattacharyya** and **Prof. G. Ravi Kumar** for their critical comments and valuable suggestions.

I especially thank **Dr. Vimal Pandey** for mentoring and helping me throughout my Ph.D. in every possible way. Also, I thank **Dr. Anwita Mudiraj** for her suggestions and moral support.

I thank, **Prof. J. S. S. Prakash**, Head, Dept. of Biotechnology and former **Prof. K. P. M. S. V. Padmasree, Prof. Anand Kondapi, Prof. Niyaz Ahmed and Prof. P. Prakash Babu** for providing the necessary facilities in the department to carry out my research work.

I am grateful to present Dean **Prof. S. Dayananda**, School of Life Sciences, and former Deans **Prof. K. Ramaiah, Prof. P. Reddanna, Late Prof. Aparna Dutta Gupta, Prof. A. S. Raghavendra**, for providing all the facilities in the school.

I am thankful to my friends in the UoH campus for all the fun time and thoughts sharing, specially **Mukesh jee, Tripti, Dr. Indira, Dushyant, Ravi, Pratul, Rajat**.

I am deeply thankful to **Kristina and her family** for being there for me and all the support.

I am also thankful to **Hermann, Moritz, Lilei, Yana, Barbara, Leonie and Lena** for being nice friends and fun to work with.

I express my whole-hearted thanks to **Dr. Manas Panigrahi** (Dept. of Neurosurgery, Krishna

Institute of Medical Sciences (KIMS)), **Dr. Chandrashekhar** (Dept. of Neurosurgery, Krishna Institute of Medical Sciences (KIMS)), **Dr. Satish** (Dept. of Pathology, Nizam Institute of Medical Sciences (NIMS)) for providing tumor samples and their constant support throughout the course of my work. I thank all the residents of neurosurgery and pathology for their cooperation.

I am thankful to my lab members **Dr. Vimal, Dr. Parimala, Dr. Ranjana, Dr. Apoorv Suresh, Dr. Prabhakar, Dr. Ramu, Dr. Kamusha Valli, Dr. Nobel Kumar, Dr. Sireesh Kumar, Mr. Karthik, Dr. Ravindra, Dr. Deepak babu, Dr. Praveen, Ms. Ruchi, Mr. Kishore, Ms. Neera, Ms. Shubhangee, Mr. Rahul, Ms. Shailaja** for their encouragement and support during this time.

Special thanks to **Muthyam anna** for managing the things in the lab.

I thank **Dr. Madhu Babu, Prof. Anand Kondapi, Dr. Suresh Yenugu, Prof. Brahmanandam and their students** for allowing me to use their facilities.

I thank the **office staff** of Dept. of Biotechnology, Ms. Nalini for Confocal, Mr. Ramesh for FACS assistance.

I thank all the funding bodies (**CSIR, DBT, DST, FIST, CREBB, UPE** for their financial assistance to the department and school.

I thank **BBL, CSIR-UGC** for providing the fellowships during my Ph.D.

Special thanks to **Uli and DAAD** for providing me the fellowship.

I thank **Almighty and my family** for showering the blessings and moral support.

Table of Contents

List of abbreviations

Abbreviations	Meaning
AA:	Anaplastic astrocytoma
APS:	Ammonium persulfate
BBB:	Blood-brain barrier
BCL2:	B-cell lymphoma 2
Bcl-2:	B-cell lymphoma protein-2
BSA:	Bovine serum albumin
CM:	Conditioned medium
CNS:	Central nervous system
CNV:	Copy number variations
Cox-2:	Cyclo-oxygenase-2
CSCs:	Cancer stem cells
Ct:	Cycle threshold
DA:	Diffuse astrocytoma
DAPI:	4,6-Diamidino-2-phenylindol
DAB:	Diamino benzidine
DCFH-DA:	Dichloro-dihydro-fluorescein diacetate
DMSO:	Dimethyl sulfoxide
DNA:	Deoxyribonucleic acid
dNTP:	Deoxynucleoside triphosphate
DSB:	Double-strand breaks
DTT:	1,4-Dithiothreitol
ECM:	Extracellular matrix
EDTA:	Ethylene diamine tetra acetate

Abbreviations	Meaning

e.g.:	Exempli gratia / for example
EGF:	Epidermal growth factor
EGFR:	Epidermal growth factor receptor
ENPs:	Early neoplastic proliferations
ENU:	n-Ethyl n-nitrosourea
FBS:	Fetal Bovine Serum
GAPDH:	Glycerinealdehyde-3-phosphate dehydrogenase
GBM:	Glioblastoma multiforme
GFAP:	Glial fibrillary acidic protein
GPX:	Glutathione peroxidase
GSC:	Glioblastoma stem cell
GSK3β:	Glycogen synthase kinase 3β
GST:	Glutathione-S-transferase
HBMvEC:	Human Brain Microvascular Endothelial Cells
HRP:	Horseradish peroxidase
LFAC:	Large Focal Adhesion Complex
MAPK:	Mitogen activated protein kinase
MEM:	Modified eagle's medium
MGMT:	O6-methylguanin-DNA-methyltransferase
MKK:	MAP kinase kinases
MMP:	Matrix metalloproteinase
mRNA:	Messenger RNA
NF-κB:	Nuclear factor κB
NMRI-Rj:	NMRI-Foxn1nu/Foxn1nu
NP-40:	Igepal

Abbreviations	Meaning
NPC:	Neuronal precursor cells
NSCs:	Neural stem cells
o/n:	Over night
PA:	Pilocytic astrocytoma
PCR:	Polymerase chain reaction
PI:	Propidium iodide
PMSF:	Phenyl methyl sulphonyl fluoride
PNS:	Peripheral nervous system
P/S:	Penicillin (100 U/ml)/streptomycin (100 µg/ml)
PVDF:	Polyvinylidene fluoride
RIPA:	Radioimmunoprecipitation assay
SDS:	Sodium dodecyl sulfate
SDS-PAGE:	Sodium dodecyl sulfate - polyacrylamide gel electrophoresis
TBS:	Tris-buffered saline
TBST:	Tris-buffered saline-Tween 20
TMZ:	Temozolamide
TP53:	Tumor protein p53
VEGF:	Vascular endothelial growth factor
WHO:	World health organization
5-Aza-dC:	5-Aza-2′-deoxycytidine

Summary

Glioblastoma (GBM) is the most aggressive brain tumor in adults. Resistance mechanisms in GBM present an array of challenges to understand its biology and to develop novel therapeutic strategies. Despite multidisciplinary treatments, overall survival remains poor in glioma patients. Although novel therapeutic approaches are being explored, no outstanding effects on the survival of GBM patients have been achieved so far. This substantiates the need to develop new therapeutic strategies. Hence, understanding glioma biology and the mechanisms responsible for its high malignancy is of central importance. In this regard, we have examined the impact of the tumor suppressor gene (TSG) *MTUS1*, coding for ATIP1, in glioma malignancy as well as how its expression might influence GBM therapy. *MTUS1* has been reported as a TSG in various cancers but there are no reports in glioma. We found that ATIP1 was significantly downregulated in high-grade glioma (HGG), GBM cells and GSC. In glioma cells, ATIP1 mitigates proliferation, clonogenic outgrowth and is accompanied by cell motility reduction and can be used as a biological marker to predict therapy outcomes. Glioma specimens, GBM cells and glioma stem cells (GSC) were analysed for ATIP1 expression by PCR, immunoblot and immunohistology. In order to analyse the role of *MTUS1* promoter-methylation, Decitabine treatment and bisulfite sequencing (BSS) were used. We found that in HGG, decitabine treatment results in enhanced expression of ATIP1 and promoter methylation might play a crucial role in *MTUS1* downregulation. In glioma-bearing mice, ATIP1 prolonged the overall and median survival. The effect of temozolomide (TMZ) and tumor irradiation on ATIP1 expression and its influence on survival were examined *in vitro* and *in vivo*. TMZ treatment recovered ATIP1 expression both *in vitro* and *in vivo*. However, surprisingly, increased ATIP1 expression resulted in an increased repair of irradiation-induced DNA damage and protects GBM cells against cell death induced by irradiation. The impact of ATIP1 in irradiation-induced DNA repair was examined by

counting phospho-γH2A.X foci post-radiation treatment. Where the higher expression of ATIP1 results in the rapid repair of DSB compared to the mock cells.

Our findings indicate that in glioma ATIP1 serves as a tumor suppressor regulating cell motility, proliferation and DNA repair, and its downregulation is involved in the progression of this tumor. Additionally, it should be taken in mind that in ATIP1 expressing HGG its higher expression might interfere with the tumor irradiation therapy.

Chapter 1

Review of literature

1. Review of literature

1.1. Glioblastoma

Glioblastoma (GBM) are the most commonly occurring, highly malignant and therapy-resistant primary brain tumors with an unfavorable prognosis and median survival of fewer than 20 months, even with optimal therapy [1]. GBMs can either arise *de novo* which are termed as primary GBM or they can reappear, progress and transform into GBM, which are known as secondary GBMs.

The high malignancy of GBM is based on its characteristics of a highly proliferating tumor that grows invasively into the surrounding CNS parenchyma with the most prominent symptoms of deficits, headaches and seizures. GBMs are mostly located at the frontal lobe followed by temporal and parietal lobes [2] and represents massive necrosis as well as hemorrhage (Figure 1). The optimal glioma therapy comprises of maximal safe surgical resection of the tumor, radiotherapy and chemotherapy. Besides, GBM are highly resistant to irradiation and most chemotherapeutics. This is mainly based on the existence of an extremely resistant subpopulation of GBM cells known as glioma stem cells (GSCs) which are supposed to be responsible for tumor initiation and recurrence [3, 4]. Although novel therapeutic approaches are being explored, no outstanding effects on the survival of GBM patients have been achieved so far. The overall median survival is 12.1 months post tumor resection and radiotherapy and 14.6 months with the combination of TMZ [5]. Although the beneficial effect of the combined therapy is restricted to those in whose tumor the promoter of the DNA repair enzyme methylguanine-methyltransferase (MGMT) is methylated, allowing the efficacy of alkylating chemotherapy [6, 7]. The etiology of glioma is unknown, studies show some molecular interactions with longer overall survival, for instance O6-MGMT hypermethylation; although, any molecular alteration is not accepted as a prognostic factor.

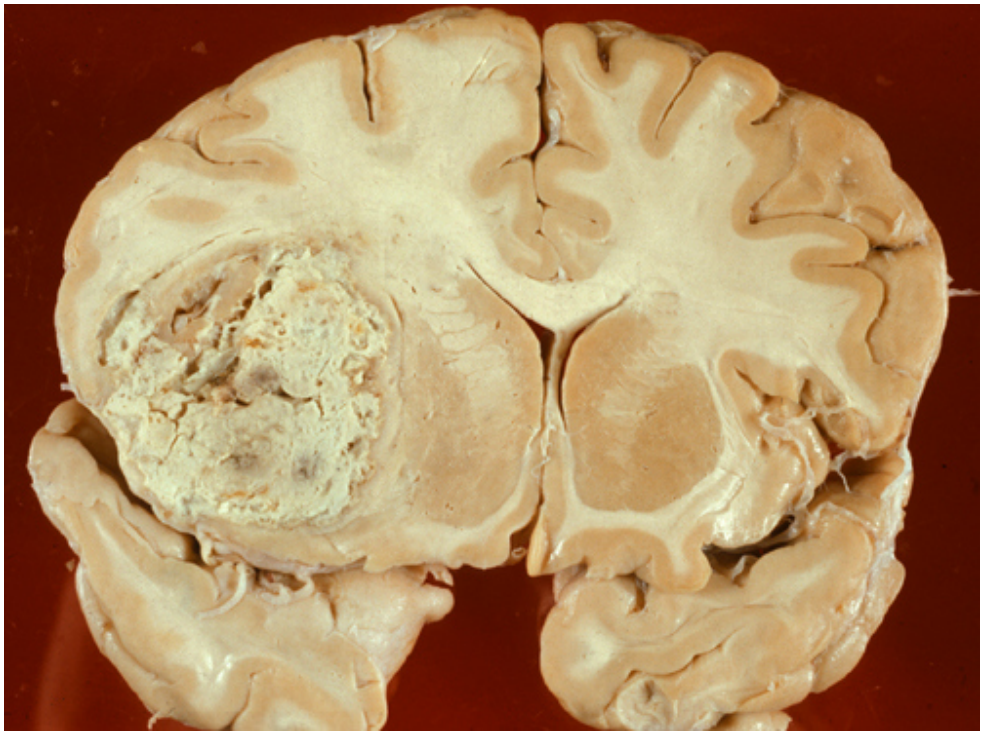

Figure 1. Formalin-fixed brain. Figure representing poorly defined intra-axial mass with variegated appearance due to necrosis and hemorrhage. Source: http://neuropathology-web.org/chapter7/chapter7bGliomas.html, status from 24.06.2018.

It has been shown that patients with IDH1 and IDH2 mutations have a improved medical prognosis [8]. IDH mutations provoke fluctuations in the metabolic pathways culminating in metabolic reprogramming. R132H mutation has been reported to rattle the IDH1 ability of isocitrate conversion to α-ketoglutarate (α-KG) rather results in the accumulation of D-2-hydroxyglutarate (D-2-HG) in an NADPH dependent aspect [9]. D-2-HG can act as a competitive inhibitor against the enzymes which need α-KG as a co-factor, such as DNA demethylases. This results in genomic CpG hypermethylation and altered transcription. Reduced α-KG levels might impact the hypoxia-inducible factor subunit HIF-1α because α-KG is required for prolyl hydroxylases (PHD) to hydroxylate and elevate the degradation of HIF. In addition to the molecular alterations, IDH mutations also play a crucial role in CpG

island hypermethylation resulting in epigenetic reprogramming as well [10, 11]. Mutations in IDH1/2 are associated with better prognosis in glioma patients [12, 13] and are prevalent in different forms of cancers including >70% of grade II-III gliomas and secondary glioblastomas (GBM), leukemias, sarcomas and other tumors [14-16]. IDH mutations are most frequent in grade II and grade III astrocytomas and oligodendrogliomas compared to GBMs, all oligodendrogliomas are IDH1 mutant at R132 or the analogous residue R172. The mutations are rare in primary GBM (5%) and frequent in secondary GBM (70-80%) [17, 18]. A higher relative prevalence of IDH mutation in secondary GBM advise that lower grade glioma with IDH mutation reoccurs as a higher grade tumor after undergoing malignant transformation [9]. Although GBM shares mutual clinical demonstration and histology, it has been identified as a heterogeneous tumor, which suggests that future treatments might involve individualization for patient's tumor genotype or proteomic potrait.

1.2 Glioma classification

Gliomas are the tumors originating from the glial cells which are the most persistent intrinsic tumors of the central nervous system. Glioma comprise two principal subgroups: diffuse glioma and non-diffuse glioma (gliomas showing circumcised growth pattern). In 2016 WHO reclassified the CNS tumors, including the molecular parameters along with the histological parameters. Glioma specifies to the glial tumors consisting primarily of glioblastoma, astrocytoma, oligodendroglioma and ependymoma. GBM is subdivided in IDH-wildtype, IDH-mutant and not otherwise specified (NOS) in case the IDH status cannot be certified. IDH-wild-type GBM is principally associated with de novo primary GBM and IDH-mutant GBM with secondary GBM developing from lower-grade gliomas [19] (Figure 2). IDH-wild-type GBM are prevalent in older patients with median age of 62 years at diagnosis, while GBM which are IDH-mutant affects younger patients with a median age of 44 years. IDH-wildtype tumors count for 90% of GBM cases. Additionally, these tumors are further classified into giant

cell GBM, gliosarcoma, and epithelioid GBM [20] also, glioma is further classified based on the origin of the tumor cells (Figure 3) [21].

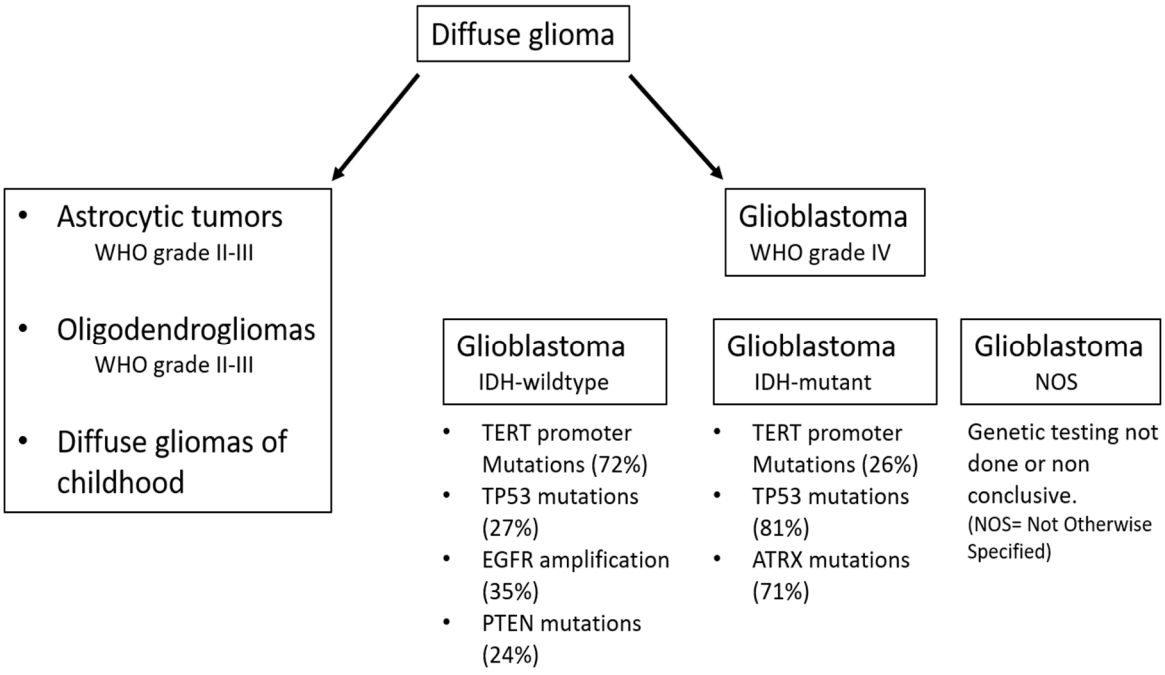

Figure 2. The molecular aspect of glioma classification. Molecular changes which are responsible for the classification of glioma are Isocitrate dehydrogenase (IDH) mutations, Tumor Protein 53 (TP53) mutations, α-thalassemia/mental retardation syndrome X-linked (ATRX), Telomerase Reverse Transcriptase (TERT) mutations, loss of Phosphatase and Tensin Homologue which is deleted in chromosome ten (PTEN) mutations, overexpression of Epidermal Growth Factor Receptor (EGFR), silencing of O6-methylguanine-DNA methyltransferase gene (MGMT) as a consequence of hypermethylation in the promoter region.

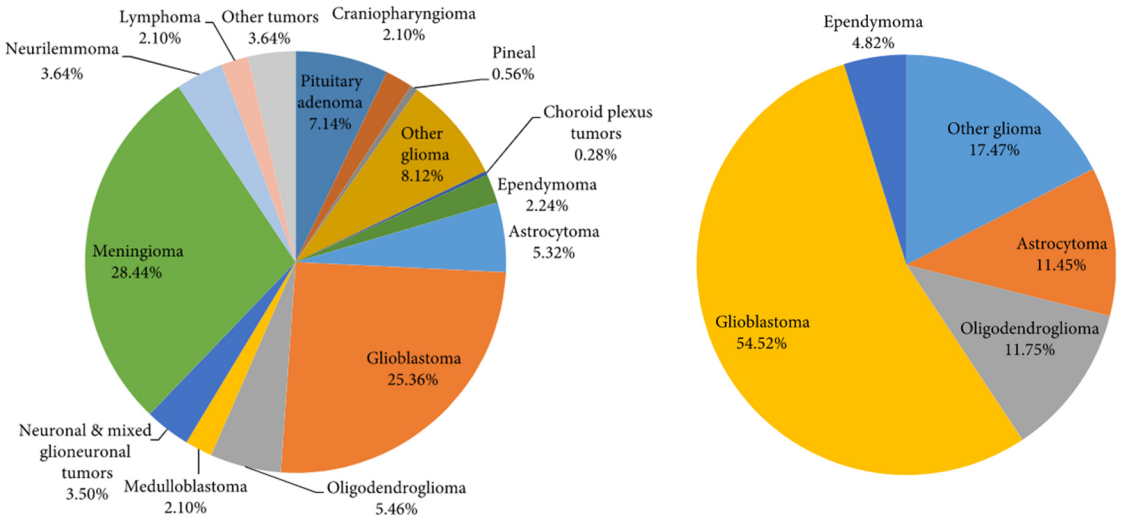

Figure 3. Distribution of primary CNS tumor type and primary CNS gliomas. Characterized by World Health Organization (WHO) guidelines. The samples were classified based on the inclusion criteria for IDH1/2, histologic subtypes and other molecular characterization. (*Adapted from Amna Almutrafi et al., https://doi.org/10.1155/2020/1429615)*

1.2.1 Pilocytic astrocytoma (PA), WHO Grade I

PA is basically a distinct form of astrocytoma in children and young adults and it is most common brain tumor in children. Prominent location of PAs are in the cerebellum, hypothalamus and optic chiasm. The vast majority of PAs show BRAF activation, which is most usually caused by fusion of BRAF with KIAA1549, a contiguous gene on 7q34, producing a fusion gene that lacks BRAF regulatory domain. Fusion of KIA1549: BRAF activates MAPK oncogenic signalling cascade, which is responsible in the progression of PA (https://neuropathology-web.org/chapter7/chapter7cOthergliomas.html#pa).

1.2.2 Diffuse astrocytoma (DA), WHO Grade II

DA is intermittent in young adults. They arise almost anywhere in the CNS but are most frequent in the cerebral hemispheres, especially the frontal lobes. DA's are difficult to demarcate and determine, involving a large part of the brain diffusely. Histological features include spindle-shaped, stellate, fiber-like processes or a plump with a immense eosinophilic cytoplasmic mass also termed as gemistocytic astrocytoma. Das displays mild atypia and rare mitosis, with time DA's gradually transforms over time into anaplastic astrocytoma and later to glioblastoma. DA's cause seizures, deficits and grow slowly for several years.

1.2.3 Oligodendroglioma and Oligoastrocytoma

These tumors originate from oligodendrocytes of the brain and usually consist of 13-14% of gliomas. They are considered low-grade glioma (LGG), they are slow-growing and emerge mostly in the cerebral hemispheres. Complete deletion of the short arm of chromosome 1(1p) and the long arm of chromosome 19 (19q) (1p/19q co-deletion) is a specific pathognomonic biomarker for oligodendroglioma. A diffuse glioma that appears to be astrocytic but harbours IDH mutation and 1p/19q co-deletion classify as oligodendroglioma. Hence, all oligodendrogliomas are IDH1 mutant at R132 or the analogous residue R172. These tumors are classified as low grade (WHO grade II) or high grade (WHO grade III) based on cellularity, anaplasia, mitotic activity, microvascular proliferation and necrosis. Median survival for grade II and grade III oligodendrogliomas is about 11 and 4-5 years respectively and even shorter for oligoastrocytomas.

1.2.4 Anaplastic astrocytoma (AA), WHO Grade III

AA is an intermediate existence amidst Grade II and GBM. AAs either develop from pre-existing grade II DA's and also contribute to transform into glioblastoma. Mostly, it is

comparable to Grade II DA but consists of higher cellularity and a higher proliferative index. Clinically, AA is evolving more rapidly and has a reduced survival (3-5 years).

1.2.5 Glioblastoma multiforme (GBM), WHO Grade IV

GBM is the most malignant form of glioma. Although it occurs most frequently in middle-aged adults and the most commonly occurs in frontal and temporal lobes of brain although it is not age specific and can affect any region of the CNS. GBM arises most commonly de novo (primary glioblastoma) which are highly aggressive and common in older patients. Some GBMs arise by malignant transformation of low-grade astrocytomas (secondary glioblastoma). Histologically, glioblastoma represents high cellularity, cellular and nuclear anaplasia defining the classification "multiforme", mitoses, microvascular proliferation, pseudopallisading and necrosis.

1.3 Challenges in glioma treatment

Cancers are classified in hierarchies and originated by a cancer stem cell (CSC), this is proven by the model where transplantation of cancer cells subpopulation can commence and retain the tumor upon grafting. Apart from the insufficiency of clinical demonstration, studying the cancer stem cell model is difficult due to the inadequacy of the markers that persistently define CSCs. Solid tumors always represent heterogeneity in the expression of particular markers. CD133 (prominin-1) is the best-characterized surface marker in GBM, but CD133 negative cells also trigger tumors upon xenografting and it has been proposed that the true GBM stem cell (GSC) is present in the CD133 negative cells population. Hence CSC population which are sorted with surface marker cannot be always defined and functional affirmation of CSC activity with permitted tumor initiation assays is necessary.

1.3.1 Glioma stem cells

Cellular origin of glioma is still unclear, which provides an opportunity for understanding the disease. The transformation of differentiated glia is assumed to be the mechanism of gliomagenesis but this hypothesis is controversial and fails to explain the origin of mixed gliomas such as oligoastrocytoma [22]. Neural stem cells (NSC) and the glial progenitor cells are the dividing cells present in multiple regions of the postnatal brain, which makes them the only brain cells capable of transforming. NSCs are self-renewing and multipotent, have been isolated from the subventricular zone [22], the lining of the lateral ventricles, the dentate gyrus [23], within the hippocampus and the subcortical white matter [24]. The glial progenitor cells with the self-renewing capability produce astrocytes and oligodendrocytes that have been observed throughout the neuraxis [25], including the cortex [26], the corpus callosum [27], subventricular zone [28]. Abnormalities in these stem cells and progenitor components, in addition to differentiated adult glia, can lead to neoplastic transformation.

1.3.2 Tumor recurrence

Recurrence of GBM is one of the most major concerns and largely undefined for the treatment of the disease for the subsequent reasons: 1). Absence of uniformity for the interpretation and criteria for tumor recurrence; 2). Variation in the institutional medicinal regimen approach; 3). Presence of the clonal heterogeneity in these tumors, including the tumor recurrence location and various mechanisms involved which result in the subtypes or subclones of GBM [29]. The infiltrative characteristics of GBM cells make it problematic to eradicate these cells microscopically even after macroscopic tumor resection. Studies have shown that GBM recurrence most often occurs within 2 to 3 cm radius from the border of original lesion [30-32]. Even though the epidemiology of GBM is acknowledged, the discrepancy of various

institutions in defining recurrence and treatment options results in uncertainty in the GBM recurrence profile.

From an evolutionary aspect, the divergence in the subpopulation development of tumor cells within the same tumor is a result of therapy failure, resistance to the treatments and finally recurrence of the malignancy (Figure 4). Recurrences are often directed by branched subclonal divergent mutations, which are not even present in the primary GBM and the driver mutation was lost in recurrence [33]. Reports have also suggested that immense retention of initial tumor mutations are responsible for GBM recurrence, following a linear model of evolution, whereas a spatially inaccessible tumor recurrence was confined to lesser mutations from the original tumor and trailed a branched model of evolution for recurrence [34]. These studies clearly represent the role of genetic and epigenetic events in a clonal selection of GBM tumor cells and document both linear and branched divergent sub-clonal evolution.

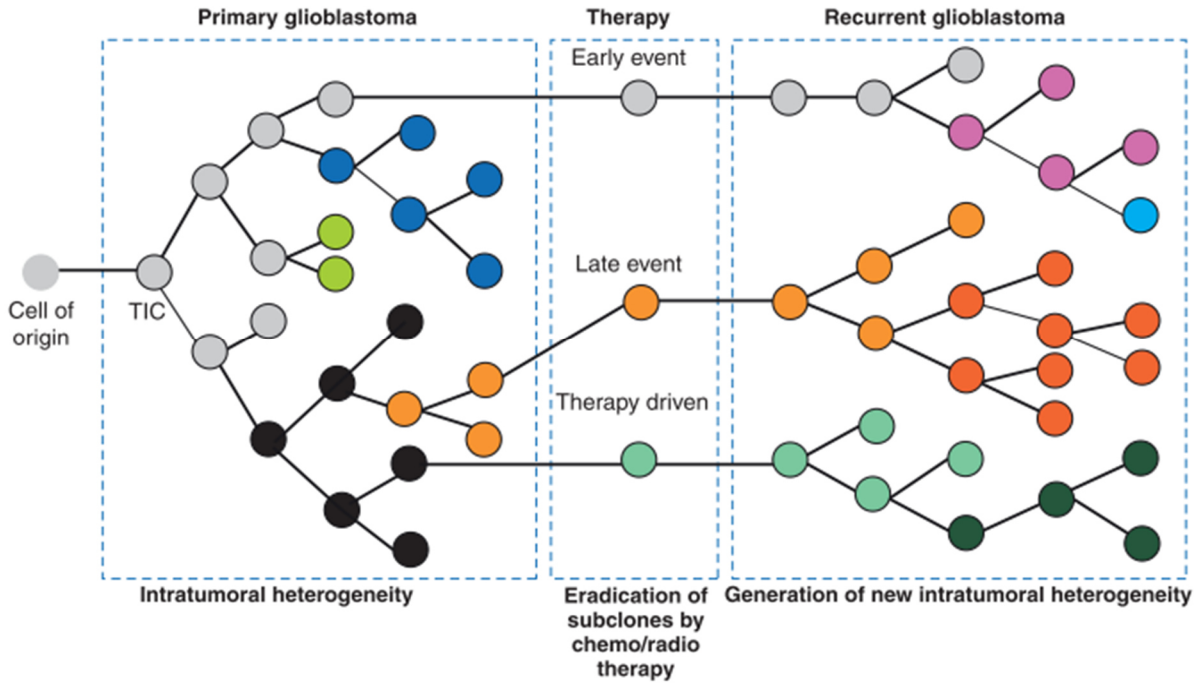

Figure 4. Recurrence and therapy resistance in glioma. Representation of how sub-clonal population in primary GBM rescue itself from therapy and leads to treatment-refractory, heterogeneous recurrent glioblastoma. After acquiring mutation, a normal cell gives rise to further multiple sub-clonal GBM populations with selectable traits against stress (distinct coloured circles) along with therapy. Primary GBM therapy give rise to the compilation of a sub-clonal cell population (early or late event sub-clone) or gives rise to therapy-driven-resistant sub-clone. This treatment-resistant sub-clonal population of cells further leads to tumor relapse and ultimately to a heterogenous recurrent glioblastoma with clonal heterogeneity from primary glioblastoma.

1.3.3 Immunosuppressive mechanisms

Tumors create an immunosuppressive network that assists them to escape the immune attack. Several studies have delineated the immunosuppressive nature of glioma, resulting in deregulation of an anti-tumor immune response. GBM can escape immune regulation by modulating several pathways and mechanisms such as secretion of immunosuppressive cytokines [35]; activation of negative regulatory pathways in lymphocytes. The most

prominent example is increased expression of programmed death ligand-1 (PD-L1) that binds to programmed death-1 on activated T cells and induces T cell exhaustion [36], indolamine 2,3 dioxygenase (IDO) which restricts the presentation of antigens to the immune cells [37] and evasion of immune recognition by modulating Major Histocompatibility Complex expression (MHC) [38]. Macrophages that are associated with glioma secrete interleukin (IL)-10 and transforming growth factor (TGF-β), which decreases immune cells activity [39, 40]. Tumor cells produce suppressive factors which mediate the effect of Treg cells population expansion through tumor-associated macrophages and dendritic cells, tumor-associated Treg cells leads to the immunosuppression of both innate and adaptive immune response [41].

One of the immunosuppressive mechanisms is by expression of cell surface immunosuppressive factors on glioma cells such as CD95 (Fas/Apoptosis antigen 1) ligand on their surface, which binds to its receptor on T cells resulting in apoptosis of and thus reduce infiltration of T cells in the tumor microenvironment [42, 43]. The challenges for immunotherapy consist of several factors such as insufficiency of tumor-specific antigens, overcoming self-tolerance and tumor heterogeneity. Although T cells are present in fewer number in the glioblastoma microenvironment, infiltration of T cell correlates positively with the clinical outcomes of the patients.

A healthy brain consists of fewer immune cells although rupture in the BBB results in an influx of immune cells [44, 45]. Brain antigens move towards the lymph nodes where the Antigen Presenting Cells (APC) represent them to the naïve T cells. This results into the of activation of T cells ultimately leading to the upregulation of α4 and β1integrins. These regulations allow the T cells to bind to the vascular cell adhesion molecule (VCAM)-1 on the vascular cells and to cross the BBB.

Checkpoint blockade therapies have been successful in the recent past and provided an illustration of targeted immunotherapies with higher effectiveness but to a restricted patient population [46]. This advocates that checkpoint-mediated regulation is the basis of immunosuppression for those tumors. Understanding the immunosuppressive mechanisms in GBM will definitely benefit to develop novel GBM immunotherapeutic advancements.

1.4 Treatment options

The treatment options depend largely on the respective grades of glioma, established on the potential of tumor growth and aggressiveness. Treatment factors which is associated with an individual patient are the tumor location, potential symptoms and potential benefits versus risks of other treatment options.

1.4.1Surgical intervention

Most common initial treatment is surgical resection in glioma, which requires opening of the skull also known as craniotomy. The tumor location plays a crucial role in surgical resection, if the tumors are near the important areas of the brain, intraoperative MRI or intraoperative brain mapping is performed. Various studies have shown that surgical resection alone, doubles survival and also assists in improving patient's response to chemotherapy and radiotherapy [47-49]. Unfortunately, due to the highly invasive character of GBM, it is almost impossible to perform a complete resection of the tumor and the residual tumor can behave in a more invasive and malignant manner.

1.4.2 Chemotherapy treatment

This is a treatment option for glioma and recurrent gliomas [50], several chemotherapeutic agents are currently being examined for their potential in the treatment of GBM. Nitrosourea studies have dominated the randomized control trials in glioma, which have shown that some

of the nitrosourea (BCNU) provide survival benefit to some extent (about 2 months) [4]. Mostly used drug for glioblastoma treatment is TMZ, which can easily cross the BBB, which is an orally administered DNA alkylating agent commercially available as Temodal®. TMZ promotes cytotoxicity through methylation guanine residues in DNA at O6 and N7 positions and adenine at N3 position [51]. These alterations lead to subsequent nucleotide mispairing during the replication process (O6 guanine with thymine instead of cytosine). This results in single or double-strand DNA breaks inducing cell cycle arrest in the G2/M phase and ultimately leading to apoptosis. The cytotoxicity of the chemotherapeutic drugs associated with DNA alkylation is dependent on the possible drug resistance mechanisms, primarily the suppression of DNA repair pathway.

1.4.3 Radiation therapy

Some types of gliomas are subjected to radiation therapy, particularly, which are located in the areas difficult to resect with surgery. There are three types of radiotherapy used for glioma treatment: a). external beam radiation therapy; b). Stereotactic radiosurgery; c). internal radiation. In the 1960s and early 1970s radiation therapy was the first postsurgical adjuvant therapy that reported significant efficacy by almost doubling the survival, even though the exact mechanism was not understood [4]. Stereotactic radiosurgery is administered as 60 Gy in 30 fractions for 6 weeks, although it should be started only after 2 weeks of surgery for adequate wound healing. In radiotherapy, fractionation of the dose is delivered to tumor cells relative to normal cells, fractionation allows the normal cells to repair the damage between fractions.

1.4.4 Anti-angiogenic treatment

Normal brain vasculature is peculiarly organized, consisting of endothelial cells, pericytes and astrocytes. These cells are responsible for forming and maintaining the BBB. Brain tumors

disrupt the brain vasculature by angiogenesis and metastasis [52]. Tumor angiogenesis or neo-angiogenesis is a characteristic of tumor cells for their growth as well as metastasis, anti-angiogenic treatment is a highly promising therapeutic aspect [53]. Anti-angiogenic drugs are classified based on their functionality into three categories: a). drugs constraining the expansion of endothelial cells (Thalidomide) [54]; b). drugs blocking angiogenesis signalling pathway (anti-VEGF antibodies, Avastin; interferon-alpha, inhibits the production of bFGF and VEGF) [55]; c). drugs that block extracellular matrix degradation (inhibitors of MMPs) [56].

1.4.5 Immunotherapy

Cancer immunotherapy activates the host's lymphocytes to recognize and eradicate the cancer cells. Immunotherapy has shown impressive therapeutic outcomes in distinct metastatic cancer types such as non-small cell lung cancer, non-Hodgkin lymphoma and melanoma. A modified immune environment in GBM results in tumor advancements and troubles the therapeutic options. Different forms of immunotherapies are followed in recent past including passive, active and adoptive immunotherapeutic approaches. Genetically synthetic immunoglobulin T cell receptor molecules, chimeric antigen receptors (CARs) are modified in a specific way to perceive specific antigens which will lead to T cells activation [57]. Since CAR-T cells showed promising results, several CARs have been developed and used to target glioma, including CARs targeting IL13Rα2 (present in almost 75% of glioma and associated with PI3K/Akt /mTOR pathway), EGFRvIII (50% of EGFR amplified glioma contain constitutively active oncogenic EGFRvIII), human epidermal growth factor receptor 2 (HER2, overexpressed in many cancer types) and CD70 (novel antigen) [58]. The escape variants from CAR-T cell therapy can ultimately lead to tumor recurrence.

After treatments, MRI scans are performed to check tumor growth. These scans represent the effectiveness of the treatment and if there is the presence of recurrent tumor growth. Future

treatment strategies for glioma should focus on sensitization of GBM to immune therapies along with other therapeutic options since GBM are very low immunogenic tumors located in the immune-suppressive microenvironment. Combinational adjuvant therapies can offer drastic opportunities to fulfill novel therapeutic outcomes in glioma.

1.5 New therapy options

As mentioned above, current optimal GBM therapy includes maximal safe surgical resection, chemotherapy (TMZ) and radiotherapy. Unfortunately, these therapies are not provide benefit to the overall survival probability in GBM patients and have been unsuccessful to provide substantial results at the clinical trials. Although there might be various reasons for these failed attempts which resulted in a significant gain of knowledge that can guide us towards new directions with future therapeutic studies. As brain metastases represent one of the major challenges in glioma treatment, recent molecular treatment in extra-cerebral tumor types has been proven to be useful in some patients with brain metastases. Such as EGFR and ALK inhibitors in non-small cell lung cancer, BRAF inhibitors in melanoma, HER-2-targeting agents in breast cancer, immune checkpoint inhibitors of CTLA4 or PD1 in melanoma or non-small cell lung cancer and bevacizumab in patients with radio-necrosis of corticosteroid-refractory brain edema [59].

New therapeutic strategies as a novel therapeutics include tumor-treating fields (TTF). TTF is an antimitotic treatment that selectively targets actively dividing GBM cells by transiting low intensity, intermediate frequency (range 100-500kHz) alternating electric fields through transducer arrays applied to the scalp [60] [61]. TTF might interfere with the appropriate arrangements of the mitotic spindle leading to activation of spindle assembly checkpoint (SAC) which eventually similarly results in apoptosis with anti-microtubule agents. This approach helps achieve a compelling escalation in the overall survival in GBM patients [1]. Another

approach for GBM would be CAR T-cell therapy, which has demonstrated the feasibility and safety and has opened the door to personalized cancer treatment. Here, T cells are genetically engineered to express chimeric antigen receptors (CARs) which further will be guided against definite antigens. CARs are artificial fusion proteins that incorporate an extracellular antigen-recognition domain, a transmembrane domain and an intracellular T-cell signalling domain [62]. Later CARs engage with their associated antigen, which leads to the outcome of activation of primary T cells. One of the major challenges for using CAR T cell therapies for GBM is its immunosuppressive microenvironment. After CAR T cells enter in the tumor microenvironment, they encounter several challenges by microenvironment such as tumor derived soluble factors, cytokines, immune cells leading to immunosuppression along with physical and metabolic barriers [63]. Some other factors which affect the CAR T cell therapies are the tumor heterogeneity, antigen loss and T cell proliferation and endurance. In hematologic malignancies, amplification of T-cell is required in peripheral blood for achieving clinical adequacy. In solid tumors, the peripheral blood is not involved in therapeutic response, hence it is difficult to determine an effective CAR T cell dose and frequency of administration [58].

1.6 Aim of the study

Since GBM is highly aggressive, even the advancements in the therapeutics approach is not able to increase the median survival which remains 14-16 months for several years. Therefore, development of new therapeutic approaches is extremely important. Because, the molecular mechanisms involved in gliomagenesis is poorly understood, we also have to focus towards the understanding of molecular pathways which leads to gliomagenesis and therapeutic resistance. Along with this there are several other challenges which restricts the therapeutic advancements such as highly invasive and neo-angiogenic nature of GBM cells, BBB which restricts the availability of particular drugs in the tumor niche, highly immunosuppressive nature of GBM, mutations and molecular alterations. Therefore, I pursued the goal to

understand more about the complex molecular mechanisms by focussing on Microtubule Associated Tumor Suppressor 1 (*MTUS1*). *MTUS1* encodes a family of Angiotensin Type II receptor Interacting Protein (ATIP) through alternative splicing (ATIP1, ATIP2, ATIP3a, ATIP3b, ATIP4). In this study we focussed particularly on ATIP1 since it is ubiquitously expressed and it has the highest expression in brain as compared to any other isoform [64]. We think that the elucidation of the role of *MTUS1* in GBM might help to develop new strategies that target the *MTUS1* associated pathways and that might help to slow down or even to block the progression of GBM. In order to achieve this, we framed the objectives and asked following questions:

1. How *MTUS1*/ATIP1 expression is regulated in glioma and what might lead to its altered regulation? To answer this question, we did the dtabase mining in the R2: Genomics and Visualization Platform where we analysed different datasets to check MTUS1 expression levels in glioma samples compared to control samples. We also analysed *MTUS1*/ATIP1 expression in clinical glioma samples and patient derived GSCs. Also, in order to understand the reason alterations in *MTUS1*/ATIP1 alterations we studied the methylation pattern in its transcription start site (TSS).

2. Does *MTUS1*/ATIP1 act as a tumor suppressor? Role of *MTUS1*/ATIP1 in glioma migration and invasion based on molecular mechanistic evaluations? After exploring the expression of ATIP1 *in vitro* and clinical samples, we tried to understand the biological role of ATIP1 and how it affects gliomagenesis. We performed *in vitro* functional assays with overexpressed ATIP1 stable cell lines

3. How does chemo and radiotherapy in glioblastoma cells, modulates *MTUS1*/ATIP1 expression? We also wanted to explore the effect of available therapeutic approaches in glioma on ATIP1 expression. Hence we treated respective cells with chemo and

radiotherapy and performed western blot analysis and TMZ treated *in vivo* experiments in orthotopic glioma model using Wistar rats.

4. Does *MTUS1*/ATIP1 regulates DNA repair and how does it affect glioma therapies? Based on the findings of the previous objectives we further wanted to explore if ATIP1 expression is inflecting radiation induced DNA repair. Hence, we analysed dynamics of ϒH2A.X formation and elimination in order to find out the ATIP1 mediated ds-DNA repair mechanisms.

Chapter 2

Materials and methods

2. Materials and methods

2.1 Materials

2.1.1 Equipments

Equipment	Manufacturer
10 / 100 / 1000 µl pipettes	Eppendorf (Hamburg, Germany)
7500 Fast Real Time PCR	Applied Biosystems (Darmstadt, Germany)
Accu Jet Pipette Pro Controller	Hirschmann (Eberstadt, Germany)
Biofuge Pico centrifuge	Heraeus (Hanau, Germany)
Biorad Immunoblot Equipment	Biorad (Munich, Germany)
ChemiDocTM Imaging System	Biorad (Munich, Germany)
CO2 Incubator	Sanyo (Munich, Germany)
CyAn ADP flow cytometer	Beckman Coulter (Krefeld, Germany)
Eclipse TS100 microscope	Nikon (Kingston, UK)
Multiscan EX	Thermo Electron Corporation (Karlsruhe, Germany)
Gammacell-40 Irradiator	MDS Nordion (Toronto, Canada)

Equipment	Manufacturer
10 µl Hamilton syringe, 701 N, 26s ga,	Hamilton (Bonaduz, Switzerland)
Hera Safe Clean Bench	Heraeus (Hanau, Germany)
LSM 510 META Confocal microscope	Carl Zeiss (Oberkochen, Germany)
MACS MultiStand	Miltenyi (Bergisch Gladbach, Germany)
MilliQ Integral (ultrapure water preparation)	Millipore/Merck (Darmstadt, Germany)
MiniMACS Separator	Miltenyi (Bergisch Gladbach, Germany)
Mouse stereotaxic instrument	Stoelting (Dublin, Ireland)
Multifuge 3 S-R centrifuge	Heraeus (Hanau, Germany)
Multipipettes	Eppendorf (Hamburg, Germany)
NanoDrop ND 1000	Peqlab (Erlangen, Germany)
Neubauer cell counting chamber	Marienfeld (Bad Mergentheim, Germany)
Power Pac power supply unit	Biorad (Munich, Germany)
Thermomixer Comfort	Eppendorf (Hamburg, Germany)

2.1.2 Consumables

Consumable	Manufacturer
Assay plate white, 96 well format	Corning (New York, USA)
Cell culture flasks T25 / T75 / T125	Thermo Fisher Scientific (MA, USA) and Greiner Bio-One (Frickenhausen, Germany)
8.0 µm pore size Cell culture insert size, 24 well format	Becton Dickinson (Heidelberg, Germany)
Cell scraper	Corning (New York, USA)
Combitips advanced 2.5 / 5 ml	Eppendorf (Hamburg, Germany)
Falcon centrifuge tubes 15 / 50 ml	Corning (New York, USA)
Filter paper	Peqlab (Erlangen, Deutschland)
Microlance 3 needles	Becton Dickinson (Heidelberg, Germany)
Microscope slides 76x26 mm	R. Langenbrick (Emmendingen, Germany)
Microscopical cover slips	R. Langenbrick (Emmendingen, Germany)
MS columns	Miltenyi (Bergisch Gladbach, Germany)
MycoAlert mycoplasma detection kit	Lonza (Cologne, Germany)
PERMA-HAND silk suture, black braided, 6-0, 11 mm, 3/8 circle	Ethicon (Somerville, NJ, USA)
Pipette tips	Ratiolab (Dreieich, Germany)

Consumable	Manufacturer
Nitro-cellolose 0.45 µ transfer membrane	GE Healthcare (Chicago, USA)
Polypropylene tubes 1.3 / 5 ml	Greiner Bio-One (Frickenhausen, Germany)
PVDF 0.45 µ transfer membrane	Serva (Heidelberg, Germany)
Reaction tubes 0.5 / 1.5 / 2 ml	Greiner Bio-One (Frickenhausen, Germany)
RNA-Isolation kit	Macherey-Nagel (Düren, Germany)
RT-qPCR adhesive film	Biozym Scientific (Hessisch Oldendorf, Germany)
RT-qPCR plates	Thermo Fisher Scientific (MA, USA)
Serological pipettes 5 / 10 / 25 ml	Corning (New York, USA)
Surgical blades, sterile	B. Braun (Melsungen, Germany)
Syringes Inject-F/Inject Solo 1-20 ml	B. Braun (Melsungen, Germany)
Water (ultrapure)	Milli Q Integral (Millipore/Merck, Darmstadt, Germany)
Well plates 6 / 12 / 24 / 48 / 96	Becton Dickinson (Heidelberg, Germany)

2.1.3 Chemicals, media, and reagents

Material	Manufacturer
1,4-Dithiothreitol (DTT)	Sigma-Aldrich (Taufkirchen, Germany)
Accutase	Sigma-Aldrich (Taufkirchen, Germany)
Acetic acid	Merck (Darmstadt, Germany)
Acrylamide	Carl Roth (Karlsruhe, Germany)
Adenosine 5′-triphosphate disodium salt (ATP)	Sigma-Aldrich (Taufkirchen, Germany)
Ammonium persulfate (APS)	Carl Roth (Karlsruhe, Germany)
Ascorbic acid	Sigma-Aldrich (Taufkirchen, Germany)
BIOMYC-1 / 2 / 3 antibiotic solution 100X	PromoCell (Heidelberg, Germany)
Bovine serum albumin (BSA)	Carl Roth (Karlsruhe, Germany)
Bradford reagent	Carl Roth (Karlsruhe, Germany)
Bromophenol blue	Merck (Darmstadt, Germany)
Calcium chloride	Sigma-Aldrich (Taufkirchen, Germany)
Coenzyme A, trilithium salt	Merck (Darmstadt, Germany)
Collagen I, rat tail	Enzo Life Sciences (New York, USA)

Material	Manufacturer
Crystal violet (CV)	Merck (Darmstadt, Germany)
D-glucose	Sigma-Aldrich (Taufkirchen, Germany)
Dimethyl sulfoxide (DMSO)	Carl Roth (Karlsruhe, Germany)
dNTP´s 20 mM	Peqlab (Erlangen, Germany)
Dulbecco's modified eagle's medium (DMEM)	Sigma-Aldrich (Taufkirchen, Germany)
Dulbecco's phosphate buffered saline (PBS)	Sigma-Aldrich (Taufkirchen, Germany)
Endothelial basic medium (EBM-2)	Lonza (Basel, Switzerland)
Endothelial growth medium (EGM-2)	Lonza (Basel, Switzerland)
Ethanol 99%	Merck (Darmstadt, Germany)
Ethylene glycol-bis(2-aminoethylether)-N,N,N′,N′-tetraacetic acid (EGTA)	Sigma-Aldrich (Taufkirchen, Germany)
Ethylenediaminetetraacetic acid (EDTA)	Sigma-Aldrich (Taufkirchen, Germany)
Fetal bovine serum (FBS)	Sigma-Aldrich (Taufkirchen, Germany)
Glycerol	Carl Roth (Karlsruhe, Germany)

Material	Manufacturer
Glycine	Carl Roth (Karlsruhe, Germany)
Gly-Gly	Sigma-Aldrich (Taufkirchen, Germany)
Goat serum	Sigma-Aldrich (Taufkirchen, Germany)
H2O2	Sigma-Aldrich (Taufkirchen, Germany)
Haematoxylin	Merck (Darmstadt, Germany)
Hygromycin B	Invivogen (Toulouse, France)
Igepal (NP-40)	Sigma-Aldrich (Taufkirchen, Germany)
Isopropanol	Merck (Darmstadt, Germany)
K2HPO4	Carl Roth (Karlsruhe, Germany)
L-Glutamine 200 mM	Sigma-Aldrich (Taufkirchen, Germany)
Magnesium sulfate	VWR (Darmstadt, Germany)
Matrigel matrix basement membrane	Corning (New York, USA)
Methanol	VWR (Darmstadt, Germany)
M-MLV reverse transcriptase	Promega (Madison, USA)
M-MLV RT 5xBuffer	Promega (Madison, USA)
Modified eagle's medium (MEM)	Sigma-Aldrich (Taufkirchen, Germany)

Material	Manufacturer
Normal rabbit IgG	Santa Cruz Biotechnology (Heidelberg, Germany)
Oligo dT-nucleotide 100 µM	Sigma-Aldrich (Taufkirchen, Germany)
Paraformaldehyde	AppliChem (Darmstadt, Germany)
Penicillin/Streptomycin (100x)	PAA Laboratories (Cölbe, Germany)
Poly-L-lysine hydrobromide	Sigma-Aldrich (Taufkirchen, Germany)
Ponceau S	Merck (Darmstadt, Germany)
Propidium iodide (PI)	Sigma-Aldrich (Taufkirchen, Germany)
Protein marker PanReac	AppliChem (Darmstadt, Germany)
Proteinase inhibitor cocktail set III	EMD Chemicals (San Diego, USA)
Chalbio.	
Ribonuclease A from bovine pancreas	Sigma-Aldrich (Taufkirchen, Germany)
RPMI1640 medium HEPES modification	Sigma-Aldrich (Taufkirchen, Germany)
Skim milk powder	Carl Roth (Karlsruhe, Germany)
Sodium chloride	Merck (Darmstadt, Germany)
Sodium citrate	Merck (Darmstadt, Germany)

Material	Manufacturer
Sodium dodecyl sulfate (SDS)	Carl Roth (Karlsruhe, Germany)
ß-Mercaptoethanol	Carl Roth (Karlsruhe, Germany)
Sybr Green PCR master mix	Thermo Fisher Scientific (MA, USA)
Temozolomide (TMZ)	Sigma-Aldrich (Taufkirchen, Germany)
Tetramethylethylenediamine (TEMED)	Carl Roth (Karlsruhe, Germany)
Thiazolyl blue tetrazolium bromide (MTT)	Sigma-Aldrich (Taufkirchen, Germany)
Triton X-100	Sigma-Aldrich (Taufkirchen, Germany)
Trizma base (Tris)	Sigma-Aldrich (Taufkirchen, Germany)
Trizma hydrochloride (Tris HCl)	Sigma-Aldrich (Taufkirchen, Germany)
Trypan blue 0.4%	Sigma-Aldrich (Taufkirchen, Germany)
Trypsin-EDTA	Sigma-Aldrich (Taufkirchen, Germany)
Tween-20	Carl Roth (Karlsruhe, Germany)
VECTASHIELD Antifade mounting medium with DAPI	Vector laboratories (Burlingame, USA)
VECTASHIELD HardSet mounting medium with DAPI	Vector laboratories (Burlingame, USA)
Clarity Western ECL HRP substrate	Biorad (Munich, Germany)

2.1.4 Antibodies immunoblot

Antibody	Manufacturer
Goat anti-mouse IgG-horseradish peroxidase (HRP), secondary antibody	Santa Cruz Biotechnology (Heidelberg, Germany)
Goat anti-rabbit IgG-HRP, secondary antibody	Santa Cruz Biotechnology (Heidelberg, Germany)
Rabbit polyclonal anti-human ATIP1	BIOSS (Massachusetts, USA)
Mouse anti-human MMP-2	Oncogene (Massachusetts, USA)
Mouse monoclonal anti-human GAPDH	Millipore (Massachusetts, USA)
Rabbit monoclonal anti-human E-cadherin	Cell Signaling (Danvers, MA, USA)
Mouse monoclonal anti-human MMP-9	Santa Cruz Biotechnology (Heidelberg, Germany)
Rabbit monoclonal anti-human p-ERK	Cell Signaling (Danvers, MA, USA)
Rabbit monoclonal anti-human ERK	Cell Signaling (Danvers, MA, USA)
Mouse monoclonal anti-human ERK	Santa Cruz Biotechnology (Heidelberg, Germany)
Rabbit monoclonal anti-human p-AKT	Cell Signaling (Danvers, MA, USA)
Rabbit monoclonal anti-human AKT	Cell Signaling (Danvers, MA, USA)

Antibody	Manufacturer
Mouse monoclonal anti-human Bcl-2	Santa Cruz Biotechnology (Heidelberg, Germany)
Mouse monoclonal anti-human Bax	Santa Cruz Biotechnology (Heidelberg, Germany)

2.1.9 Cell lines and primary cells

Name	Description	Source
C6	Rat GBM cell line (p53WT)	NCCS (Pune, India)
HBMvEC	Human Brain Microvascular Endothelial cells	
LK7	Human derived glioma stem cells	University Clinics, Tübingen, Germany
LK31	Human derived glioma stem cells	University Clinics, Tübingen, Germany
LN-308	Human astrocytoma cell line (p53-/-)	N. de Tribolet (Lausanne, Switzerland)
LN-18	Human astrocytoma cell line ($p53^{mut}$)	N. de Tribolet (Lausanne, Switzerland)

Name	Description	Source
LNT-229	Human GBM cell line ($p53^{WT}$)	N. de Tribolet (Lausanne, Switzerland)
LNT-229	Human GBM cell line (temperature-sensitive ($p53^{V135A}$) p53)	
NHA	Normal Human Astrocytes	Lonza (Basel, Switzerland)
NIH/3T3	Murine embryonic fibroblast cell line	ATCC (Manassas, USA)
U87MG	Human GBM cell line (p53WT)	ATCC (Manassas, USA)
R11	Human derived glioma stem cells	University Clinics, Tübingen, Germany
R28	Human derived glioma stem cells	University Clinics, Tübingen, Germany
LK7	Human derived glioma stem cells	University Clinics, Tübingen, Germany
LK31	Human derived glioma stem cells	University Clinics, Tübingen, Germany

2.1.11 Software

Software	Manufacturer
qPCR 7500 Software v 4.2.0.	Applied Biosystems (Darmstadt, Germany)
Ascent Software 2.6	Thermo Fisher Scientific (MA, USA)
Axiovision SE64	Carl Zeiss (Oberkochen, Germany)
MS Office	Microsoft (Redmond, WA, USA)
ImageJ	Johannes Schindelin, Albert Cardona, Mark Longair, Benjamin Schmid, and others
FlowJo V10	FlowJo, LLC (Ashland, OR, USA)
Graphpad Prism 8	Graphpad (San Diego, CA, USA)
Image Lab Version 6.0	Biorad (Munich, Germany)
NanoDrop 1000	Thermo Fisher Scientific (MA, USA)

2.2. Methods

2.2.1 Cell culture and reagents.

Human GBM cell lines LNT-229 ($p53^{WT)}$, LN-308 ($p53^{del}$) and LN18 ($p53^{mut}$) were kindly provided by N. de Tribolet (Lausanne, Switzerland), U87-MG ($p53^{WT}$) were obtained from ATCC (Manassas, USA). LNT-229-$p53^{ts}$ cells expressing a p53 temperature-sensitive mutant (V135A) were grown at 38.5ºC to express mutant p53 or at 32.5ºC to express wild-type p53 [65, 66]. C6 ($p53^{WT}$) rat glioma cells were obtained from NCCS, Pune, India. The cells were maintained in DMEM (Sigma Aldrich, MO, USA) containing 10% fetal bovine serum (FCS), penicillin (10,000 U/ml) and streptomycin (100mg/ml; Gibco, NY, USA). GSC lines R11, R28 were a kind gift from C. Beier (University of Regensburg) [3]. The above-mentioned cell lines have been sent for authentication to the DSMZ-German Collection of Microorganism and Cell Cultures in 2012. Thereon, the cells were frozen at -145°C in individual labelled and electronically documented vials. After taking in culture GSC were further used for maximal 15 passages. LK7, LK28 and LK31, derived from patients with primary GBM were obtained from S. Huber (Radio-Oncology, University Hospital Tübingen) and were maintained up to passage 30. R11, R28 and LK-cells were maintained as spheres in stem cell-permissive DMEM-F12 medium supplemented with 20ng/ml of human recombinant epidermal growth factor (EGF; BD Biosciences, Heidelberg, Germany), human recombinant basic fibroblast growth factor (bFGF; R&D Systems, Wiesbaden, Germany), human leukemia inhibitory factor (LIF; Millipore, Billerica, MA, USA), 2% B27 supplement (Life Technologies, Carlsbad, CA, USA), penicillin (10,000 U/ml) and streptomycin (100mg/ml, Gibco, NY, USA). Normal human astrocytes (NHA, passages 2-4, Lonza, Basel, Switzerland) were maintained in supplemented ABM medium (Lonza, Basel, Switzerland). Human brain microvascular endothelial cells (HBMvEC) obtained from iXCells (San Diego, CA, USA) were cultured in supplemented

EGM-2 medium (Lonza, Basel, Switzerland). All cell lines (except LNT-229 $p53^{ts}$) were maintained at 37°C in a 5% CO_2 humidified atmosphere. To generate ATIP1 overexpressing glioma cells, ATIP1 was amplified from cDNA of normal human brain tissue obtained from the National Institute of Mental Health and Neurosciences (NIMHANS), Bengaluru, India and was cloned into pCDNA3.1-Myc to express myc-tagged ATIP1 (Table 1). Glioma cells were transfected with pCDNA3.1-myc or pCDNA3.1-myc-ATIP1 using Effectene (Qiagen, Hilden, Germany) and positive cells were selected using G418. Decitabine (5-Aza-2'-deoxycytidine: 5-Aza-dC; Sigma Aldrich, MO, USA) treatment was performed in standard growth medium for 72 h with a repeated change of the medium every 24 h. To determine clonogenic survival, 1000 cells were seeded in 6 well plates. After approximately 10 doubling times the cells were fixed with 4% paraformaldehyde (PFA) and stained with crystal violet as previously described [67].

2.2.2 Mycoplasma detection

All cell lines were periodically tested for mycoplasma contamination using the Lonza MycoAlert mycoplasma detection kit. Briefly, 500 µl of cell culture supernatant was centrifuged for 5 min at 2000 rpm and 40 µl of MycoAlert reagent was added, incubated for 5 min and luminescence was measured using a luminometer (value A). Further, 40 µl MycoAlert substrate was added, incubated for 10 min and luminescence was measure again (value B). If value B represents equal to or higher than value A, the cells were classified as mycoplasma positive according to the manufacturer´s protocol. Mycoplasma positive cells were treated with BIOMYC solutions 1-3 according to the manufacturer´s instructions and were analysed again. Only mycoplasma-free cells were used in experiments.

2.2.3 Clinical sample collection and processing.

This study was authorized by the Institutional Ethics Committee (IEC, Ref. No. UH/IEC2016/180). The surgically resected glioma samples were collected from the Krishna Institute of Medical Science (KIMS, Hyderabad, India). Patients diagnostics were confirmed clinically and histopathologically at the Pathology facility of KIMS Hospital, and classification of samples was done according to the WHO classification [68]. The samples were snap-frozen and kept at -80°C for further analysis. Normal brain tissue samples were collected from the National Institute of Mental Health and Neurosciences (NIMHANS), Bengaluru, India. The specimens consisted of 4 normal brain samples along with 4 epileptic brain samples, 6 WHO grade I glioma, 27 WHO grade II glioma, 20 WHO grade III glioma and 23 WHO grade IV glioma. Amongst these 2 patients from grade I, 4 patients in grade II, 5 patients in grade III and 7 patients in grade IV were classified as recurrent glioma cases. None of the patients had received pre-operative chemotherapy, radiotherapy and targeted therapy except recurrent glioma patients. The samples were further processed for RNA and protein isolation and analysis of ATIP1 expression and its molecular correlations.

2.2.4 RNA isolation

For quantitative reverse transcription-polymerase chain reaction (RT-PCR), total RNA was isolated from the tumor tissues using TRIzol reagent (Sigma-Aldrich, MO, USA) according to manufactures instructions. RNA concentration and purity were determined by measurement at 230, 260, and 280 nm using a NanoDrop spectrophotometer and stored at -80°C.

2.2.5 cDNA synthesis

One microgram of total RNA was reverse transcribed into complementary DNA (cDNA) using the cDNA synthesis kit (Takara Bio, USA). In a final volume of 10 µl, 1 µg of respective RNA was incubated with oligodT primer, 1 µl dNTP mix for 5 mins at 65°C. After a short

centrifugation, 4 µl of 5X primescript buffer, 0.5 µl RNase inhibitor, subsequently 1 µl Primescript RTase was added followed by one hour incubation period at 42°C. The enzyme was inactivated at 95°C for 5 mins and diluted accordingly in RNase-free water.

Table 1. Primers used to amplify ATIP1 cDNA

Primer	Sequence (5'-3')
ATIP1 Forward	CGGATCCATGTTGTTGTCTCCCAAATTC
ATIP1 Reverse	GCTCGAGTCATCTGGGTGAAATGCTG

2.2.6 Semi-quantitative PCR (sq-PCR) and Quantitative real-time PCR (RT-qPCR)

To quantify the differences in expression of respective in variable control and glioma samples, sq-PCR and RT-qPCR were used. Respective primers were designed for amplification using the NCBI nucleotide database software (Table 2). For normalization, a primer pair targeting the housekeeping gene glyceraldehyde-3-phosphate dehydrogenase (GAPDH) was used.

cDNAs were diluted 1:3 in water and subsequently, 1 µl of pre-diluted cDNA was used for respective PCRs. Water and reaction mixture without polymerase was used as a negative control. Real-time qPCR plates were sealed with adhesive film and subjected to quick spin. Real-time quantitative PCR using SYBR Green (Takara Bio, USA). ABI7500 qPCR system and Software v 4.2.0. (Applied Biosystems Incorporation, Darmstadt, Germany). Cycling conditions were as followed: 95°C for 5 min, 40 cycles at 95°C for 15 s, 60°C for 1 min and 72°C for 30 s.

The resulting cycle threshold (Ct) values were analysed using excel. The Ct value is specified as the first cycle with a fluorescent signal clearly above the threshold. The target values were normalized to the housekeeping value (ΔCt) and then relate to the control value (ΔΔCt), the final value is depicted as an n-fold expression to the control. Final relative mRNA expression was quantified as mentioned above, $E^{\Delta\Delta CT}$ (gene of interest)/$E^{\Delta\Delta CT}$ (housekeeping gene).

Table 2. Primers used for quantitative-PCR analysis

Primer	Sequence (5'-3')
ATIP1 Forward	GGAGAGCTAGTCACTGCTTCAACC
ATIP1 Reverse	GTCCCGAAGCTTTTCATACTCCC
SHP1 Forward	GGAGTCGGAGTACGGGAACAT
SHP1 Reverse	ATCCTCCTTGTGTTTGGACGA
MMS2 Forward	ATTGGGCCACCAAGGACAAA
MMS2 Reverse	TAACACTGGTATGCTCCGGG
GAPDH Forward	TGACCCCTTCATTGACCTCA
GAPDH Reverse	GAGATGATGACCCTTTTGGCT

2.2.7 Immunoblotting

2.2.7.1 Generation of protein lysates

The confluent cell monolayers were washed with PBS twice and were collected using a cell scraper for the generation of protein lysates. The cells were centrifuged at 1200 rpm for 5 minutes and the supernatant was removed. Pellets were washed with ice-cold 1X PBS and lysed for 30 mins at 4°C in 1X cell lysis buffer. The samples were passed through a 27-gauge syringe 10-20 times. Further, respective samples were centrifuged at 12000 rpm for 20 minutes and the clear supernatant was collected and procured at -20°C.

Lysis buffer	Concentration
Tris HCl pH 8	50 mM
Sodium chloride	120 mM
EDTA	5 mM
NP-40	0.5 %
Millipore water	
Proteinase inhibitor cocktail	10 µl in 2 ml lysis buffer short before usage

2.2.7.2 Bradford protein assay

The respective concentrations of protein in whole-cell lysates were quantified by using Bradford reagent. For the standard curve, respective concentration of BSA solution (0, 1, 2, 4, 6, 8, 10 and 12 µg) was diluted in water. For lysates, 1 µl of sample in 50 µl of water were used in triplicates. Further 150 µl of 1:5 pre-diluted Bradford reagent was added and the absorbance was recorded at 595 nm. The means for respective samples were used to calculate the protein concentration on basis of the standard curve.

2.2.7.3 SDS polyacrylamide gel electrophoresis (SDS-PAGE)

To separate the protein based on their size SDS-PAGE is used. Proteins were denatured in SDS loading dye supplemented with bromophenol blue and β-mercaptoethanol. An equal amount of proteins (20 µg to 50 µg) was resolved on 10-12% SDS-polyacrylamide gel and subjected to electrophoresis.

2.2.7.4 Protein transfer

To transfer the resolved proteins from acrylamide gel to nitrocellulose or PVDF membrane (after activation in methanol for 1 minute), the gels were subjected to transfer at 100 V for one hour in 1X transfer buffer.

2.2.7.5 Immunoblot antibody incubation and detection

After transfer, the membranes were blocked in 5% non-fat milk (1 h, RT) and further probed with respective indicated primary antibodies overnight at 4°C. The following primary antibodies were diluted as per manufacturer recommendations. After incubation, blots were washed in 1X TBST and probed with HRP-conjugated secondary antibodies at a dilution of 1:5000 in blocking solution (1 h, RT), washed three times in TBST. The blots were developed using WesternBright ECL chemiluminescence detection reagents (Bio-Rad, CA, USA). Protein expression was imaged and quantified using the ChemiDocTM imaging system and Image Lab Software (Bio-Rad, Munich, Germany).

2..2.8 Immunohistochemistry

2.2.8.1 Brain tissues from animal experiments

Rodent brain tissues were fixed with 4% PFA for 24 hours, subjected to dehydration using a 20-30% sucrose solution and cryo-sectioned for histological analysis using a Leica Cryomicrotome CM3050S (Leica, Wetzlar, Germany). The sections were heated on a slide warmer for 10 min at 72ºC and rehydrated in PBS for 10 mins and heat-mediated antigen retrieval was performed by boiling the sections in Tris-EDTA buffer pH 9 for 20 mins. Non-specific peroxidase activity was quenched by 9:1 methanol/30% hydrogen peroxide solution for 10 mins and sections were washed in PBST twice (10 min each) sections were blocked using 2% BSA for 45 min at room temperature followed by overnight immunostaining with

respective primary antibody incubation at 4ºC. Further, the sections were washed with PBS and incubated with Polydetector HRP label for 45 mins at RT followed by incubation with diaminobenzidine (DAB) chromogen (Bio SB, CA, USA) for 20 min. Sections were counterstained with hematoxylin and washed out with tap water for 10 min. After subsequent dehydration in 70 %, 80 %, 90 % and 100 % ethanol and clearing with 100 % xylene, sections were mounted with DPX mountant (SRL, India) using coverslips. The sections were examined and the images were captured using an Olympus camera attached to the microscope (Olympus, Tokyo, Japan) and using Axioplan 2 microscope and imaging software (Carl Zeiss, Oberkochen, Germany).

2.2.8.2 Histological studies in clinical glioma specimens

Paraffin-embedded control and glioma brain sections were obtained from KIMS hospital, post-diagnostic confirmations. Respective brain sections were deparaffinized in xylene (5 min). Followed by rehydration of the section in ethanol (100 %, 90 %, 80 % and 70 %, 2 min each) and water (5 min). Further, heat-mediated antigen retrieval was performed by boiling the sections in Tris-EDTA buffer pH 9 for 20 mins. Non-specific peroxidase activity was quenched by 9:1 methanol/30% hydrogen peroxide solution for 10 mins and sections were washed in PBST twice (10 min each) sections were blocked with 2% BSA for 45 min at room temperature followed by overnight immunostaining with respective primary antibody incubation at 4ºC. Further, the sections were washed with PBS and incubated with Polydetector HRP label for 45 mins at RT followed by incubation with diaminobenzidine (DAB) chromogen (Bio SB, CA, USA) for 20 min. Sections were counterstained with hematoxylin and washed out with tap water for 10 min. After subsequent dehydration in 70 %, 80 %, 90 % and 100 % ethanol and clearing with 100 % xylene, sections were mounted with DPX mountant (SRL, India) using coverslips. The sections were examined and the images were taken using an Olympus camera attached to the microscope (Olympus, Tokyo, Japan).

2.2.9 Methylation pattern analysis

2.2.9.1 CpG island identification

The CpG island in the proximal region or *MTUS1* coding region was identified using Methprimer software (Beijing, China). The criteria used for prediction were: Island size > 100, GC Percent > 50.0, Obs/Exp > 0.6.

2.2.9.2 Genomic DNA isolation, bisulfite conversion and PCR

Genomic DNA was isolated from established glioma cells (LNT-229, LN-308), GSCs (LK7, LK31, R11, and R28) and human astrocytes using a Qiagen DNA extraction kit (Qiagen, Hilden, Germany). The genomic DNA was subjected to bisulfite conversion using the DNA Lightening conversion kit (Zymo Research GmbH, Freiberg, Germany) according to the manufacture's protocol. The bisulfite converted DNA was used for amplification of the predicted *MTUS1* promoter regions and purified using hot start Platinum Taq Polymerase according to manufacturer's guidelines (Invitrogen, CA, USA).

Table 3. Primers used for amplification of Bisulfite-converted DNA

Primers	Sequence (5'-3')
Distal region-Forward	GAGGTAAGTAGGAGTTAGATTTTTTATT
Distal region-Reverse	AAAAAACAACCCTCAAAAAACCTAAAT
Proximal region-Forward	GATGGTGGTTGGTTTTGGTTTTT
Proximal region-Reverse	CACTTACCCACAACTCCTTCAAA

2.2.9.3 TA-TOPO cloning and sanger sequencing.

The purified PCR fragment was further cloned in the pCR2.1 vector using the TA-TOPO cloning kit (Invitrogen, Karlsruhe, Germany). Positive clones were selected through blue-white screening and colony PCR. The positive clones were sent for Sanger sequencing (Eurofins, Ebersberg, Germany) and the methylation pattern was analysed using QUMA software (CDB, Riken, Japan). The raw fastq sequence files were uploaded on Sequence Read Archive (SRA, NCBI) server with accession ID: PRJNA633153.

2.2.9.4 Decitabine (5-Aza-2′-deoxycytidine: 5-Aza-dC) treatment.

The GSC (LK7, R11, R28) established glioma cells (U87-MG, LNT-229 and LN-308) were seeded and allowed to adhere and treated with different concentrations (0 µM, 10 µM and 30 µM) of decitabine (Sigma Aldrich, MO, USA). The treatment was performed in a standard growth medium for 72 h with a repeated change of the medium every 24 h. Further, the cells were collected and harvested for RNA and protein isolation for analyzing ATIP1-expression post decitabine treatment using qRT-PCR and immunoblotting.

2.2.10 Functional analysis of ATIP1 overexpression

2.2.10.1 Molecular cloning, establishing ATIP1 overexpression cell lines and functional analysis.

To construct ATIP1 plasmids, pCDNA3.1-Myc (vector) was digested with BamHI and XhoI and ATIP1 is PCR amplified and inserted into the vector backbone. The primers used are described in Table 4. LNT-229 and LN-308 cell lines were transfected with pCDNA3.1-Myc or pCDNA3.1-Myc-ATIP1 constructs using effectine transfection reagent (Qiagen, Hilden, Germany). After 48 hours, the stable transfectants were cultured and selected in DMEM

complete media supplemented with 400 µM G418 selection media. The colonies were screened and used for further analysis.

Table 4. Primers used for ATIP1-pcDNA3.1 construct

Primer	Sequence (5'-3')
ATIP1 Forward (BamHI)	CGGATCCATGTTGTTGTCTCCCAAATTC
ATIP1 Reverse (XhoI)	GCTCGAGTCATCTGGGTGAAATGCTG

2.2.10.2 Wound healing assay.

Wound healing assay inspects the migration capability of the cells. The pcDNA3.1 (mock, EV) and pcDNA3.1-ATIP1 overexpressed cells LNT-229 and LN-308 cells were cultured in a 6-well plate (2×10^5 cells/well). After the cells were about 80% confluent the monolayers were treated with mitomycin A (2.5 µg/ml) for 3 hours which results in the inhibition of cell proliferation. Further, the monolayer was scratched and cultivated in optimal conditions. The migrating cells images were captured using a camera assisted with a light microscope at the interval of every 24 hours post scratching (0h, 24h, and 48 h). The rate of migration was measured and analysed by ImageJ software.

2.2.10.3 Transwell migration and matrigel invasion assay.

To analyse the migrating capability of the cells, a transwell migration assay was performed. Chambers for transwell migration assays consist of a 24 well plate filled with a chemoattractant and respective insert. Inserts separate the lower chamber from the upper chamber which contains the cells and allowed to migrate through 8 µ pores. 2×10^4 cells (~200 µl) of control, pcDNA3.1 (mock, EV) and pcDNA3.1-ATIP1 overexpressed cells from LNT-229 and LN-308 were collected in serum reduced media and seeded into the upper chamber of 8 µ transwell inserts (Corning, NY, USA). For Matrigel invasion, 2×10^4 cells (~200 µl) were plated into

Matrigel-coated inserts (Corning, NY, USA) in serum reduced media. The lower chamber in both assays is filled with 500 µl NIH/3T3 conditioned media (CM) to serve as a chemoattractant. The CM was obtained 48 h after seeding 10×10^6 NIH/3T3 mouse fibroblast cells in 20 ml of complete culture medium, clarified from cell debris by centrifugation (1200 rpm, 5 min), and stored at -80°C. The plates were incubated at 37°C and allowed to grow for 20 hours for migration and 36 hours for the invasion assay. Post incubation the cells were fixed with ice-cold methanol for 10 min, stained with 1% hematoxylin for 10 min and washed with water. The membranes were cut with a scalpel and embedded in the mounting medium on a microscopic slide covered with a glass coverslip and observed under a light microscope to analyse the migration and invasion of the cells. The migrated and invaded cells were counted from images at 10 fold magnification (5 visual fields per membrane) with ImageJ software.

2.2.10.4 Clonogenic survival assay.

The efficiency of single cancer cells to grow into colonies was analysed by seeding, control and stably expressing EV and ATIP1 overexpressing LNT-229 (500 cells) and LN-308 (1000 cells). Cells were seeded in 6 well plates per well and allowed to grow in G418 selection media. The cells were allowed to grow for 12-15 days when the colonies became visible (~ >50 cells) and media was changed every 3 days. Further, cells were stained with crystal violet and counted using ImageJ software.

2.2.10.5 Crystal violet staining

The density of adherent growing cells was quantified by crystal violet staining. The medium was aspirated and fixed with 4% paraformaldehyde for 10 mins. Crystal violet staining solution (0.5% crystal violet, 20% methanol) was added, after 5 min of incubation the staining solution was removed and the cell culture plates were washed with tap water. After drying, sodium

citrate (0.1 M sodium citrate, 50% ethanol) was added, and absorbance was measured at 560 nm using a Multiscan ELISA reader.

2.2.10.6 Cell viability (MTT) assay

To analyse cell viability, a thiazolyl blue tetrazolium bromide (MTT) assay was performed which examines the mitochondrial activity of viable cells. Soluble MTT is converted into insoluble formazan by intracellular NAD(P)H-dependent oxidoreductases in viable cells. In this regard, MTT was added to the cell culture medium at a final concentration of 500 µg/ml. Upon the formation of blue formazan crystals (after ~ 4 h incubation at 37°C) the medium was removed, DMSO was added to solve the formazan crystals and absorbance was measured at 570 nm using a Multiscan ELISA reader.

2.2.10.7 Focal adhesion complex analysis using double immunofluorescence.

To visualize the effect of ATIP1 in cancer cell migration and invasion we analysed the focal adhesion complex. $1x10^5$ LNT-229 and LN-308 EV and ATIP1 overexpressing cells were seeded on coverslips coated with poly-L-Lysine in 12-well plates. Post 48 hours the cells were fixed with 4% paraformaldehyde for 10 min at room temperature, the cells were washed with PBS + 0.25% Triton-X-100 for 2 mins at room temperature to perforate the cells. The cells were washed with PBS and blocked with 2% BSA at room temperature for 1 hour. Further, the cells were incubated with vinculin antibody (1:100) in blocking solution at 4°C overnight. For localizing of focal adhesions, Alexa Flour 488 coupled goat anti-rabbit IgG antibody was used (1 h, RT). The secondary antibody was diluted as recommended by the manufacturer. Staining was accomplished using the Actin Cytoskeleton and Focal Adhesion Staining Kit (Millipore, Schwalbach, Germany), which allows the detection of actin filaments (by phalloidin), or focal contacts (by vinculin antibody) as well as of the nucleus (DAPI). Finally, the coverslips with

cells were mounted on slides with DAPI containing VECTASHIELD Antifade mounting medium. Quantification of migration, invasion and adhesion (focal adhesion complexes and of vinculin-positive cells) was done using Image J software [69].

2.2.10.8 siRNA transfection.

To knock down *MTUS1*, LNT-229 or LN-308 cells at 60-80% confluency were transfected with either 50 nM of control non-target or *MTUS1* siRNA mixes (Santa Cruz Biotechnology, Texas, USA) containing a mix of three to five different siRNAs using the Viromer Blue transfection reagent (Biontech, Mainz, Germany). Whole-cell lysates were prepared from the transfected cells 72 hours later.

2.2.10.9 Cell cycle analysis

The number of cells were determined in each phase of the cell cycle (G1, S or G2-M), LNT-229 and LN-308 EV and ATIP1 overexpressing cells were seeded in 60 mm plates. After 48 h the cells were washed in PBS, trypsinized and washed again with PBS. The cells were fixed in 70 % ice-cold ethanol (overnight, 4°C). Further, the cells were washed twice with PBS, to stain the DNA the cells were washed twice with flow cytometry buffer and incubated in dark with PI/RNase A buffer (50 µg/ml PI, 100 µg/ml RNase A in flow cytometry buffer; 30 min). The cells in different phases were analysed using a CyAn ADP flow cytometer. Analyses were performed on a CyAn ADP flow cytometer and analysed using FlowJo software (FlowJoLCC, BD Life Sciences, Heidelberg, Germany).

2.2.11 Animal experiments

2.2.11.1 Xenograft mice model for survival analysis

These experiments were conducted in accordance with appropriate guidelines and approved by the regional ethics committee in Tübingen, Germany (permit number N10-18G). Athymic four-

six-week-old female NMRi-FoxN1^{nu}/FOXN1^{nu} mice were procured from Janvier (Le Genest-Saint-Isle, France). For survival analysis, we used 16 animals in total (8 animals per cohort) and in addition, we used 3 animals in a separate cohort that were analysed for immunohistochemistry.

Mice were stereotactically implanted with 2 × 10^4 LNT229-pcDNA3.1 (Sham cohort, n=11) or LNT-229-pcDNA3.1-ATIP1 stably transfected glioma cells (ATIP1 overexpressed cohort, n=11) into the right striatum. The cells were diluted in 2 µl of PBS and implanted with an injection rate of 1 µl/min using the following coordinates: 2 mm right, 1 mm frontal of bregma and 3 mm depth using Hamilton syringe [70]. Survival was determined by the generation of Kaplan-Meier survival curves (n=8) and histological studies (n=3) were performed as mentioned above. The mice were sacrificed as soon as they developed weight loss, neurological or tumor-associated symptoms. For immunohistochemical analyses, the mice were sacrificed three weeks after intracranial implantation of the tumor cells.

2.11.2 Stereotactic intracranial tumor implantation for TMZ treatment

These animal experiments were approved by the Committee for the Purpose of Control and Supervision of Experiments on Animals (CPCSEA), Government of India and with permission of the Institutional Animal Ethics Committee (IAEC), University of Hyderabad. Experimental Wistar rats (220-275g) were procured from the National Institute of Nutrition (NIN), Hyderabad, India. Rats were anesthetized by intraperitoneal injection of xylazine and ketamine, 10mg/kg and 50mg/kg respectively. Stereotaxic implantation was performed as described previously [71]. Briefly, the rats were stabilized in the stereotactic apparatus and a scalp incision was performed. C6 rat glioma cell suspension (1 × 10^5 cells in 10ul DMEM) was injected through a drilled burr hole using a Hamilton syringe and the cavity was filled with dental cement. On the 7th day of implantation, two rats were randomly selected, sacrificed and

screened for the presence of tumors by H&E staining. Rats were further divided into sham and TMZ treated cohorts (n=6), rats were treated by i.p injections of TMZ (10mg/kg) on alternate days for three doses based on existing literature [72]. Sham rats were treated with 10% DMSO saline (vehicle). Animals were sacrificed on the 14th day of tumor implantation, perfused with ice-cold PBS followed by in situ fixation with 4% PFA. Brain tissues were further harvested and used for histology and immunohistochemical analysis.

2.11 Radio sensitivity analysis

2.11.1 Clonogenic assay post irradiation

To determine the effect of *MTUS1*/ATIP1 on the glioma cell´s sensitivity towards irradiation, ATIP1 overexpressing or control cells as well as LNT-229-p53^{ts} cells (grown at 32.5°C or 38°C) were irradiated using a Gammacell GC-40 exactor (Nordion, Ontario, Canada). The cells were plated in 6 well plates and further divided and irradiated with 1Gy, 2Gy, and 4Gy. Post irradiation the cells were allowed to grow in optimal conditions (32.5°C or 38.5°C) and the clonogenic abilities of the irradiated cells were analysed. Cell viability was assessed by incubating the cells in methyl-thiazole tetrazolium (MTT, 5mg/ml) for 4 h at 37°C as described above. To analyse the expression of ATIP1 post-irradiation the lysates were made at represented time points after 4Gy irradiation.

2.11.2 Role of *MTUS1*/ATIP1 in DNA repair

To determine the effect of ATIP1 on the glioma cell´s sensitivity towards irradiation, ATIP1 overexpressing or EV control cells as well as LNT-229-p53^{ts} cells (grown at 32.5°C or 38°C) were irradiated using a Gammacell GC-40 exactor (Nordion, Ontario, Canada). To determine clonogenic survival, the cells were seeded as described above. Cell viability was assessed by incubating the cells in methyl-thiazole tetrazolium (MTT, 5 mg/ml) for 4 h at 37° C, the

formazan crystals thus formed were solubilized in DMSO and absorbance was measured at 570 nm. To investigate the dynamics of Histone H2A.X phosphorylation (γH2A.X) after irradiation, the cells were stained using an anti-phospho^{S139}-H2A.X (Ser139) antibody (Millipore, Schwalbach, Germany). Briefly, the cells were fixed with 2% PFA for 10 mins at represented time periods and washed with PBS. Cells were perforated with PBS+0.2% Triton-X-100 for 10 mins, washed with PBS and subjected for blocking with 2% BSA for 45 mins at RT. Further, the cells were probed with pH2A.X primary antibody (Millipore, Schwalbach, Germany) in 1:300 dilution. After primary antibody incubation, the cells were washed with 1x PBS for 15 mins at RT followed by incubation with secondary antibody (Millipore, Schwalbach, Germany) for 1 hour at RT. The cells were washed with 1x PBS and mounted with antifade reagent vectashield with DAPI (Vector Laboratories, CA, USA). All the images were captured with a laser scanning confocal microscope (Carl Zeiss LSM 510). Quantification of phospho-γH2A.X foci, representing DNA double-strand breaks, was performed using Image J software.

2.12 Data acquisition and statistical analysis.

For survival analysis in human cohorts, the "R2: Genomics Analysis and visualization" platform (https://hgserver1.amc.nl/cgi-bin/r2/main.cgi) was used. All experiments were performed independently at least thrice unless mentioned otherwise. Statistical analysis was performed using multiple pairwise comparisons for *in vitro* data. The Log-rank (Mantel-Cox) test was implemented for *in vivo* survival analysis using GraphPad Prism version 8. Statistical comparisons were made using the student's two tailed-unpaired *t*-tests. Correlation analysis between p-ERK and ATIP1 relative expression was performed using the parametric Pearson's test. Results are represented as mean ± standard error mean (SEM). *P*-values of <0.05 are considered as statistically significant (ns: not significant; * $P < 0.05$, ** $P < 0.01$, *** $P < 0.001$, **** $P < 0.0001$).

Chapter 3

Microtubule Associated Tumor Suppressor 1 (*MTUS1*) gene regulation in glioma: epigenetic aspect

3.1 Introduction

3.1.1 Tumor suppressor genes (TSG)

Genes related to cancer can be classified under two categories of proto-oncogenes and tumor suppressor genes (TSGs). Proto-oncogenes are broadly convoluted with the pathways which regulate cell growth. Mutations and alterations in these genes result in the transformation of normal cells into cancerous cells. Proto-oncogenes harbours dominant mutations and the mutated variants are recognised as oncogenes [73]. Tumor suppressors are the crucial genes that regulate several cellular functions in cell growth, cell proliferation, cell cycle progression, DNA repair mechanisms and other crucial cellular functions. Dysfunctional TSG often results in dysregulated cell growth which is a crucial mechanism for cancer development [74].

As mentioned earlier, cancer results from an aggregation of genetic and epigenetic changes in two varieties of genes i.e. TSG and proto-oncogenes, linking the cell cycle control to tumorigenesis. Genetic alterations comprises genetic mutations, genomic instability, loss of heterozygosity and gene copy number variations (CNV) [75]. Whereas, epigenetic mutations include histone modifications, DNA methylation and loss of imprinting (LOI). These alterations result in the inactivation of tumor suppressor genes and activation of dominant oncogenes culminating in carcinogenesis. Loss of function mutations in TSG has been identified in various cancers including lung, ovarian, pancreatic, uterine head and neck, breast and bladder cancer [76-79]. Inactivation of tumor suppressor results in loss of function i.e both maternal and paternal copies of a genes coding for the tumor suppressor must be altered for tumorigenesis to occur.

3.1.2 Types of tumor suppressor

TSGs can be broadly classified into five types based on their functions [74], a. genes encoding intracellular proteins which are crucial in regulation of cell cycle (e.g., pRB and p16) [80]. b. genes which encodes receptors or signal transducers responsible for coordinating the signals that inhibit cell proliferation [e.g., adenomatous polyposis coli (APC) and transforming growth factor (TGF)-β] [81] c. genes that encode the checkpoint-control proteins, which are useful in inducing cell cycle arrest in case of DNA damage or chromosomal defects [e.g., p16, p14, and breast cancer type 1 susceptibility protein (BRCA1)] [82] d. genes encoding proteins appropriate for the induction of apoptosis (e.g., p53) [83] e. genes which encodes proteins involved in DNA repair [e.g., DNA mismatch repair protein 2 (MSH2) and p53] [84].

3.1.3 Microtubule-Associated Tumor Suppressor

The expression of the tumor suppressor gene, microtubule-associated tumor suppressor (*MTUS1*) has been reported to be lost in various cancer types like colon, ovarian, pancreas, bladder, gastric and lung cancer [85, 86]. *MTUS1* encodes a family of angiotensin II (AT2) receptor-interacting proteins (ATIP). Alternative splicing results in five different isoforms of ATIP (ATIP1, ATIP2, ATIP3a, ATIP3b, and ATIP4) [64, 87, 88]. Angiotensin II (AngII) is the active end product of the Renin-Angiotensin System (RAS), responsible to maintain vascular integrity throughout the body [89]. There are two main receptors for AngII, AngII type I receptor (AT_1R) and type 2 receptor (AT_2R) belonging to G-Protein Coupled Receptor (GPCR). AT_1R is responsible to modulate the blood pressure, stress response, cellular growth and proliferation and whereas the role of AT_2R remains unclear in many physiological and pathophysiological situations but, it counteracts AT_1R by promoting vasodilation, apoptosis and antigrowth effects [90] (Figure 3).

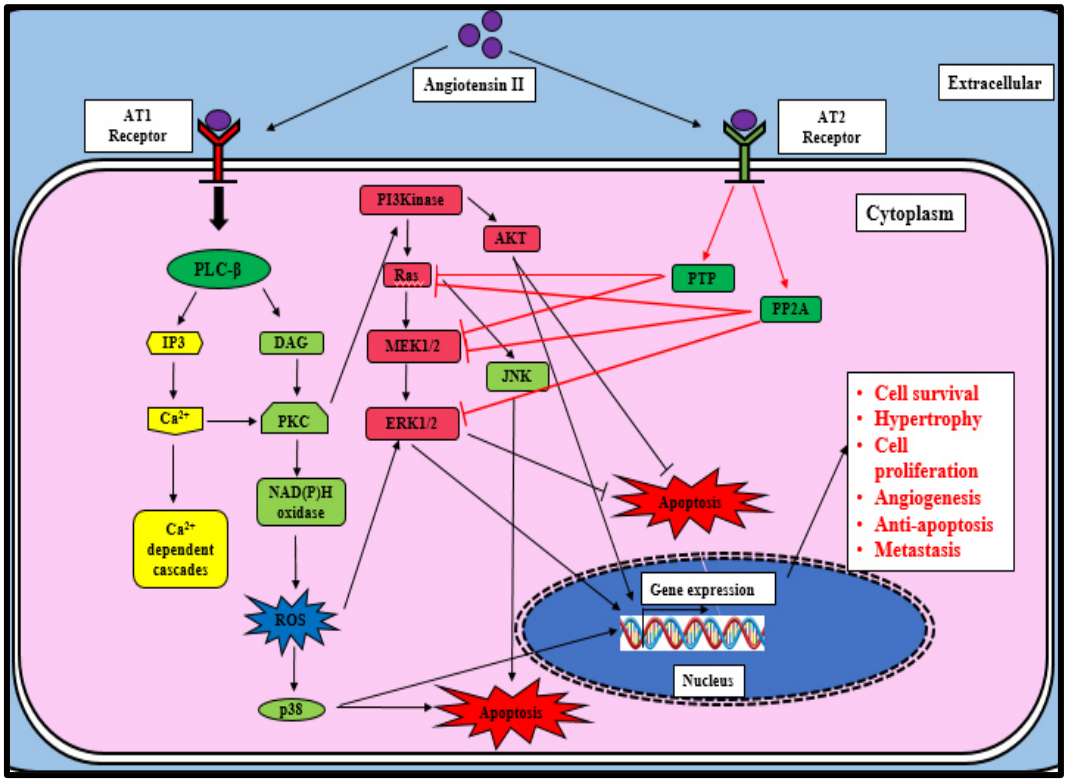

Figure 5. Schematic representation of Renin Angiotensin Aldosterone System (RAAS). RAAS pathway consists of two receptors AT1 and AT2 antagonistic to each other. The AT1 receptor-mediated pathway is responsible for the inhibition of apoptosis and results in cancer progression. Whereas AT2 receptor signalling results in inhibition of progression of apoptosis by inhibiting AT1 signalling pathway hence inhibits cancer progression.

Besides the important role of maintaining vascular integrity and homeostasis at the level of the angiotensin II (AngII)/angiotensin receptor system (AT_xR) through the Renin Angiotensin Aldosterone System (RAAS) [89], RAAS also plays a crucial role in cancer biology and affects tumor growth by remodeling the tumor microenvironment [91]. In oral squamous cell carcinoma, ATIP1 is regulated by p53 and inhibits epidermal growth factor (EGF) mediated ERK phosphorylation, cell proliferation and migration, indicating that ATIP1 serves as a tumor suppressor [92, 93]. In the central nervous system (CNS), ATIP1 is the most abundant transcript expressed in all brain regions except the cerebellum and fetal brain and is involved

in neural differentiation [64, 94, 95], suggesting that it might play a crucial role in physiological functions via different intracellular mechanisms. Recent studies have shown that after angiotensin II receptor (AT_2R) stimulation, ATIP1 interacts with the Src homology region 2 domain-containing phosphatase-1 (SHP-1). This complex is translocated to the nucleus where it transactivates the ubiquitin-conjugating enzyme methyl methanesulfonate sensitive 2 (*MMS2/UBE2V2*), involved in the error-free-post-replication repair pathway [96].

3.2 Epigenetics

At the genome level, GBM characteristics are regulated at the genetic and epigenetic level, this may contribute to the heterogeneity of GBM cell populations. In tumor cells, alterations in the genome are always detectable in the form of deletions, amplifications or mutations [97]. Epigenetics refers to the heritable traits without alterations in the DNA sequence. Epigenetic alterations are a result of multiple collaborative regulatory pathways such as DNA methylation, DNA binding transcription factors, long-non-coding RNAs (lncRNAs), ATP dependent nucleosome remodelling and post-translational modification (PTM) of histone proteins [98]. Once these epigenetic patterns are resolved, they have propagated separately over several cell generations in a highly co-ordinated manner. These epigenetic marks are linked to the regulation of gene expression and their alterations play an important role in tumorigenesis, although very little is known about the mechanisms underlying these alterations [99, 100].

3.2.1 DNA methylation

Covalent transfer of a methyl group to a DNA base results to the phenomena of DNA methylation leading to epigenetic modifications in the DNA. DNA methylation is chemically stable, which makes it a reliable way to transmit epigenetic information to regulate appropriate gene expression [101]. Methylation on cytosine orchestrate an fundamental role in genome

regulation and modifications in DNA methylation. In cancer, these modifications include hypomethylation of oncogenes and hypermethylation of tumor suppressor genes [102, 103]. The standard way for detection of m5C is bisulfite sequencing which represents methylation at specific base pairs in the genome or area of interest. Currently, methylation alterations are understood to develop in cancerous tissues all together with changes in normal tissue differentiation [104]. Methylation of a CpG site within or near a gene is able to alter its expression. Methylation in DNA is mediated by DNA methyltransferases (DNMTs), which comprises three proteins distributed into two families, based on their role in *de novo* methylation (DNMT3A and DNMT3B) or in the conservation of methylation marks (DNMT1) [101]. DNMT3A and DNMT3B are responsible for establishing the methylation pattern during early development and the patterns of methylated and unmethylated CpGs are propagated from generation to generation with the help of DNMT1 [105-107]. Deregulation of either of the major DNMTs (DNMT1, DNMT3a, DNMT3b) causes global demethylation and can lead to death in mice [108] and in human cancer cells, disruption of DNMT1 consequently results in irregular progression of the cell cycle [109].

DNA methylation pattern in promoter region of MGMT (O6-methylguanine-DNA-methyltransferase) gene was shown to be a prognostic marker for GBM patients treated with TMZ. Patients with silenced MGMT gene expression due to promoter hypermethylation were found to have a favourable outcome, as compared to patients with an unmethylated MGMT promoter. Hypermethylation modifications are perhaps excellent tumor markers and based on their unpredictable nature of epigenetic gene silencing makes this process an alluring target for cancer therapy [110].

3.2.2 Post-translational modifications

The other major form of epigenetic modification includes covalent post-translational modifications of histone proteins. Histones are principal protein components of chromatin and DNA wraps around these proteins, harbouring post-translational modifications. These modifications are carried out by the histone-modifying enzyme complexes influencing the overall chromatin structure and triggering functional consequences. There are several types of post-translational modifications including acetylation, methylation, ubiquitination, SUMOylation, citrullination [111]. The central regulators responsible for these modifications are histone deacetylases (HDACs), histone acetyltransferases (HATs) and methyltransferases. Core histones H2A, H2B, H3 and H4 together form nucleosome particles that package 147bp of DNA and the linker-histone H1 packages more DNA between core particles resulting in chromatin [112].

The eukaryotic genomes are a result of highly compact nucleosome particles which affect gene expression and chromatin-related processes. To overcome this limitation, histone acetylation plays a crucial role to open the chromatin structure which makes the DNA templates in the chromatin accessible for the transcription machinery. Acetylation is the best-studied post-translational modification, which is reversible modifications of specific residues in histone tails executed by HATs and HDACs. Dysregulations in these mechanisms results in abnormal gene expression and tumorigenesis [113].

In this objective we tried to understand the expression regulation of *MTUS1*/ATIP1 in glioma, using the databases and clinical glioma samples. We were also able to analyse the probable mechanisms involved in *MTUS1*/ATIP1 deregulation.

3. 3 Results

3.3.1 Assessment of *MTUS1*/ATIP1 expression in glioma.

In order to analyse the role of ATIP1 in glioma progression, we assessed the ATIP1 expression at the transcriptional and translational levels. We found that ATIP1 mRNA was significantly downregulated in different grades of human glioma specimens when compared with normal human brain samples, this correlates well with reduced levels of ATIP1 at the protein level. Additionally, ATIP1 expression, as well as that of the ATIP1 upstream (*SHP-1*) and downstream regulator *(MMS2/UBE2V2)* proteins, correlated with glioma progression. In HGG these genes were downregulated approximately threefold compared to normal brain tissue (Figure 1a–c, Table 1).

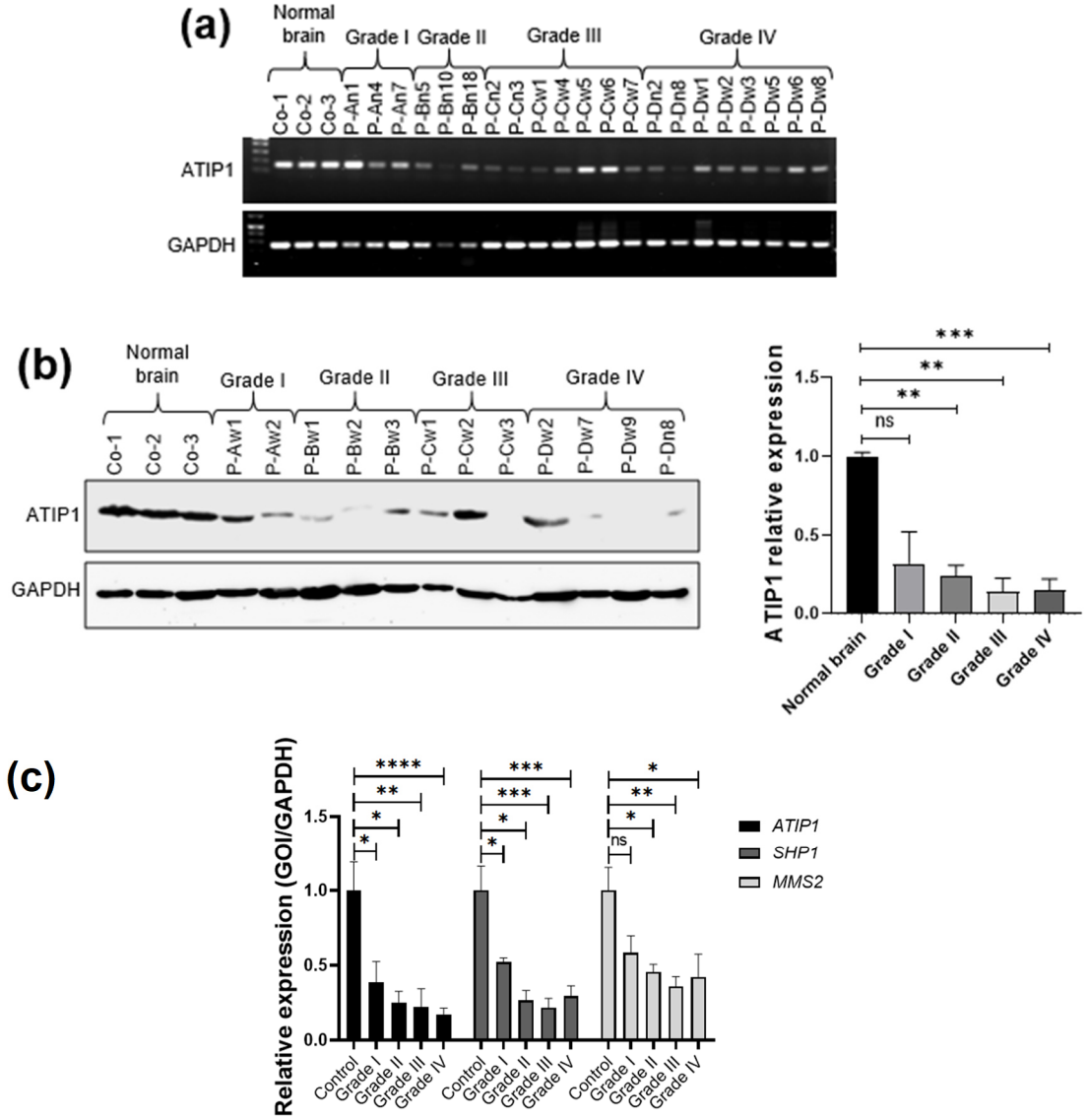

Figure 6. ATIP1 expression in normal human brain and different grades of glioma. (a). mRNA was isolated from different grades of glioma specimen and RT-PCR was performed (b) protein was isolated from respective glioma specimen and normal brain samples. Further the samples were subjected for western blot to analyse relative ATIP1 expression is respective samples and quantification in different WHO grades of glioma specimen and normal brain (normal brain, n=4; grade I, n=6; grade II, n=27; grade III, n=20; grade IV, n=23). (c). q-RT-PCR of *ATIP1* (left), *SHP1* (middle) and *MMS2* (right) in the normal human brain (control; n = 5) or glioma specimen of different WHO grades (grade I, n = 6; grade II, n = 12; grade III, n = 15; grade IV, n = 15) (n = 3, SEM; ns: not significant; * $p < 0.05$, ** $p < 0.01$, *** $p < 0.001$, *** $p < 0.001$, **** $p < 0.0001$).

3.3.2 ATIP1 expression in pilocytic, diffuse astrocytoma and recurrent gliomas

To understand the expression profile of ATIP1 in the clinical samples, although not significant, we observed a trend towards lower ATIP1 expression in diffuse glioma grades specimen (grade II-IV, n = 70) as compared to the pilocytic astrocytoma specimens (grade I, n = 6) (Figure 7a). ATIP1 expression was reduced in recurrent glioma of all WHO grades when compared to the original tumors (Figure 7b), although the difference was not significant. In order to analyse the effects of IDH mutations on ATIP1 expression, we performed a correlation analysis and found that ATIP1 was downregulated in both IDH^{WT} and IDH^{mut} HGG compared to low-grade glioma (LGG) of the same IDH status (Figure 7c, Table 5). We also correlated MGMT promoter methylation data from our GSC and glioma cell lines with ATIP1 expression. Interestingly, cells harboring a methylated MGMT promoter showed higher ATIP1 expression compared to cells presenting an unmethylated MGMT promoter (Fig. S1c, Table S2).

Table 5. p53, IDH and MGMT status of glioma cell lines [114-118]

Cells	p53	IDH	MGMT
LK7	WT	WT	u
LK28	WT	WT	m
LK31	WT	WT	m
R11	WT	WT	m
R28	WT	WT	u
LN-18	mut.	WT	u
LNT-229	WT	WT	m
LN-308	del.	WT	m
U87-MG	WT	WT	m

WT: wild type; mut: mutated; del: deleted; u: unmethylated; m: methylated

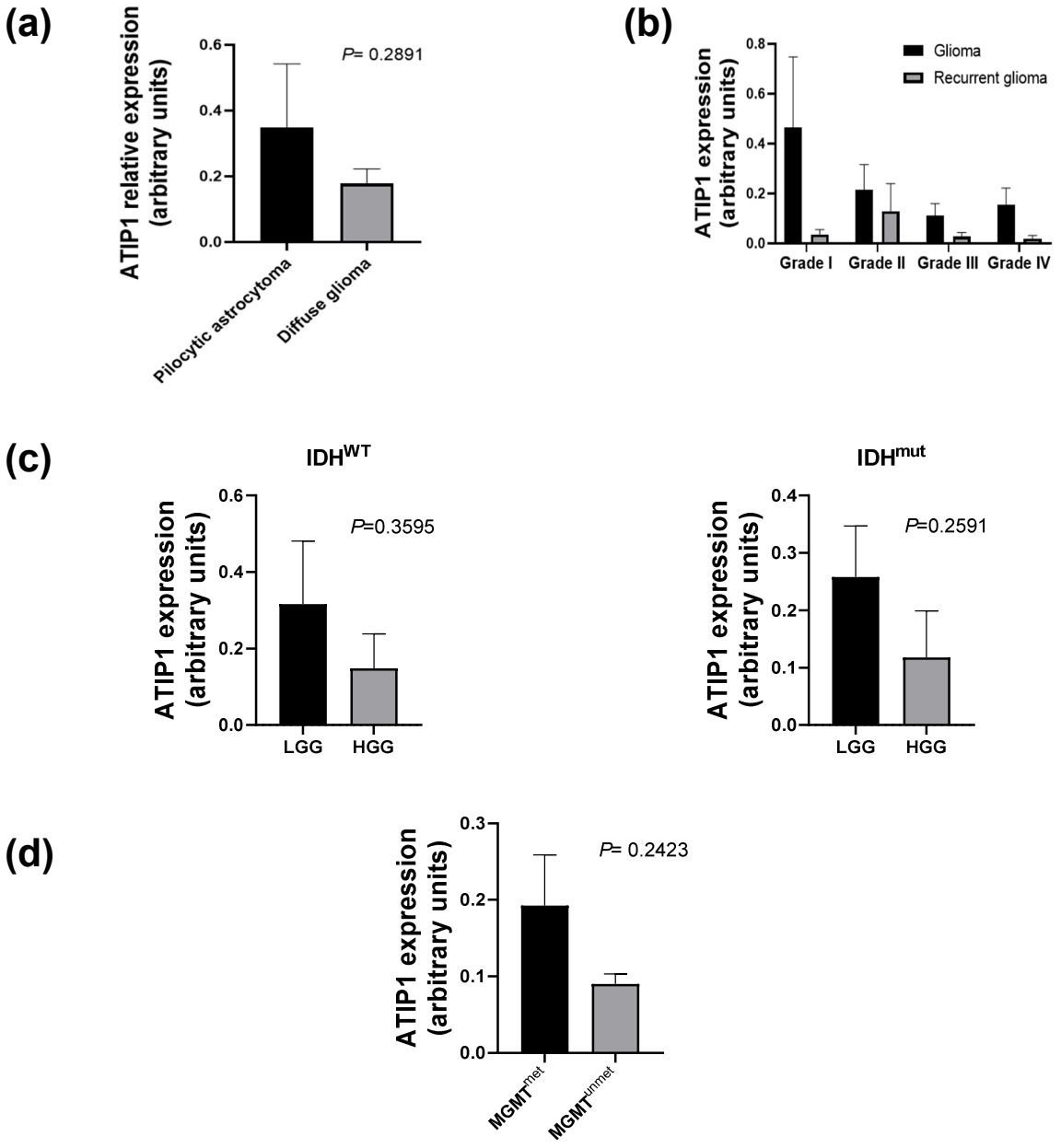

Figure 7. ATIP1 expression in glioma grades and recurrent gliomas (a). Immunoblot-based quantification of ATIP1 expression in pilocytic glioma (n = 6) and diffuse glioma (grades II-IV, n = 70). (b). ATIP1 protein expression in the tissue of original and recurrent glioma samples of different WHO grades as determined by immunoblot. (**c**)ATIP1 expression in IDH^{WT} LGG (n=10); HGG (n=12) and IDH^{mut} LGG (n=15); HGG (n=21) specimen. c. ATIP1 expression in MGMT methylated (n=6) and MGMT unmethylated promoter (n=3), patient-derived GSC and established glioma cell lines.

3.3.3 Data analysis and database mining

To determine whether elevated ATIP1-expression correlates to better survival we used the R2-database. With a p-value of 0.064, lower ATIP1 mRNA levels in human glioma correlate with a worse outcome (Figure 8a). We also determined whether lower ATIP1 expression in our cohort of glioma is associated with worse survival. Even being not significant due to the small number of cases in the ATIP1^{high} cohort, ATIP1^{high} glioma patients showed a slight trend towards a prolongated median survival (median survival not reached so far) compared to ATIP1$^{intermediate/low}$ patients (48 months) (Figure 8b).

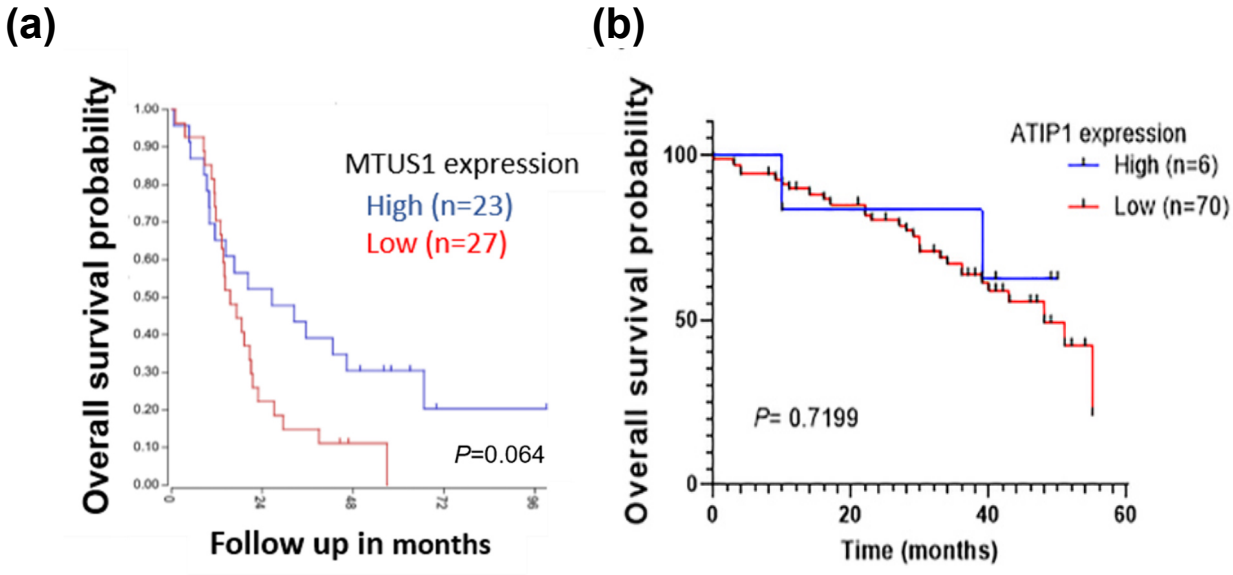

Figure 8. Kaplan-Meier survival curve of glioma patients from R2 database and Indian cohort. a. Overall survival probability of glioma patients determined by R2 database mining of glioma samples. Higher *MTUS1* expression (n=23) results in better survival compared to patients presenting low *MTUS1* expression (n=27). b. Overall survival analysis of glioma patients comparing ATIP1^{high} (n=6) and ATIP1$^{intermediate/low}$ patients (n=70, Log-Rank Mantel-Cox test).

Using the R2 database as well as the Indian cohort of glioma patients, we also determined whether in glioma patients there are age- or gender-specific differences in *MTUS1*/ATIP1 expression. We detected no significant gender or age-related changes in *MTUS1*/ATIP1 expression (Figure 9a/b). We also analysed the ATIP1 expression correlation with age and gender-specific differences in the Indian cohort as well, however, putatively due to the low number of patients in each group, no significant correlation of gender- or age-specific ATIP1 expression with patient´s survival was observed. Interestingly, in the group of elderly (>65 years) that harbor mainly HGG, no ATIP1^{high} patient was present (Figure 9c/d).

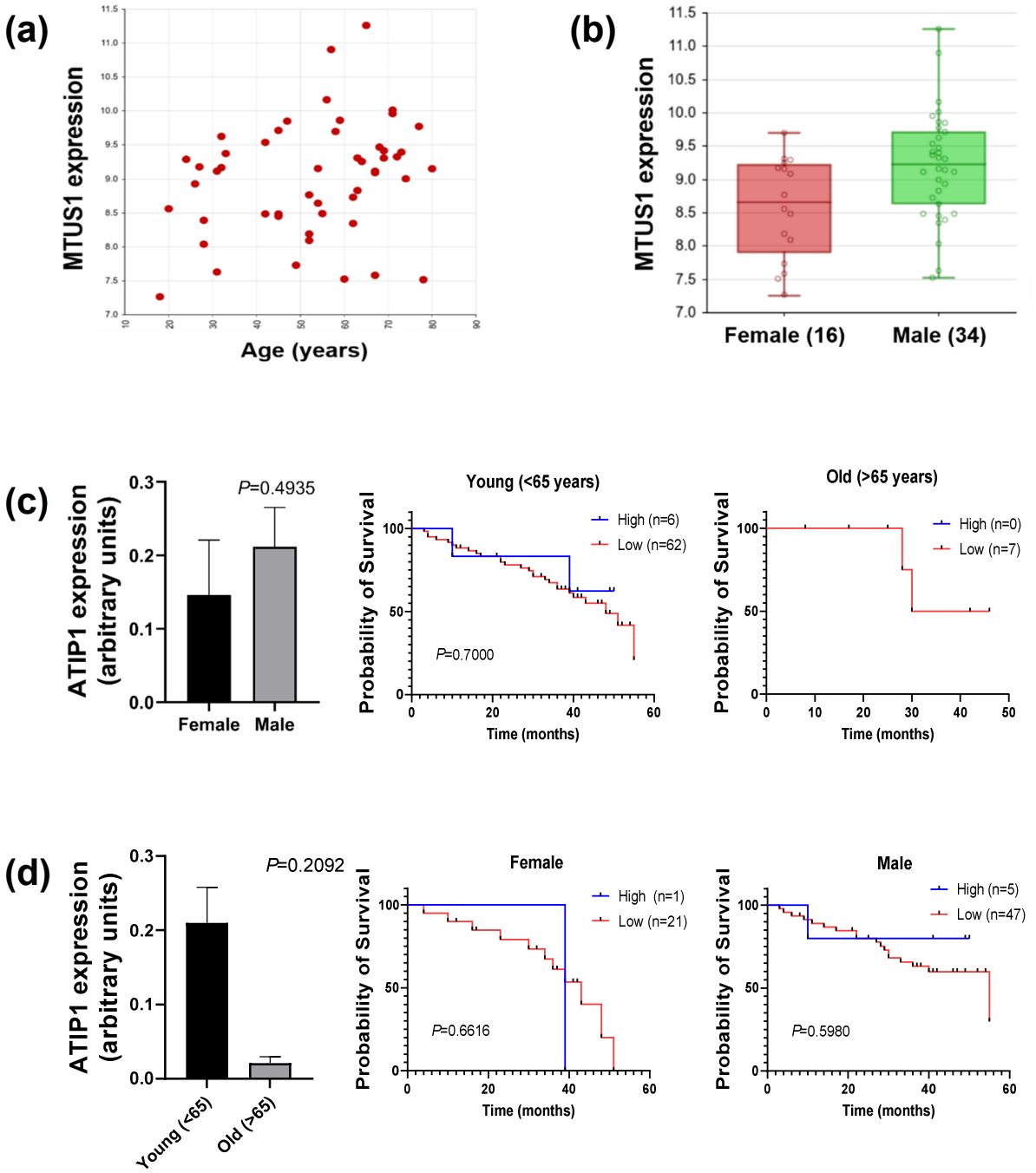

Figure 9. Kaplan-Meier survival curve of the India cohort of glioma patients. a. *MTUS1*/ATIP1 expression does not correlate to the age of glioma patients from the R2 database. b. Gender-related expression of *MTUS1*/ATIP1 in glioma patients from the R2 database. c. MTUS1 expression in younger (<65) and older (>65) glioma patients does not correlate with survival. d. MTUS1 expression in male and female glioma patients does not correlate with survival.

3.3.4 Histological analysis

The histological analysis affirms the high instance of microvascular haemorrhages, proliferation and invasion in the HGG and immunohistochemistry analysis reasserts the characteristic feature of glioma progression which is a higher expression of Ki67 and GFAP in HGG as compared to the control and LGG. In glioma specimens of different WHO grades, ATIP1 was downregulated in a grade-dependent manner indicating that downregulation of ATIP1 is correlated with an elevated malignancy of glioma (Figure 10).

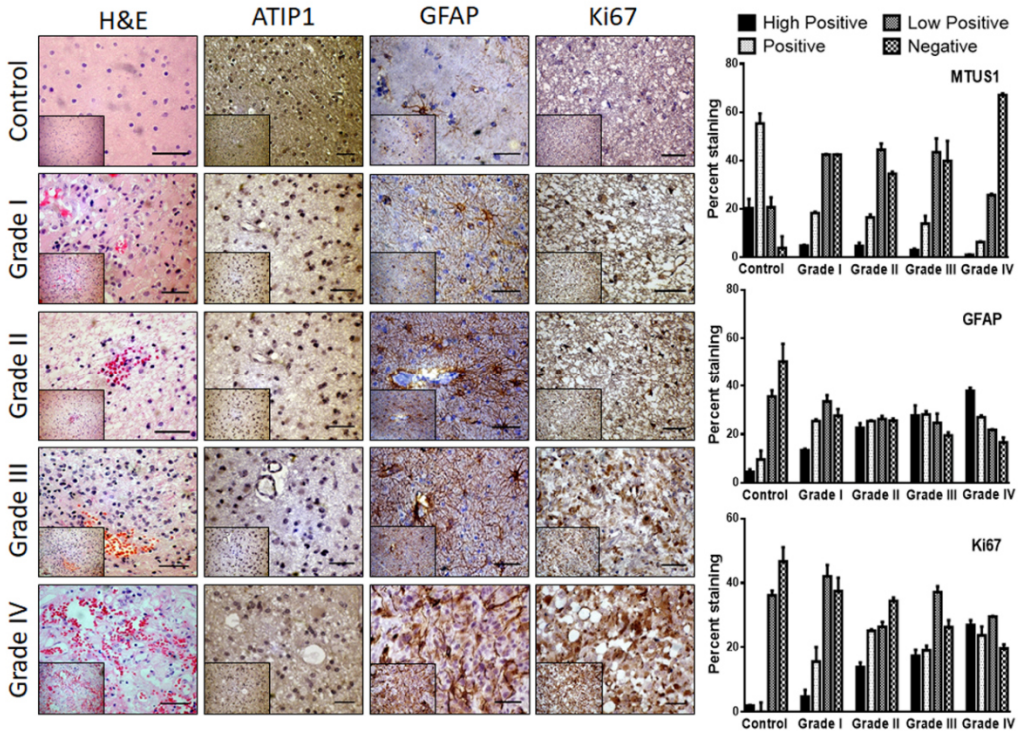

Figure 10. Histological studies with clinical glioma samples. Photomicrographs representing histopathological analysis in the normal human brain and glioma tissue sections by using H&E staining represents microvascular hemorrhages and vascularization in higher grades of glioma and immunohistochemical staining of MTUS1, GFAP (Astrocytes), Ki67 (proliferation marker) protein expression is depicted. Quantification analysis represents the percent staining of the respective proteins in glioma tissues as compared to the normal brain tissue. Scale bars represent 100μm.

3.3.5 ATIP1 expression in normal human brain cells and GSC

In order to validate ATIP1 downregulation in glioma, we analysed its expression in a panel of GSC's (LK7, LK28, LK31, R11, and R28), established glioma cell lines (U87-MG, LNT-229 and LN-308) and normal human brain cells (astrocytes and HBMvEC), significant downregulation of ATIP1 is observed mainly in GSC's as compared to the normal brain cells. However, there was no decrease in ATIP1 expression in the established glioma cell lines (Figure 11).

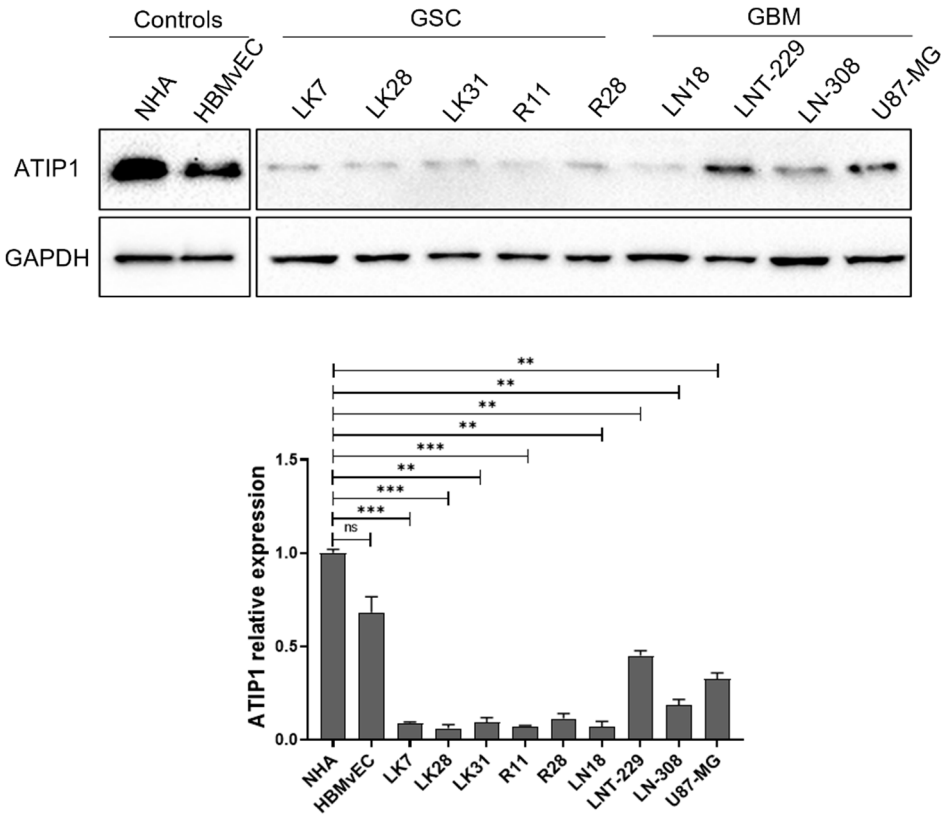

Figure 11. ATIP1 expression in GSCs and cell lines. ATIP1 protein expression in low passage GSC, glioma cells (GBM) and non-neoplastic control cells of brain origin (NHA: Normal Human Astrocytes, HBMvEC: Human Brain Microvascular Endothelial Cells; n=3, one representative experiment is shown). **b**. Quantification of ATIP1 protein expression in GBM, GSC and control cells (n=3, SEM; ns: not significant, ** $P < 0.01$, *** $P < 0.001$).

3.3.3 CpG island identification and bisulfite sequencing

Since the downregulation of TSG in cancer cells is often provoked by hypermethylation of their promoter region, we examined whether the downregulation of ATIP1 expression in glioma might be provoked by elevated methylation of the *MTUS1* promoter. For this, we first examined the methylation status of the 5´upstream *MTUS1*-TSS region. Using the MethPrimer software we identified an approximately 1000 bp long CpG island upstream of the MTUS1 coding region. After bisulfite conversion, we amplified this region except for the most proximal 200 bp of the TSS region which we, unfortunately, were not able to amplify (Figure 12a). We analysed 57 CpG (blue, proximal part) and 41 CpG (green, distal part) sites in the CpG island (Fig. 2D). Methylation pattern analysis (SRA accession ID: PRJNA633153) reveals that the tested non-neoplastic cells (NHA, HBMvEC) presented hypo-methylation in this region whilst GSC (LK7, LK28, R11, R28) and GBM cells (LNT-229, LN-308) showed elevated methylation, being the methylation pattern in the proximal part of the CpG island more variable (Figure 12b).

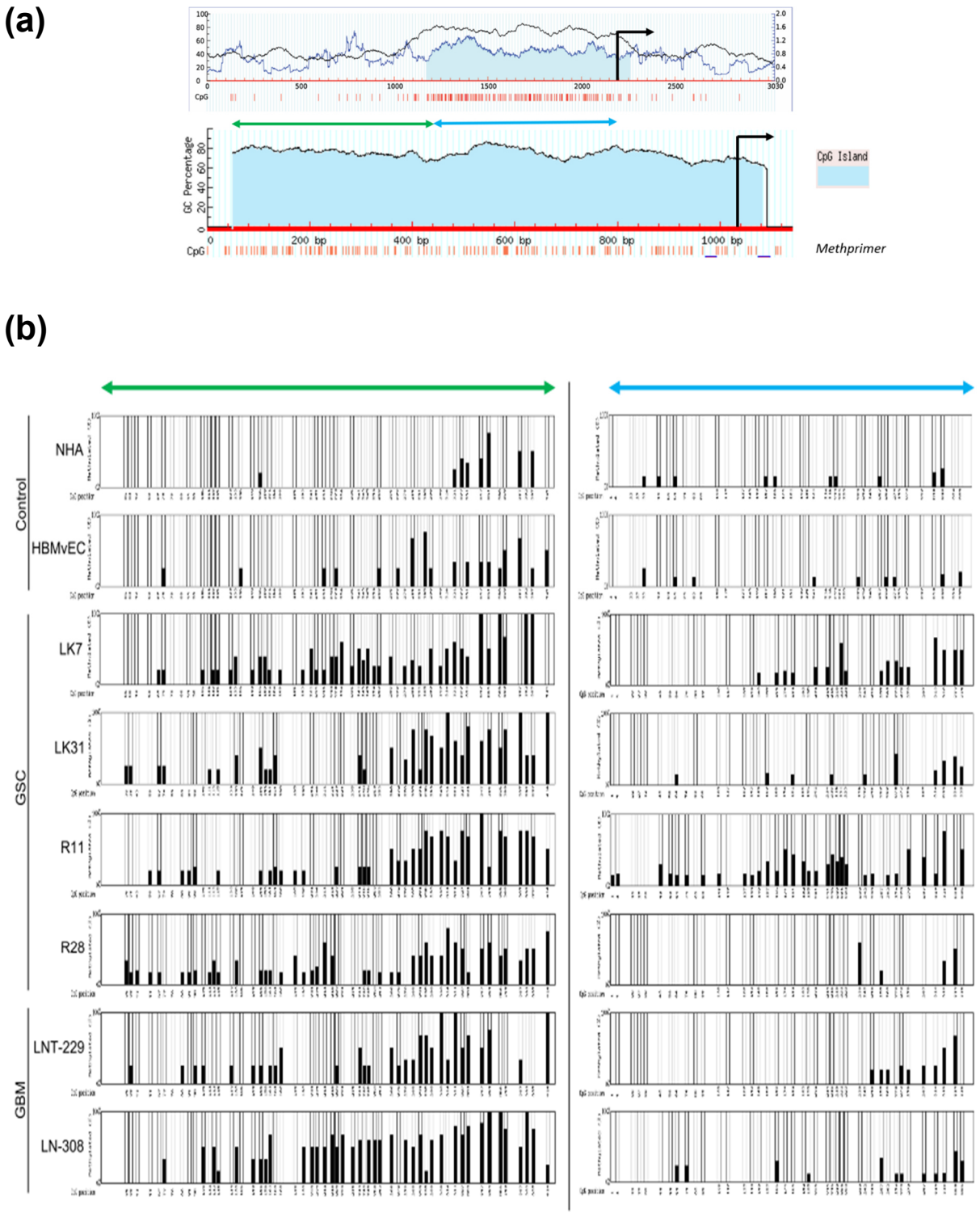

Figure 12. In glioma cells, the MTUS1 promoter region shows hypermethylation. a. Localization of a predicted CpG island in the 5′ upstream *MTUS1*-TSS region (red). The green and blue labelled regions were analysed for BSS and indicate the proximal (blue, 57 CpG) and distal (green, 41 CpG) part of the CpG island. b. Percentage of methylation in non-neoplastic primary brain cells (control), low passage GSC and glioma cells.

3.3.4 Decitabine treatment

To determine whether ATIP1-expression is dependent on hypermethylation, we subsequently treated the cells with DNA-Methyltransferase-inhibitor, decitabine. This resulted in the re-expression of ATIP1 at the transcriptional and translational levels in all GBM and GSC lines tested irrespective of the p53 expression status of these cell lines (Figure 13 a/b/c), suggesting that hypermethylation is playing a crucial role in *MTUS1*-downregulation in HGG.

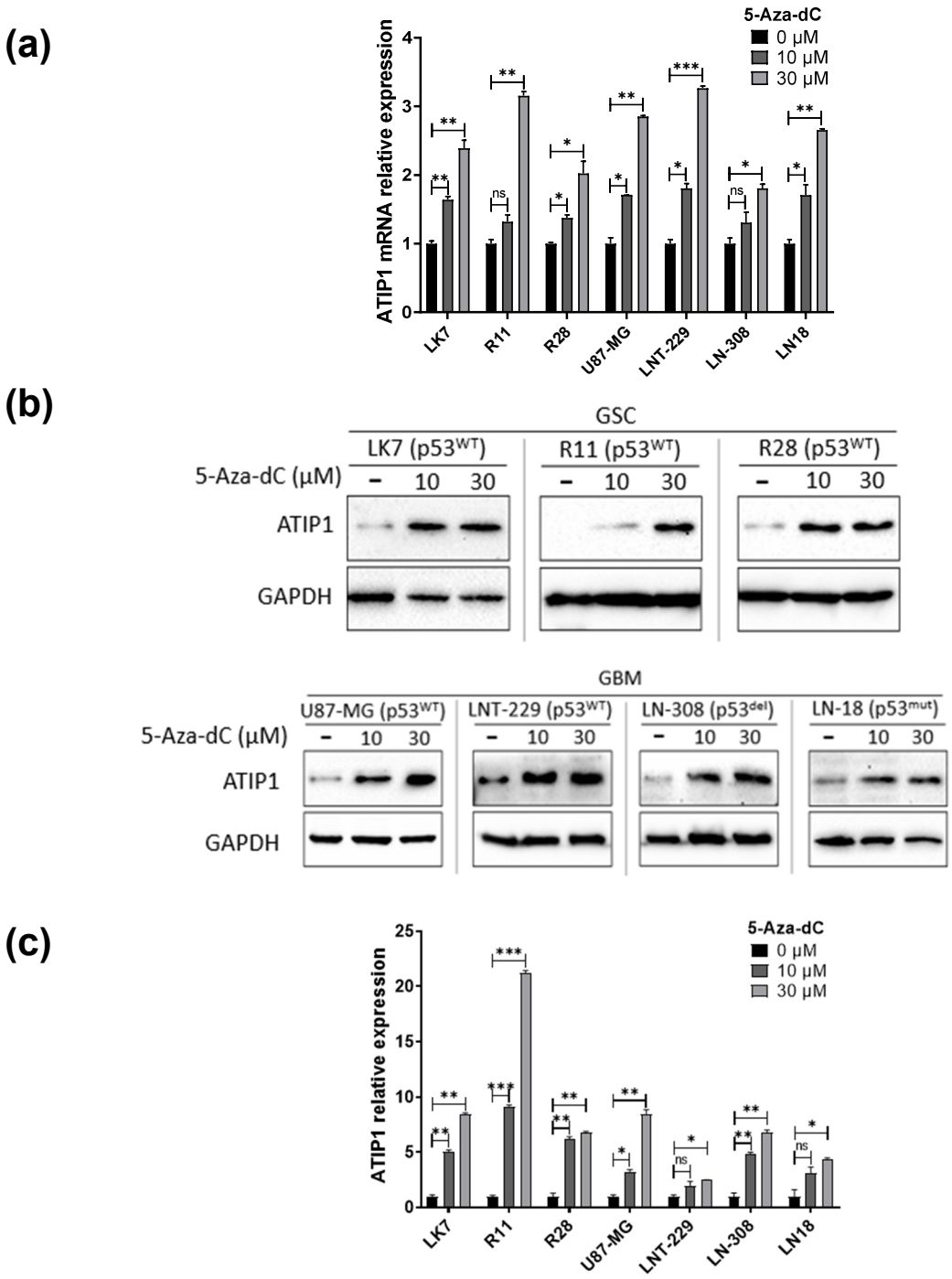

Figure 13. Decitabine (5-Aza-dC) treatment leads to the re-expression of ATIP1 both on mRNA levels in GSC and GBM. a. Relative expression of ATIP1 mRNA expression post decitabine treatment (n=3, SEM; ns, * $P < 0.05$, ** $P < 0.01$, *** $P < 0.001$). b. ATIP1 western blot, GAPDH serves as the loading control (n=3, one representative experiment is shown). c. Quantification of ATIP1 protein upon decitabine treatment at increasing concentrations (n=3, SEM; ns: not significant, * $P < 0.05$, ** $P < 0.01$, *** $P < 0.001$). e.

3.4 Discussion

Recent studies provide advancement in the new target-specific, often molecular-based and drugs developed with the current perception of the molecular biology of this destructive tumor. Although the etiology remains unclear, the existence of remarkably resistant tumor cell population, GSCs which might be responsible for treatment failure and glioma recurrence [4]. The genetic studies of GBM demonstrate the diffused distribution of genetic alterations across the entire genome, many of these alterations result in loss of TSG with a direct effect on gliomagenesis [119, 120]. Reports suggest the anti-tumor role of *MTUS1* in different cancers [87, 121-123], but has not been determined previously in glioma clinical and intracranial tumor model. This prompted us to investigate whether *MTUS1* plays any role in glioma progression and its association with the RAS pathway which might promote the advancements of novel therapies and improve responses to currently available therapies.

In this study, database mining reveals significantly low *MTUS1* expression results in poor survival in the glioma patient cohort [124], which also correlated with our observation of ATIP1 down-regulation at the transcriptional and translational level in the glioma patient samples. Whilst there seemed to be no correlation of ATIP1 expression and the IDH status of either LGG and HGG (Fig. 7c), there is a strict correlation of ATIP1 expression with glioma malignancy since ATIP1 is significantly downregulated in glioma cell lines compared with non-neoplastic cells of brain origin (Fig. 11), in HGG compared with LGG, in pilocytic astrocytomas compared to diffuse glioma (Fig.7a) as well as in recurrent gliomas compared with first time diagnosed gliomas (Fig. 1b). Studies prove that one reason for inappropriate gene regulation is epigenetic modifications and especially hypermethylation of TSG promoters [98, 113], however, there are no considerations of MTUS1 regulation with epigenetic modifications. DNA methylation is one of the most widespread epigenetic modifications responsible for gene repression. Hence, it might play a crucial role in the regulation of *MTUS1*.

Additionally, at least in GSC and glioma cell lines, we detected lower ATIP1 expression in those cells harboring an unmethylated MGMT promoter (Fig. 7d), which means in those cells that, due to enhanced repair of O6-methylguanines by MGMT, are not very vulnerable towards TMZ treatment, reflecting a more malignant type of glioma cells. With these facts, we treated glioma cells and GSCs with decitabine which resulted in elevated expression of ATIP1 in all glioma cells and low passage GSC (Fig 13), indicating that hypermethylation of the *MTUS1*-promoter might be one reason for its downregulation. Bisulfite sequencing reveals a significant increase in methylation at the CpG position in GSCs and glioma cells as compared to normal brain cells in the *MTUS1* promoter region. Unfortunately, we were not able to examine methylation of the most proximal 200 bp of the *MTUS1* CpG island. So, one could speculate that methylation in this region might also provide an impact on ATIP1 expression and might be also responsible for differences in the ATIP1 levels we observed in tumor cells and tissue (Fig. 6a/b/c/f). Although, we suggest that methylation of the proximal CpG island seems to be mainly responsible for *MTUS1* downregulation in HGG cells (LK7, LK31, R11 and R28) that provided the lowest ATIP1 levels and exhibited the highest methylation in this region (Fig. 12b).

Chapter 4

Modulations of Molecular mechanisms associated with *MTUS1*/ATIP1

4.1 Introduction

4.1.1 Alterations in the molecular signalling cascade

Genomic profiling of various tumors represents aberrant mutations in the molecular pathways, which propelled the use of molecular alterations study in glioma classification of 2016 [68]. As mentioned above, some reasons for challenging glioblastoma treatment is its complicated biology, a large number of genetic deformities and molecular signalling pathways. Molecular diversifications occur due to the overexpression or gain of function mutation in the receptor tyrosine kinase such as epidermal growth factor receptor (EGFR), platelet-derived growth factor receptor (PDGFR) and fibroblast growth factor receptor (FGFR) [125-128]. These anomalies lead to the constitutive expression of Ras/extracellular signal-related kinase (ERK), PI3K/Akt/mammalian target of rapamycin (mTOR) and other signalling cascades which are characteristics of glioma initiation and progression [129, 130]. These signalling also affect several other cascades such as autophagy and ROS production followed by DNA damage, chromosomal instability and initiation of metastasis [131, 132]. Hence, the understanding of glioma biology along with underlying mechanisms that lead to its high malignancy is of central importance. Temozolomide (TMZ), the standard therapeutic drug to treat glioma, methylates guanine residues in the DNA. Repair mechanisms that lead to resistance and that are common in tumor cells include DNA mismatch repair [6] as well as the removal of the methylation group by O^6-methylguanine-DNA methyltransferase (MGMT). Due to resistance mechanisms in GBM, the development of new therapeutic strategies is therefore necessary. For this, it is of central importance to understanding the biology of GBM in detail.

4.1.2 PI3K/AKT/mTOR signalling cascade

Recently GBM research and treatment focuses on a subpopulation of tumors known as glioma stem cells (GSCs) or cancer stem cells (CSCs). Due to the heterogeneous populations of cells

in the tumor, cells are in different stages of differentiation. Several pathways such as Wnt/β catenin, STAT3 and TGF-β are considered as key signalling cascades responsible for the maintenance of these CSC [133-135]. Some other signalling pathways which are associated with physiological and pathological conditions for instance proliferation, survival, differentiation and metabolism are phosphatidylinositol-3-kinase (PI3K)/Akt and mammalian target of rapamycin. Mutations in PI3K/Akt/mTOR pathways are frequently observed in glioblastoma, 70% of ovarian cancer which results in overactivation of PI3K/Akt/mTOR, also gastric cancer specimens have shown activated PI3K/Akt/mTOR pathways when compared with nontumor gastric mucosa [136, 137]. Besides being associated with cancer progression, recent studies have reported links between PI3K/Akt/mTOR signalling and CSC biology [138, 139]. mTOR signalling pathway maintains the self-renewal capacity and tumorigenicity in GSCs [140]. Colony formation ability and radio-resistance of CSCs are also a result of the activation of PI3K/Akt/mTOR signalling cascade.

4.1.3 MAPK/ERK signalling cascade

The MAPK family consists of two serine/threonine kinases and one double specificity threonine/tyrosine kinase, these communicating kinases are further translocated to the nucleus. MAPK/ERK pathway is involved in modulating various cellular mechanisms including cellular proliferation, differentiation, apoptosis and stress response [141, 142]. The ERK belongs to the MAPK family and any dysregulation in the Ras/ERK cascade acts as a considerable cause for cancer progression. MAPK/ERK pathways are associated with the signal transduction network. consisting of an upstream activating sequence (Ras), a MAP3K (Raf), a MAP2K (MAPK/ERK KINASE) and ERK acts as MAPK together forming the Ras-Raf-MEK-ERK pathway. Hence, ERK/MAPK consists of 4 major molecules i.e., small G-protein Ras and downstream Raf-K, MEK1/2 and ERK1/2. ERK phosphorylation results in the activation of various downstream substrates that are responsible for the stimulation of cell proliferation and differentiation [141,

142]. The localization of ERK within cells determines the target substrates as when in cytoplasm p-ERK regulates cell movement, cell adhesion, metabolism by phosphorylating cytoskeletal proteins [143]. Soon after activation, ERK dislodges from the cell membrane and enters the nucleus where it undertakes the task of phosphorylating numerous transcription regulatory factors such as carbamoyl phosphate synthetase II (CPS-II) and promoting cell cycle progression [144, 145]. Not only the subcellular location of ERK but its activity is also determined by timing, duration and intensity of signals [47]. Overactivation of MAPK/ERK pathway and subsequent phosphorylation of downstream substrates is also related to tumor formation. It has been reported that MAPK/ERK pathway promotes cell proliferation but an over-stimulated pathway can cause excessive localised growth in cellular numbers ultimately leading to tumor formation [146]. Moreover, MAPK-phosphatase expression levels were elucidated to be high in normal and benign tumors relative to invasive malignant tumors. Also, high levels of p-ERK1/2 were found in Stage II/IV patients than those in Stage I/II. That means antagonistic behaviour was displayed by MKP-1 and p-ERK1/2. Continuous overstimulation of cells due to over-activation of the ERK/MAPK pathway can promote the transformation of normal cells to invasive cancerous cells [146].

But, inhibition of the ERK/MAPK pathway can significantly reduce the survival of tumor-forming cells and promoting apoptosis [146]. It would restore tumor cells to non-transformed actively dividing cells *in vitro* and inhibit uncontrolled growth because of disrupted MAPK/ERK pathway in vivo. The MAPK/ERK signalling is predominantly activated by upstream SRC/RAS/RAF signalling, which in tumors are managed by modulation through parallel pathways culminating in the complexity within and between tumors that hinder the therapeutic approach. Inhibitors targeting the MAPK/ERK pathway are in use for over a decade now and have shown some promising results in clinical trials. The traditional inhibitors exhibit

anti-angiogenic activity, however, many of them are unsuitable for human use due to toxicity [146, 147].

4.1.4 Invasion and metastasis signalling cascade

Even with the advancements in therapeutic surgical and radiation procedures, malignant gliomas reappear within the radius of 1-2 cm of the initial tumor site. Since they have highly invasive characteristics some tumor cells invade into the non-cancerous surroundings of the brain tissue and escape the surgical removal and radiation therapy [29]. Invasion and metastasis are hallmark features of cancer involving a multi-step process utilising the integration of several molecular pathways and biochemical processes. Unlike alternative aggressive tumors, that metastasize through the circulatory or lymphatic systems to organs, HGG seldomly metastasizes outside of the brain. HGG vigorously migrates in the perivascular space surrounding the blood vessels and between the neurons and glial cells which frames the brain parenchyma [148]. To breach through these surrounding spaces, glioma cells undergo several biological transformations including enhanced mobility, degrading of Extra-cellular matrix (ECM) and stem cell phenotype, cell shrinkage to reduce cell volume, alterations in molecular pathways and gene regulation and expression of miRNAs [148]. ECM, the physical barrier, plays a pivotal role in maintaining the morphology, migration, survival and differentiation of a cell. Invasive cancer cells become morphologically polarized and establish membrane protrusions to reach forward and adhere to the ECM. Invasive glioma cells collaborate with multiple components of ECM which provides ligands that provide an anchor to pull themselves forward [148]. Along with invasion, dysregulation of the tightly regulated motility processes results in the highly migratory nature of cancer cells. Along with the ability to migrate, glioma cells must cross the physical barrier, ECM. Matrix-metalloproteinases (MMPs) are responsible for degrading the extracellular matrix proteins to create a passage for tumor cell invasion. Therefore, usually, cancer cells have a higher expression of MMPs as compared to normal cell

counterparts [149]. Also, it has been reported that molecular pathways which stimulate invasion also upregulate the expression of MMPs [150-152]. The expression of MMP-2 and MMP-9 are believed to play a crucial role in basement membrane disruptions resulting in tumor invasion, angiogenesis, tumor progression and T-lymphocytes infiltration, which is also regulated by increased hypoxia [150, 153, 154].

In general, complex signalling cascade needs a detailed investigation in order to understand its role in cancer progression, CSCs regulating mechanism and more importantly in in clinical settings. Thorough understanding of the molecular mechanisms will definitely lead us towards the development of the novel therapies essential for mitigating cancer progression.

In order to understand the functional role of ATIP1 in glioma, we overexpressed ATIP1 and established glioma stable cell lines. Using the respective cells, we performed functional analysis to understand the biological significance of ATIP1 in glioma *in vitro* and *in vivo*. This also helped us to understand the molecular mechanisms associated with glioma and ATIP1.

4.2 Result

4.2.1 Generation of ATIP1 overexpressing stable cell line

In order to elucidate the biological role of ATIP1, we generated ATIP1-overexpressing GBM cells (Figure 14a/b). After positive selection of the cells, the parental cells (LNT-229 and LN-308), control (EV: empty vector) and ATIP1 overexpressed cells (ATIP1) were subjected to immunoblot. The immunoblot and densitometric analysis represented that parental and control cells contain a basal expression level of ATIP1 and overexpressed cell lines represented a significantly high expression which confirms the stable ATIP1 overexpression in respective cell lines (Figure 14a/b). Immunofluorescence assay also confirms the ATIP1 overexpression as compared to the parental and control cells (Figure 14c).

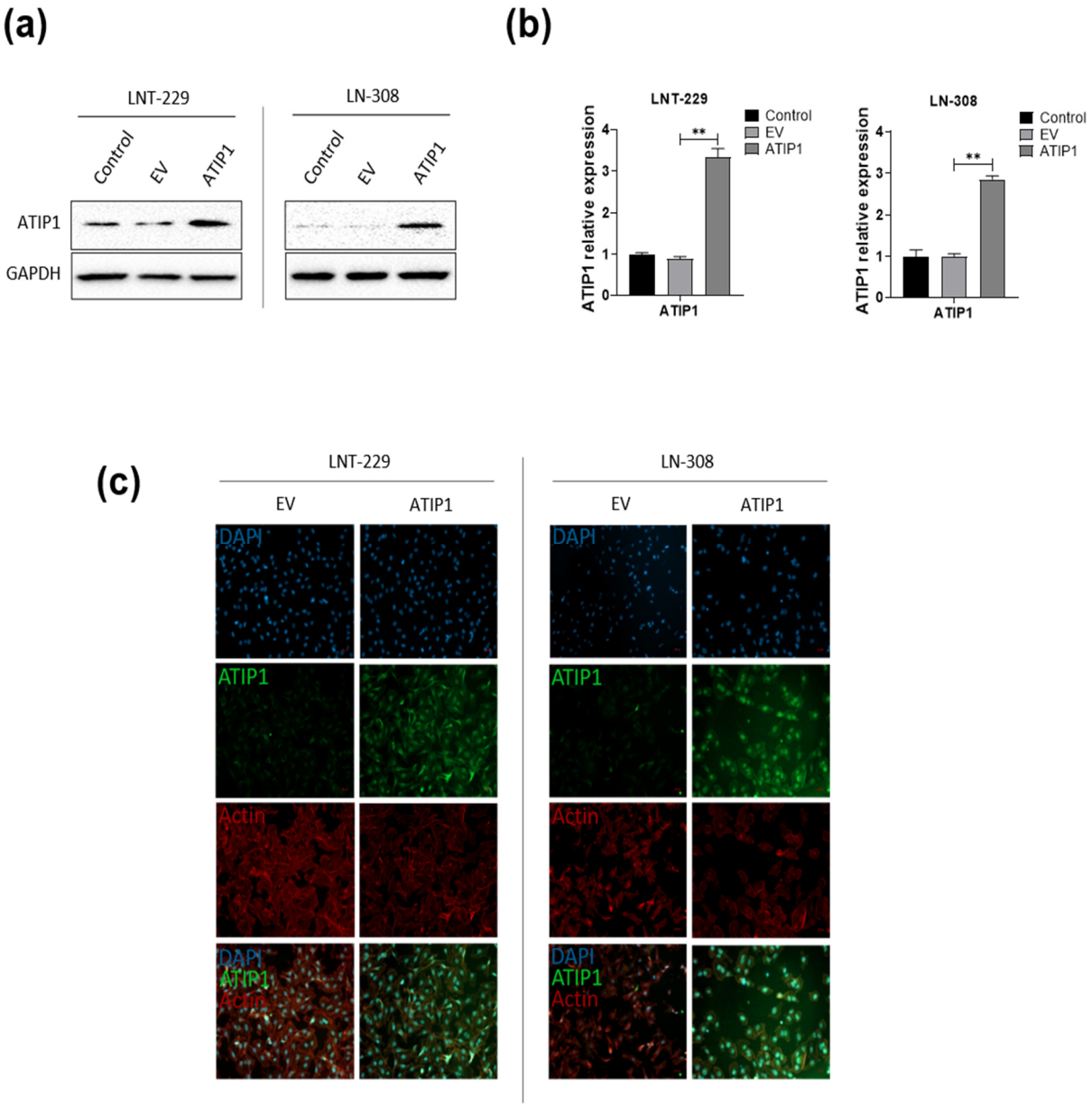

Figure 14. ATIP1 expression in control and stably transfected glioma cell lines. a. Immunoblot of whole-cell lysates derived from either LNT-229 and LN-308 parental (control) or stably transfected cells using the empty vector pcDNA3.1 (EV) or pcDNA3.1-ATIP1 (ATIP1). b. Quantification of ATIP1 as indicated in (a) (n=3, SEM, ** $P < 0.01$). c. Immunofluorescence staining of ATIP1 in EV and ATIP1-stably transfected LNT-229 and LN-308 cells (bar = 50 µm).

4.2.2 ATIP1 modulates cell proliferation, motility and survival

and analysed cell growth, clonogenic survival, migration and invasion in parental (control), mock-transfected (EV) and ATIP1-overexpressing GBM cells. The functional analysis illustrates, ATIP1 overexpression significantly mitigates proliferation, migration, and invasion as compared to the control and EV cells. As indicated in Figure 15a, ATIP1-expressing LNT-229 and LN-308 cells grew significantly slower than parental or EV cells and showed a reduced capability to form colonies (Figure 15b). Wound healing assay in the respective cells also represents that ATIP1 overexpression significantly mitigated the rate of migration as compared to EV cells (Figure 15c).

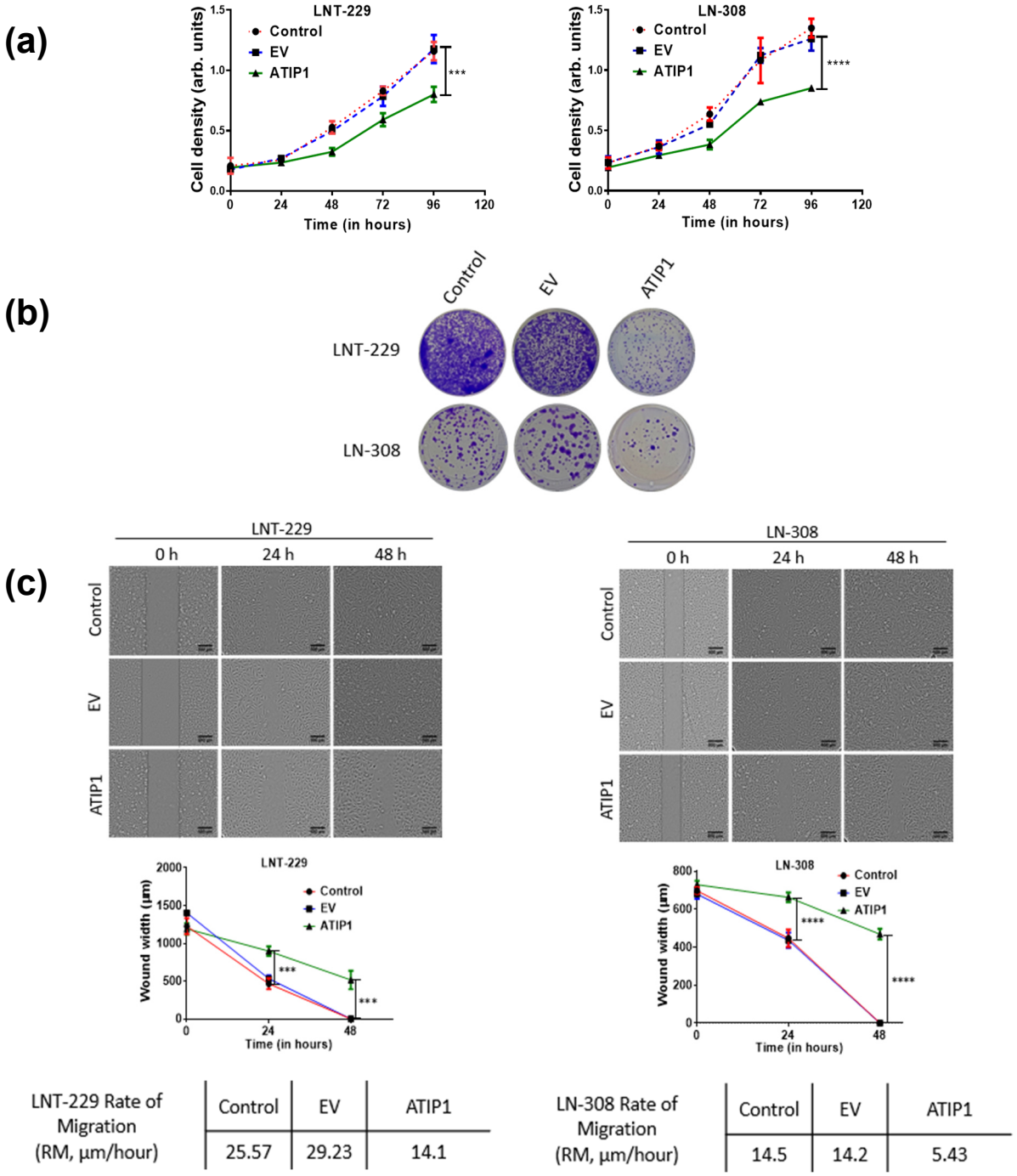

LNT-229 Rate of Migration (RM, µm/hour)	Control	EV	ATIP1
	25.57	29.23	14.1

LN-308 Rate of Migration (RM, µm/hour)	Control	EV	ATIP1
	14.5	14.2	5.43

Figure 15. ATIP1 overexpression modulates several pro-tumorigenic characteristics. Parental (control), pcDNA3.1 (EV) or pcDNA3.1-ATIP1 (ATIP1) stably transfected LNT-229 and LN-308 cells were subjected for functional assays. a. Cell density was determined by crystal violet staining at the indicated time points (n =3, SEM, *** P < 0.001, **** P < 0.0001). b. Clonogenic survival (n=3, one representative experiment is shown). c. Wound healing scratch assay of parental (control), pcDNA3.1 (EV) and pcDNA3.1-ATIP1 (ATIP1) stably transfected LNT-229 and LN-308 cells (bar = 500 µm). c. Quantification of wound closure as indicated in b. (n=3, SEM; *** *P* < 0.001).

4.2.3 ATIP1 modulates cell migration and invasion

Reduced growth was also accompanied by an elevated population of cells arrested in the G2/M cell cycle phase (Figure 16). Additionally, ATIP1-overexpression significantly mitigated the capabilities of the cells to migrate and invade (Figure 17a), accompanied by the downregulation of matrix-metalloproteinase-2 (MMP-2) and upregulation of E-cadherin (Figure 17b) [155, 156]. Reduced motility in ATIP1 cells was paralleled by a significant upregulation of vinculin-positive large focal adhesions complexes (LFAC) and associated actin stress fibers, and by a lower number of filopodia and lamellipodia (Figure 18, indicating a tighter adhesion of ATIP1 cells compared to control cells.

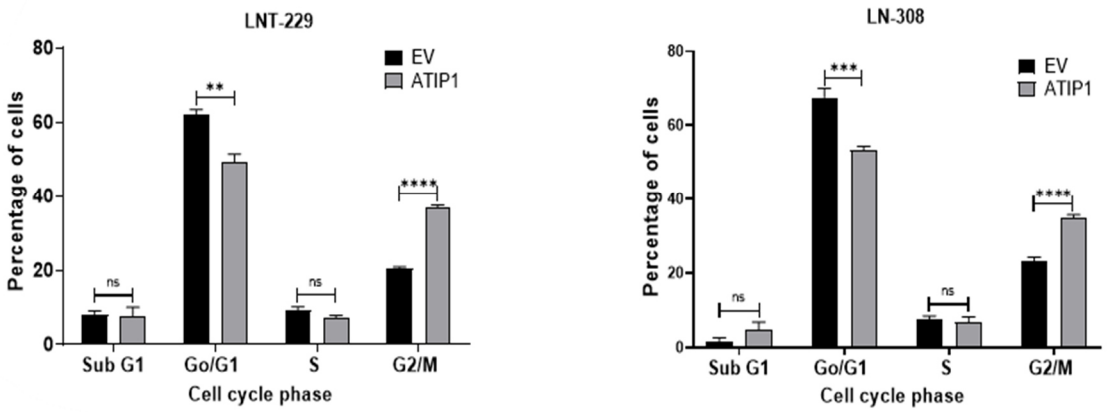

Figure 16. ATIP1 modulates cell cycle distribution and migration. a. Cell cycle analysis displaying different phases of cell cycle in pCNA3.1 (EV) and pcDNA3.1-ATIP1 (ATIP1) overexpressing LNT-229 and LN-308 cells (n=3, SEM; ns, *** $P < 0.001$, *** $P < 0.001$, **** $P < 0.0001$).

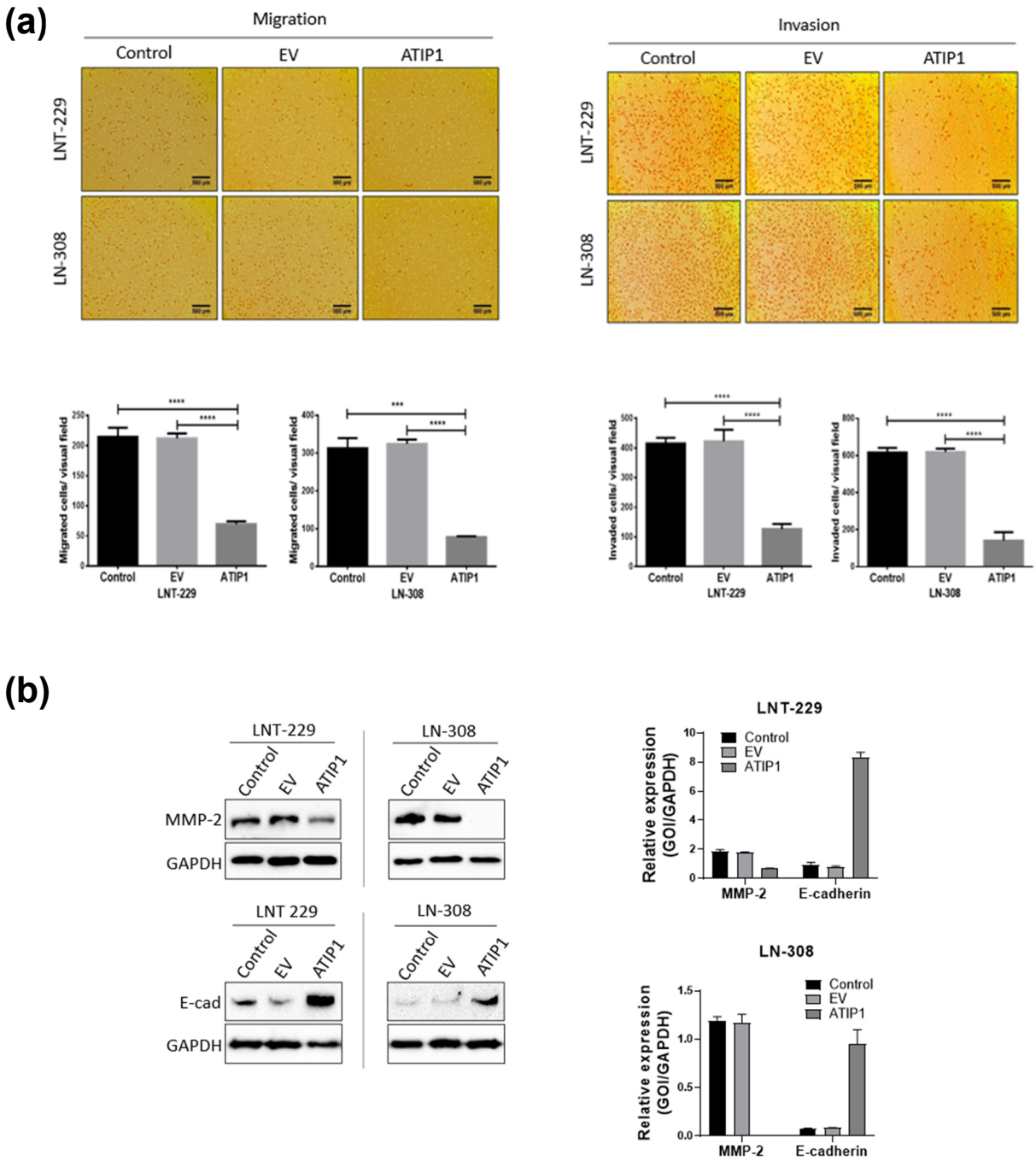

Figure 17. ATIP1 overexpression modulates several pro-tumorigenic characteristics. Parental (control), pcDNA3.1 (EV) or pcDNA3.1-ATIP1 (ATIP1) stably transfected LNT-229 and LN-308 cells a. Quantification of transwell cell migration and invasion (n=4; SEM, *** $P < 0.001$, **** $P < 0.0001$). Western blot of MMP-2 (upper panel) and E-cadherin (lower panel), GAPDH serves as a loading control (n=3, one representative experiment is shown). The right panels respectively show the quantification of MMP-2 and E-Cadherin (n=3, SEM).

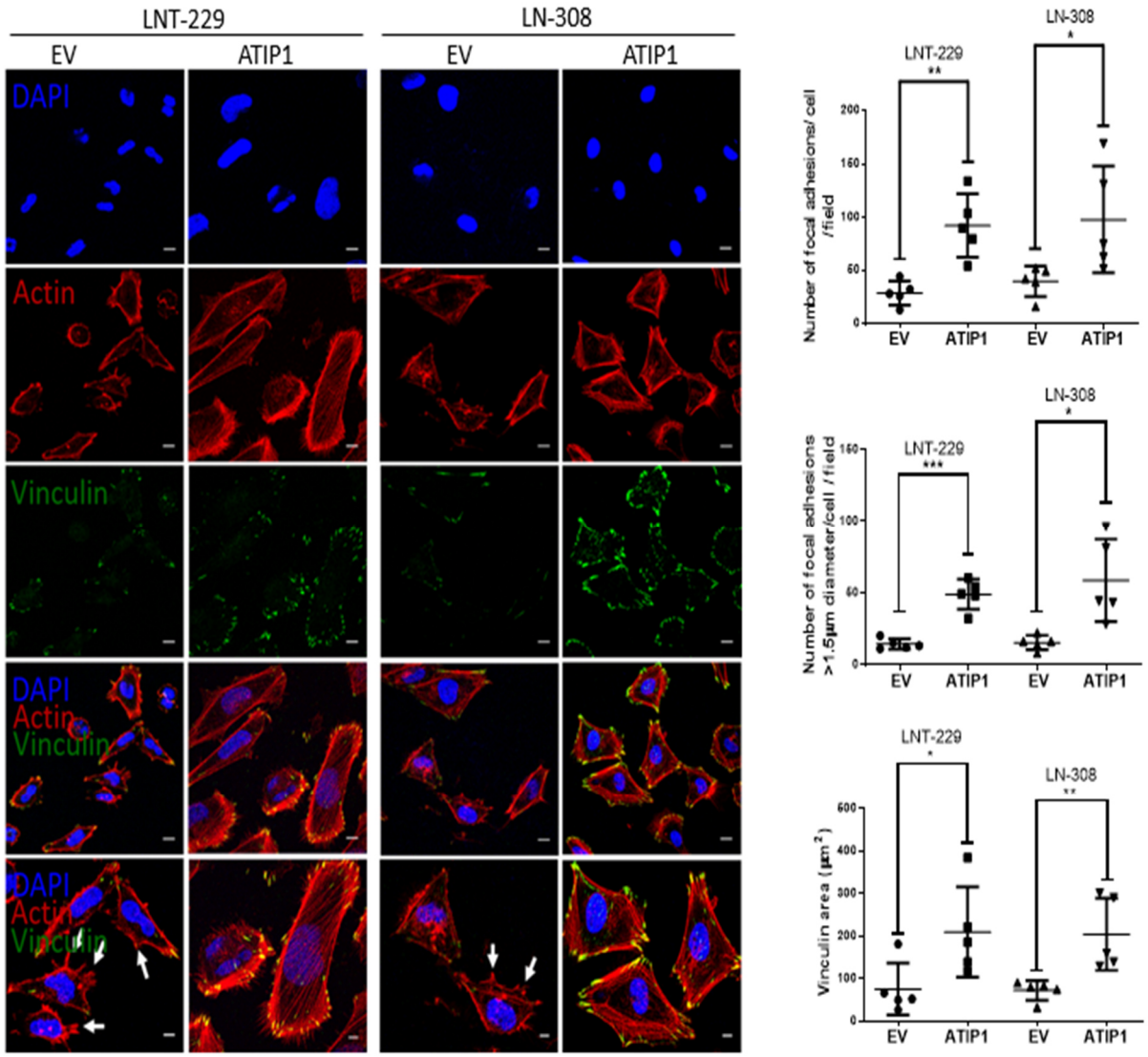

Figure 18. Focal adhesion assay for invasion analysis. Immunofluorescence analyses of actin fibers (red) and vinculin (green) indicate the higher amount of focal adhesion complexes in ATIP1 overexpressing LNT-229 and LN-308 pcDNA3.1 (EV) and pcDNA3.1-ATIP1 stably transfected cells (scale = 100 µm). Arrows indicate lamellipodia and filopodia. f. Quantification of focal adhesion complexes (upper panel), large focal adhesion contact points (middle panel) and of the total area stained for vinculin (lower panel; n=6; * $P < 0.05$, ** $P < 0.01$, *** $P < 0.001$).

To further evaluate the tumor-suppressor activity of ATIP1, we used an *in vivo* orthotopic mouse GBM model where we intracranially implanted either LNT-229-EV or LNT-229-ATIP1 cells. Mice developing LNT-229-ATIP1 tumors survived significantly longer (107.5 d) compared to the LNT-229-EV cohort (66 d, Figure 19a). Histological analyses demonstrated a significant reduction of tumor growth and Ki67 staining in the ATIP1 cohort compared to the controls (n=3; Figure 19b).

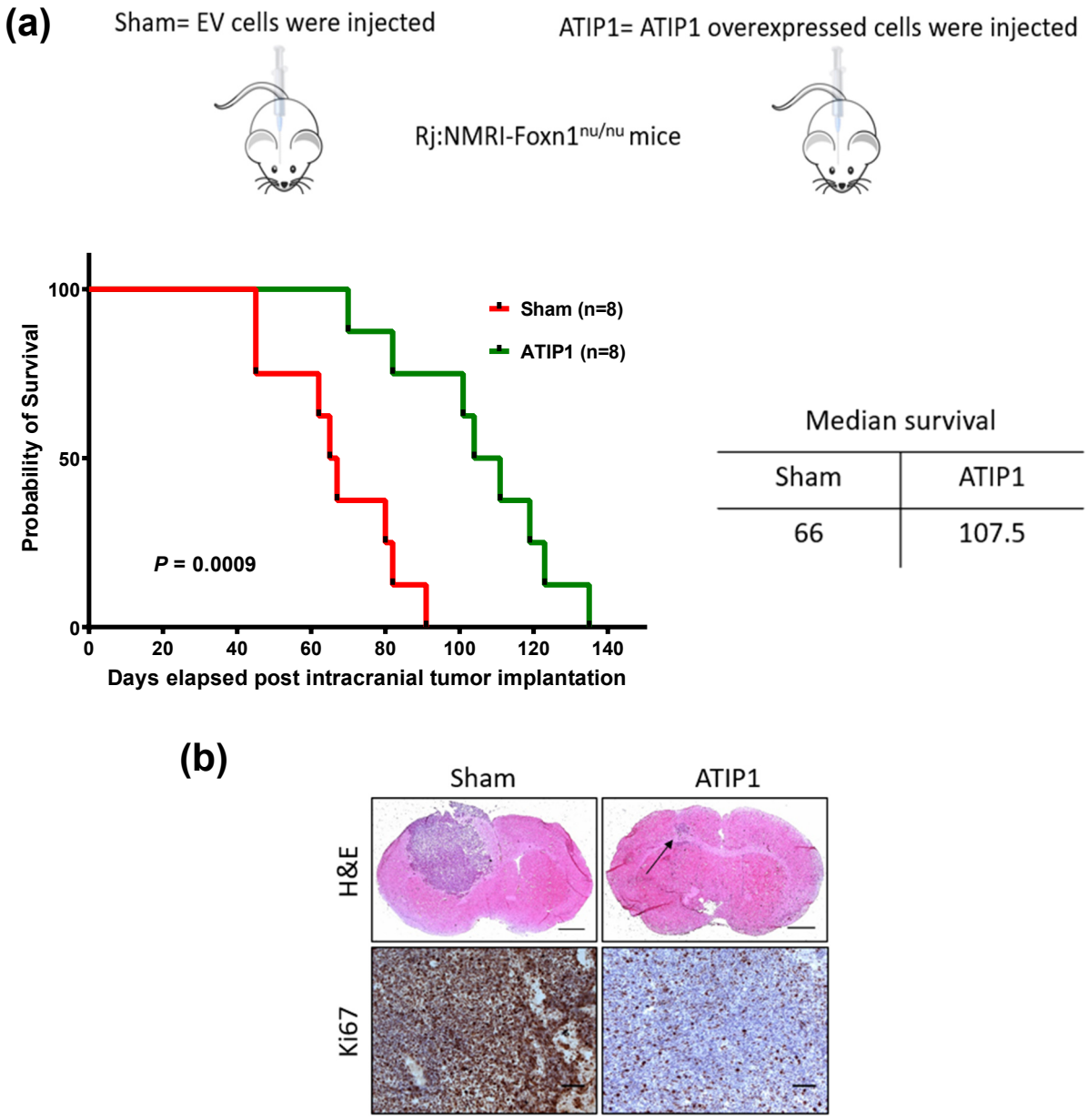

Figure 19. Role of ATIP1 overexpression on median survival and tumor progression. Survival of mice harboring either pcDNA3.1 (sham) or pcDNA3.1-ATIP1 stably transfected (ATIP1) LNT-229 gliomas (n=8 mice per group). h. Elevated ATIP1 expression reduces tumor growth and proliferation of tumor cells. H&E (upper panel, scale = 1000 µm) and Ki67 (lower panel, scale = 500 µm) staining of mice harboring gliomas developed after intrastriatal implantation of pcDNA3.1 (EV) or pcDNA3.1-ATIP1-stably transfected LNT-229 cells (n=3 mice per group, one representative picture is shown). The arrow indicates the tumor region in an LNT-229-pcDNA3.1-ATIP1-glioma bearing mouse.

4.2.4 Signalling pathway modulation post ATIP1 overexpression and survival analysis

Based on our data that ATIP1 mitigates proliferation and migration we subsequently investigated its involvement in the activation of the cancer-associated ERK and AKT signalling pathways. In ATIP1-overexpressing LNT-229 and LN-308 cells, AKT and ERK1/2 phosphorylation, as well as phosphorylation of the ERK downstream target p90RSK, were reduced (Figure 20 a/b). Additionally, pro-apoptotic BAX was upregulated and anti-apoptotic BCL-2-downregulated. To validate whether ATIP1 directly influences the activation of the above pathways and the expression of BAX and BCL-2, we knocked down *MTUS1* by siRNA. Indeed, reduced ATIP1-expression increased phospho-ERK1/2, phospho-AKT and also BAX, but reduced BCL-2 (Figure 21). We also investigated human glioma tissue for phospho-ERK and found usually lower amounts of phospho-ERK in those samples that express ATIP1 (Figure 22a). Pearson's correlation analysis represents that ATIP1 and phosho-ERK-expression are negatively correlated in clinical glioma specimens (Figure 22b).

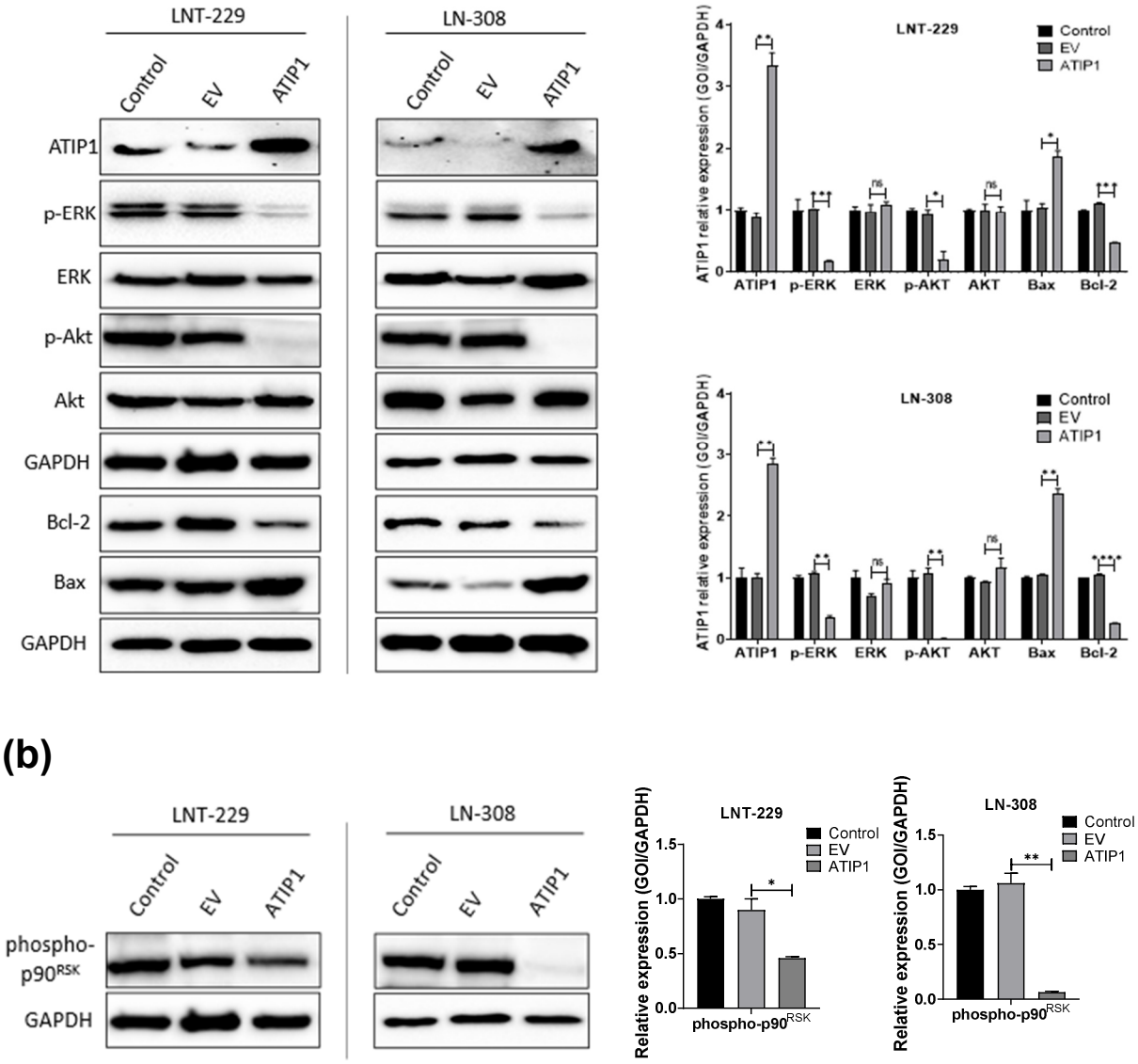

Figure 20. Enhanced expression of ATIP1 modulates the activity of glioma-associated signalling pathways. a/b. Western blot of ATIP1, p-ERK, ERK, p-AKT, AKT, BAX, BCL-2 and phosphor-p90^{RSK} in parental (control), pcDNA3.1 (EV) and pcDNA3.1-ATIP1 (ATIP1) stably transfected LNT-229 and LN-308 cells. GAPDH served as the loading control. One representative experiment out of three is shown. Quantification of the above-mentioned proteins (n=3, SEM; ns, * $P < 0.05$, ** $P < 0.01$, *** $P < 0.001$, **** $P < 0.0001$).

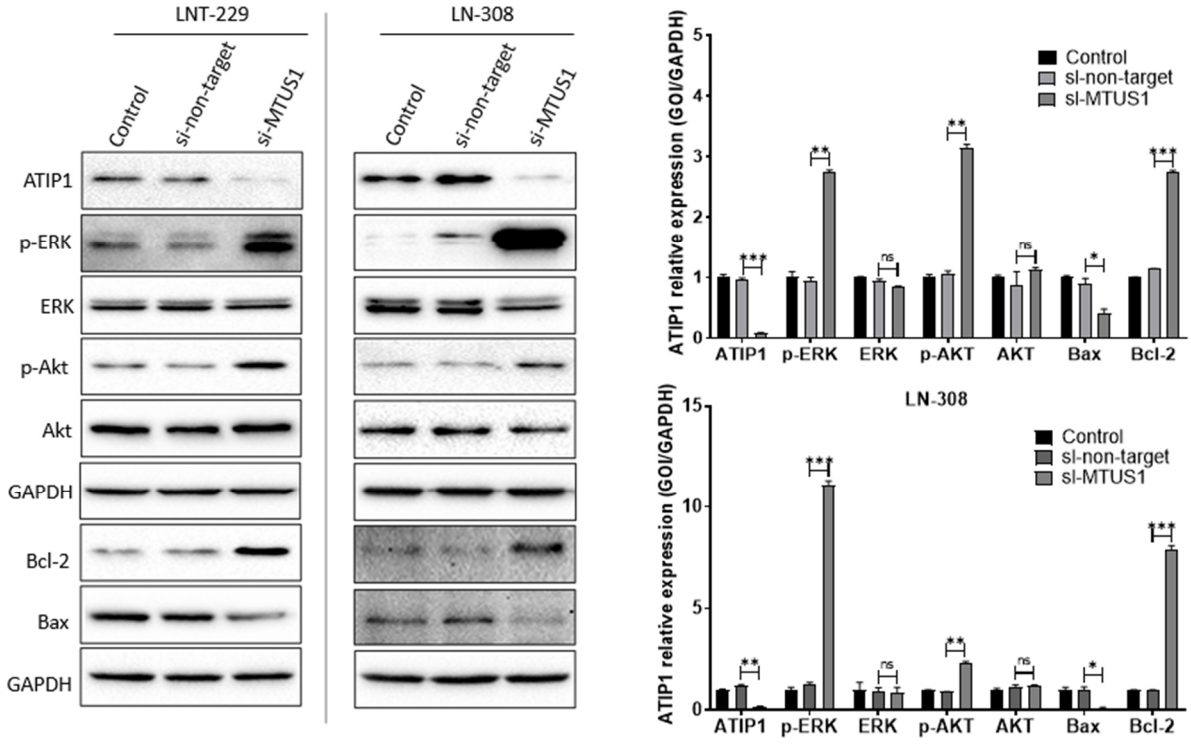

Figure 21. si-RNA mediated knockdown of ATIP1 modulates the activity of glioma-associated signalling pathways. Western blot of ATIP1, p-ERK, ERK, p-AKT, AKT, BAX and BCL-2 in parental LNT-229 and LN-308 cells after 72 h of transient si-RNA transfection of parental LNT-229 and LN-308 cells. GAPDH served as the loading control. One representative experiment out of three is shown. Quantification of the above-mentioned proteins (n=3, SEM; ns, * $P < 0.05$, ** $P < 0.01$, *** $P < 0.001$, **** $P < 0.0001$).

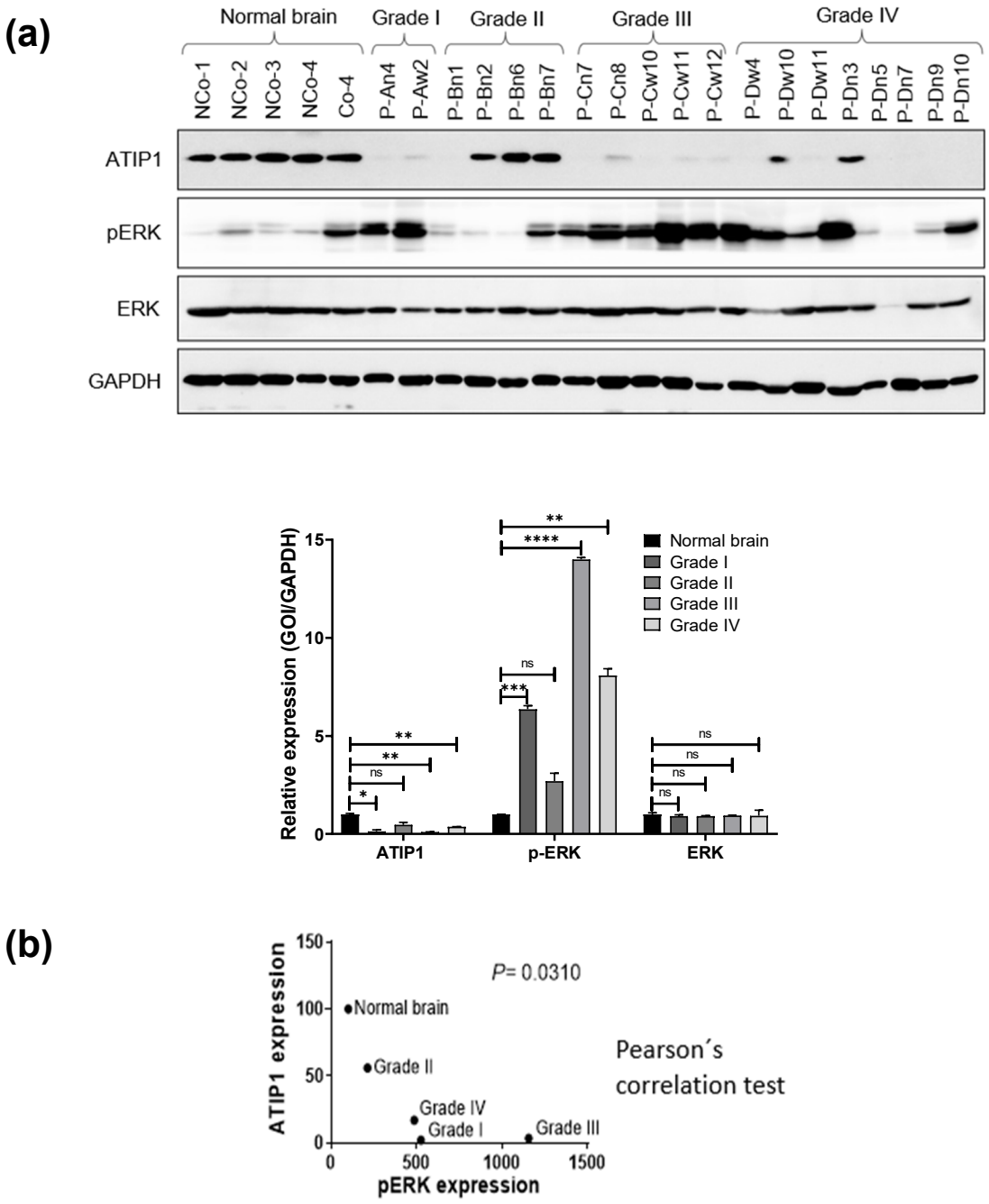

Figure 22. ATIP1 downregulation modulates the activity of glioma-associated signalling pathways. a. Western blot of ATIP1, p-ERK and ERK in glioma specimen (n=3). Quantification of the above-mentioned proteins in glioma specimen of different WHO grades (n=3, ns, * $P < 0.05$, ** $P < 0.01$, *** $P < 0.001$, **** $P < 0.0001$). b. Pearson parametric correlation test was used to analyse the significance between ATIP1 and p-ERK expression in glioma samples of different WHO grades.

4.3 Discussion

In vitro, ATIP1-overexpressing glioma cells showed a significant reduction in proliferation and migration/ invasion. In the brain, microtubules and ECM orchestrate a crucial role in neural differentiation and cell migration [157, 158] and alterations to microtubule-associated proteins are comparable with the incidence of neurodegenerative pathologies such as Alzheimer's disease [89, 90]. The functional heterogeneity of tubulins, microtubules, and their collaborative partners are considered to be the key regulators in the maintenance of the cellular homeostasis and execution of the cell stress response which is attributed to genetic code and post-translational modifications [131, 159]. Cytoskeletal proteins and proteins regulating the ECM adhesions such as integrins or focal adhesion complex members, are responsible for cell motility [160-162]. Targeting migration and invasion will serve as an essential step in the GBM therapeutics. Focal adhesions are the multi-protein structures that are responsible for linking the actin bundles and the extracellular components in different cell types. Overexpressed ATIP1 cells represent an increased expression of vinculin, a major membrane-cytoskeletal protein in the focal adhesion plaques. Loss of vinculin is associated with reduced cell adhesion preventing actin polymerization resulting in decreased cytoskeletal stiffness, cell adhesion and increased FA turnover which is necessary to deform the cell [163, 164]. Since the association of more focal adhesions with stress fibers restricts the movement of a cell. These observations indicate that ATIP1 overexpression results in higher levels of stable LFAC associated with actin stress fibers and supports the observation of reduced cell motility, whereas lower expression of ATIP1 resulted in the dissolution of stress fibers and associated focal adhesion and in an apparent increase in SFAC and a diffuse pattern of vinculin distribution which is associated with protruding lamellipodia and filopodia, respectively [160, 165]. Therefore, with an unknown mechanism ATIP1 is blocking the transition from stable LFA to more dynamic SFC, also resulting in inhib-

ition of lamellipodia and filopodia formation crucial for cell motility. Matrix metalloproteases (MMPs) are responsible for the degradation of the ECM, a decisive phenomenon that stimulates the invasion of GBM cells into the healthy brain. MMP-2 downregulation was associated with MTUS1/ATIP1 overexpression along with an increased expression of E-cadherin represents its association with reduced epithelial-mesenchymal transitions (EMT) which results in reduced tumor progression and metastasis. The immunoblot analysis showed that ATIP1 overexpression led to significant inhibition of pERK1/2 and pAKT. Moreover, immunoblot analysis from glioma patient samples represents a significantly high expression of glioma biomarker, EGFR and the inhibition of pERK1/2 and ATIP1 in the higher grades of glioma as compared to the normal brain samples. These observations explain that ATIP1 is regulating the PI3K/AKT pathway as well as modulating the apoptotic pathways as well. Furthermore, we also showed that ATIP1 overexpression results in inhibition of tumor growth and significant overall survival benefit in mice harboring LNT-229 intracranial tumors, these findings were supported with H&E staining and decreased staining for Ki67 and GFAP in LNT-229-ATIP1 overexpressed tumors as compared to LNT-229 EV tumors which correlate with low proliferation rate in ATIP1 overexpressed cells as shown in the functional assays.

Chapter 5

Effect of glioma therapeutics on *MTUS1*/ATIP1

5.1 Introduction

The challenges in glioma treatment are a concerning issue in clinical oncology, chemotherapy is difficult due to the BBB and clonal heterogeneity of this tumor. Also, clinical applications are limited by various adverse effects such as bone marrow suppression, genotoxic, teratogenic and fetotoxic effects [166]. Along with complete tumor resection, radiotherapy (RT) and now the expansion includes RT plus chemotherapy is administered to the patients after surgery, regardless of the extent of surgery. Within 6 weeks, fractionated doses of 60 Gy are co-administered along with TMZ (75 mg/m^2 body surface area per day), followed by 6 TMZ cycles (150-200mg/m^2) daily for 5 consecutive days within a 28-day cycle [48].

TMZ is the only approved drug from Food and Drug Administration (FDA) and is used as a first-line anti-cancer drug for glioblastoma and recurrent glioblastoma treatment [167]. TMZ along with RT in newly diagnosed patients resulted in a significantly longer median survival time and significantly greater 2-year survival rate than RT alone [48]. TMZ is a prodrug, an imidazotetrazine derivative with an amide group and behaves as a prodrug, which spontaneously hydrolyzes at physiological pH to 3-methyl-(triazen-1-yl)imidazole-4-carboxamide (MTIC) [168] (Figure 23a). As mentioned above the primary mechanism responsible for TMZ cytotoxicity is due to the DNA damage caused by the DNA methylation at positions N7 and O6 in guanine, resulting in prolonged DNA cuts and blockage in the cell cycle at the G2-M phase induces apoptosis [169] (Figure 23b). As mentioned above, the clinical outcomes of TMZ treatments have been compromised due to the high expression of DNA repair enzyme O^6-MGMT by protecting the tumor cells from alkylating chemotherapeutic agents [170]. MGMT has a significant impact on the outcome of anti-cancer therapy since it concludes the effectiveness of the alkylating anti-cancerous drugs.

(a)

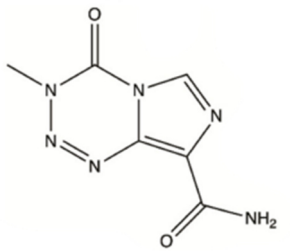

TMZ

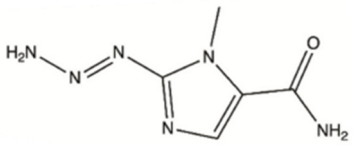

MTIC

(b)

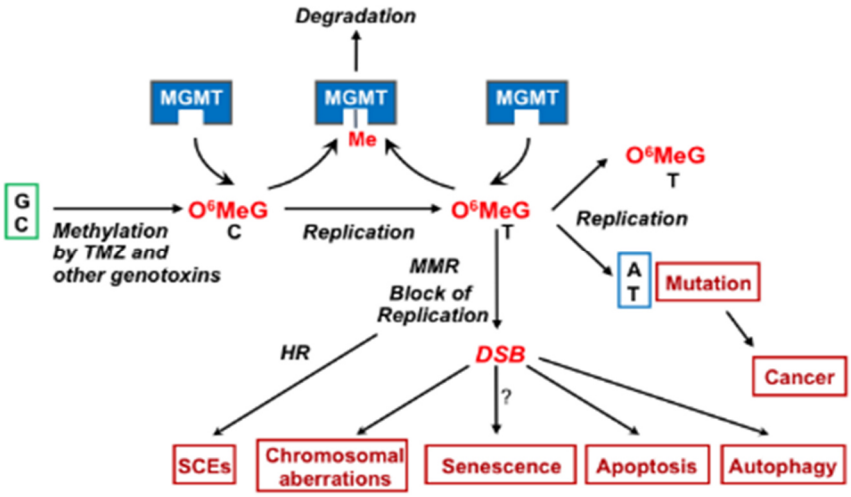

Figure 23. Temozolomide and its mode of action. a. Chemical structure of Temozolomide and biologically active product, 3-methyl-(triazen-1-yl)imidazole-4-carboxamide (MTIC). b. Representation of repair pathway of O6MeG by MGMT pre and post replication. Unrepaired lesion consequently leads to mispairing mutations resulting in cancer formation (adapted from Kaina and Christmann, 2019).

5.1.1 Resistance mechanisms

Surgical resection combined with radiation therapy and chemotherapy comprises current optimal therapy in GBM. Recently there has been a huge emphasis on the subpopulation of GBM tumor cells with stem cell characteristics. GSCs are another major cause of drug

resistance and tumor recurrence. Such individual cells are efficient in self-renewing, proliferation and differentiation which results in the complex heterogeneous tumor which is a major characteristic of glioblastoma which is a major factor responsible for resistance mechanisms. They are also known as tumor stem cells (TSC) which can be isolated from primary GBM specimens and cultured *in vitro* under optimal conditions. TSCs are defined by their capability of self-renewal and ability to form neurospheres and asymmetric cell divisions in immunocompromised mice [171, 172]. Most of the TSC expresses CD133, nestin, SOX2, LeX/SSEA-1, Bmi1, Ezh2, L1CAM and Olig2, there is no specific marker expressed exclusively for TSC [172-176].

As mentioned before TMZ is the first-line chemotherapy drug for glioma treatment but the resistance in the patients mitigates its advantages by half which is the biggest reason for the failure in chemotherapy. Various mechanisms of chemo and radiotherapeutic resistance such as efflux of the drugs by ABC transporters boosted DNA damage response, decreased apoptotic sensitivity, elevated expression of growth factors and dysregulation of transcription. The immense activity of these transporters leads to a condition known as Multi-Drug Resistance (MDR). Also, the methylation resulted from TMZ can be repaired by methyltransferase and O6 methylguanine methyltransferase (MGMT) can reverse the O6 position of guanine. Hence patients with wild type or overexpression of O6MGMT are naturally resistant to TMZ. For example, a hypomethylating agent, 5-Azacytidine deoxycytidine (5-Aza-dC; Decitabine) follows two mechanisms by which cells are resistant to 5-Aza-dC treatment: a). cells that are deficient in deoxycytidine kinase, the enzyme that activates 5-Aza-dC are completely resistant to this analog and b). increased activity of cytidine deaminase, the enzyme that inactivates 5-Aza-dC produces drug resistance.

Another mode of resistance results from the hypoxic tumor microenvironment since GBM cells are resistant to low oxygen levels which is a result of higher cell proliferation and subsequent

low supply of nutrients and oxygen due to low blood vessel density [177]. Since the hypoxic GBM cells are distant from the blood vessels results in the unavailability of anti-cancer drugs. Also, several drugs are dependent on the formation of reactive oxygen species (ROS), which is reduced in hypoxic conditions due to low oxygen supply. drugs resulting in drug resistance. Ultimately, hypoxic GBM cells become dormant and stop proliferating resulting in escape from anti-proliferative drugs [178, 179]. Increased hypoxia results in necrosis, one of the key characteristics of glioblastomas and also activates Hypoxia Inducible Factor-1 (HIF-1) transcription factor which regulates more than 40 target genes. HIF-1 is also associated with radiotherapy, studies have shown that HIF-1 protein levels increase post-radiation [180]. They explained this phenomenon by the increased presence of stress granules (protein-mRNA complexes), which leads to the blockage of translation of HIF-1mediated mRNA into target proteins. During radiation, these complexes disaggregate leading to a surge in HIF-1 regulated proteins. Also, excessive formation of free radical species post-radiation results in up-regulation of HIF-1 activity.

GBM drug resistance is determined by several mechanisms such as BBB integrity, ABC transporters, O^6MGMT, GSCs and hypoxia. Although with advancements in the glioma research independent mechanisms associated with epigenetic regulations such as histone modifications, DNA methylations are reported to be involved in resistance mechanisms [181, 182].

Here we studied the effect of glioma therapeutics (chemo and radiotherapy) on ATIP1 expression. We analysed how TMZ and different doses of radiation is affecting ATIP1 expression in glioma cells and if p53 plays any role in ATIP1 expression.

5.2 Results

5.2.1 ATIP1-overexpression doesn't affect TMZ efficacy

Our data and a previous study identified ATIP1 as TSG that regulates the expression of *MMS2* [183]. Besides, in addition to the downregulation of MTUS1 in HGG, also *MMS2* is downregulated in these tumors (Figure 6c). Being *MMS2* a member of the PRRP we suggest that, by modulating DNA-repair mechanisms, ATIP1 might interfere with glioma therapy like irradiation or TMZ-based chemotherapy. TMZ, a DNA damaging drug that is known to induce apoptosis and autophagy in glioma cells, is the only drug available for glioma treatment. However, even if ATIP1 was upregulated by TMZ, its elevated expression did not change the clonogenic survival of TMZ-treated $p53^{WT}$ and $p53^{del}$ cells (Figure 24a) indicating that TMZ-induced DNA damage repair is not influenced by ATIP1. This also suggests that TMZ, not only by inducing DNA damage but also by upregulating ATIP1 in parental and EV cells in a p53-dependent manner, overwhelms the growth of cells which under normal conditions express only low levels of ATIP1 and grow faster than cells that express high levels of ATIP1 (Figure 15a). To explore the effect of TMZ in ATIP1 expression *in vitro*, we treated GSC's (LK7, R11, and R28) and established glioma cells (U87, LNT-229, LN-308, and LN18) and with illustrated concentrations of TMZ. Interestingly we observed that cells show increased ATIP1 expression with TMZ treatment in a dose-dependent manner except for $p53^{-/-}$ (LN-308) and $p53^{mut/mut}$ (LN-18) cells (Figure 24b). TMZ-mediated ATIP1 upregulation *in vitro* reflects also into the *in vivo* findings since in rats harbouring C6 glioma ($p53^{WT}$, Fig.5D), ATIP1 levels were elevated in the TMZ cohort. Immunohistochemistry reveals that TMZ treatment led to an increase in ATIP1 and proliferation marker Ki67 protein expression, indicating reduced proliferation post-TMZ treatment and a decrease in the protein expression of astrocytic marker GFAP as compared to the tumors of the sham cohort (Figure 25).

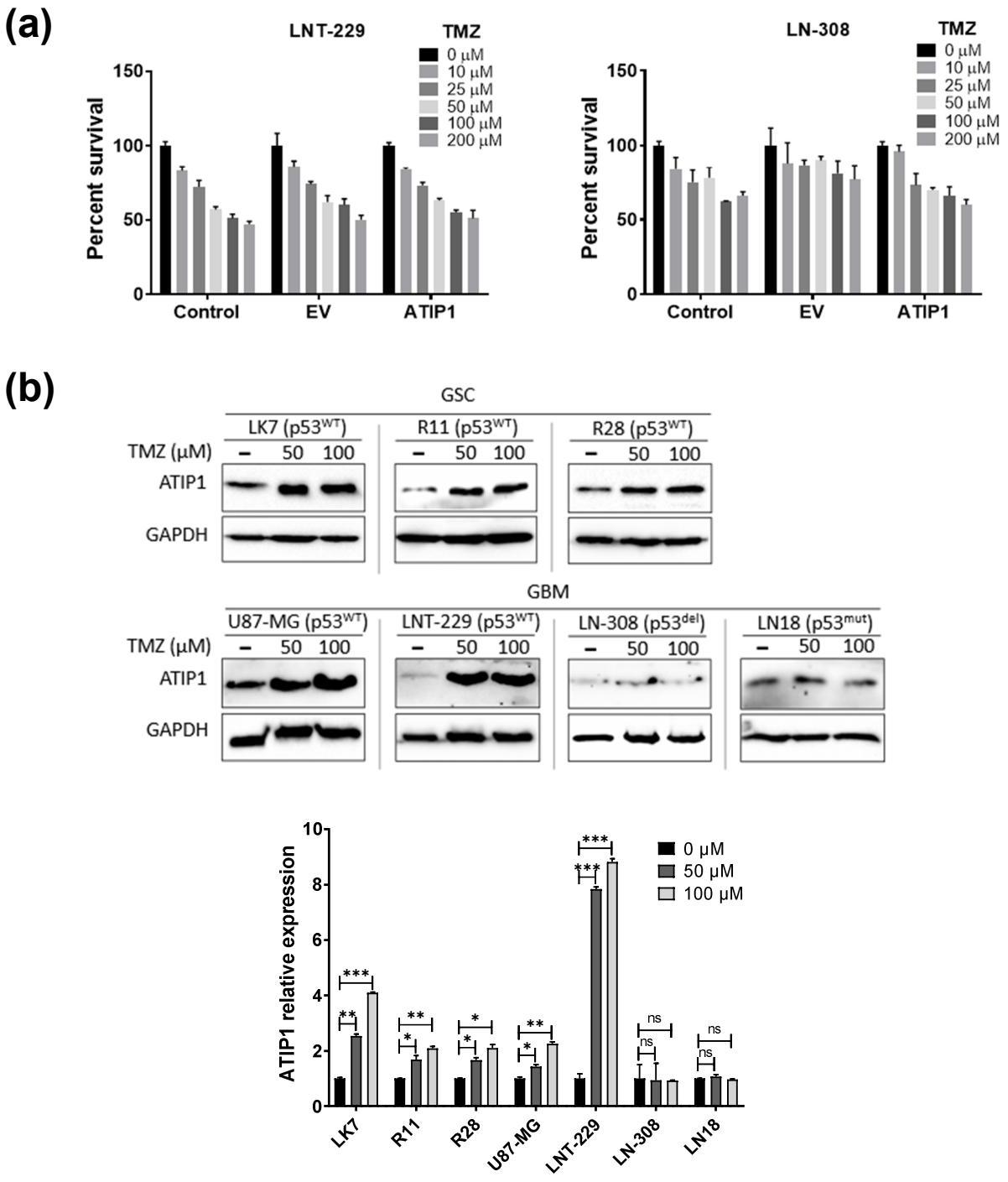

Figure 24. ATIP1 expression is modulated by TMZ Clonogenic survival of TMZ treated parental (control), pcDNA3.1 (EV) and pcDNA3.1-ATIP1 (ATIP1) stably transfected LNT-229 (upper panel) and LN-308 cells (lower panel, n=3, SEM).

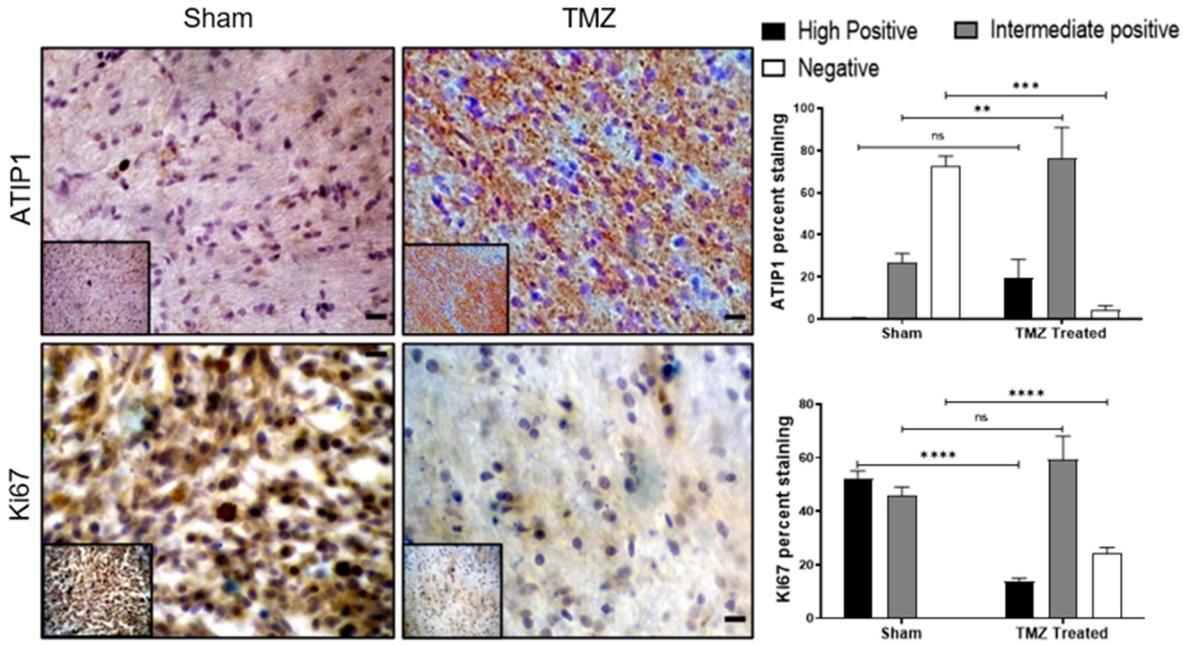

Figure 25. ATIP1 expression is modulated by TMZ ATIP1 and Ki67 expression determined by immunohistochemical staining in sham (n=6) or TMZ treated rats (n=6) harboring C6 glioma (scale = 100 μm). The right panel shows represent the quantification of the represented proteins.

5.2.2 ATIP1-expression is p53 dependent and modulates irradiation-induced growth reduction

To validate the role of p53 in the induction of ATIP1, LNT-229 $p53^{ts}$ cells were subjected to 32.5°C ($p53^{WT}$) or 38.5°C ($p53^{mut}$). A significant increase in ATIP1 was detected only if $p53^{WT}$ was present (Figure 26). Additionally, we irradiated parental LNT-229 cells and observed that the upregulation of ATIP1 was accompanied by upregulation of p53 (Figure 30), indicating that p53 is an inducer of ATIP1 also in glioma cells.

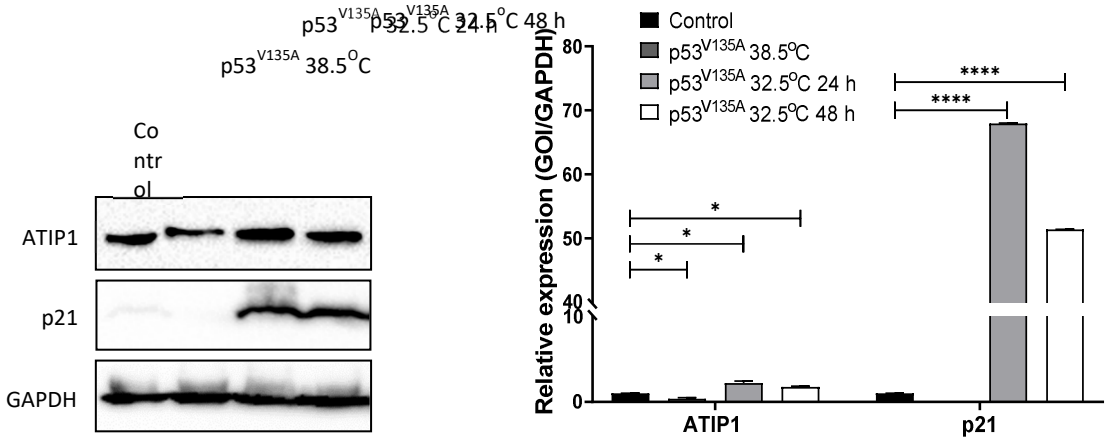

Figure 26. a. GBM and GSC cells were treated with TMZ and assessed for ATIP1 protein expression 72 h later. GAPDH serves as loading control (n=3, one representative experiment is shown). b. Quantification of protein expression after TMZ treatment as indicated in a. (n=3, SEM; ns, * $P < 0.05$, ** $P < 0.01$, *** $P < 0.001$, **** $P < 0.0001$).

5.2.2 Radiotherapy enhances ATIP1 expression

As observed for TMZ, ATIP1 was also upregulated by irradiation in $p53^{WT}$, but not in $p53^{del}$ or $p53^{mut}$ GBM cells (Figure 24b). Similarly, with irradiation to the glioblastoma cells and GSC. ATIP1 expression was significantly upregulated in p53 dependent manner (Figure 27). In order to elucidate the effect of ATIP1 overexpression on radiation treatment, clonogenic assay represented a significant increase in cell viability in ATIP1-cells after irradiation represents that elevated ATIP1 levels lead to elevated survival. Contrarily to TMZ, elevated ATIP1 level interfered with the irradiation-mediated inhibition of clonogenic survival both in $p53^{WT}$ and $p53^{del}$ cells (Figure 28a/b). To determine whether the radio-resistance we observed in the ATIP1 cells *in vitro* reflects the *in vivo* situation, we used the R2-database and correlated *MTUS1* mRNA-expression and survival in patient cohorts that did not or received radiotherapy. Whilst in untreated GBM patients elevated *MTUS1* in the tumor tissue generally correlated with better survival, in the cohort of irradiated patients possessing tumors with higher *MTUS1*-expression, this was slightly but not significantly associated with a worse outcome (Figure 28c).

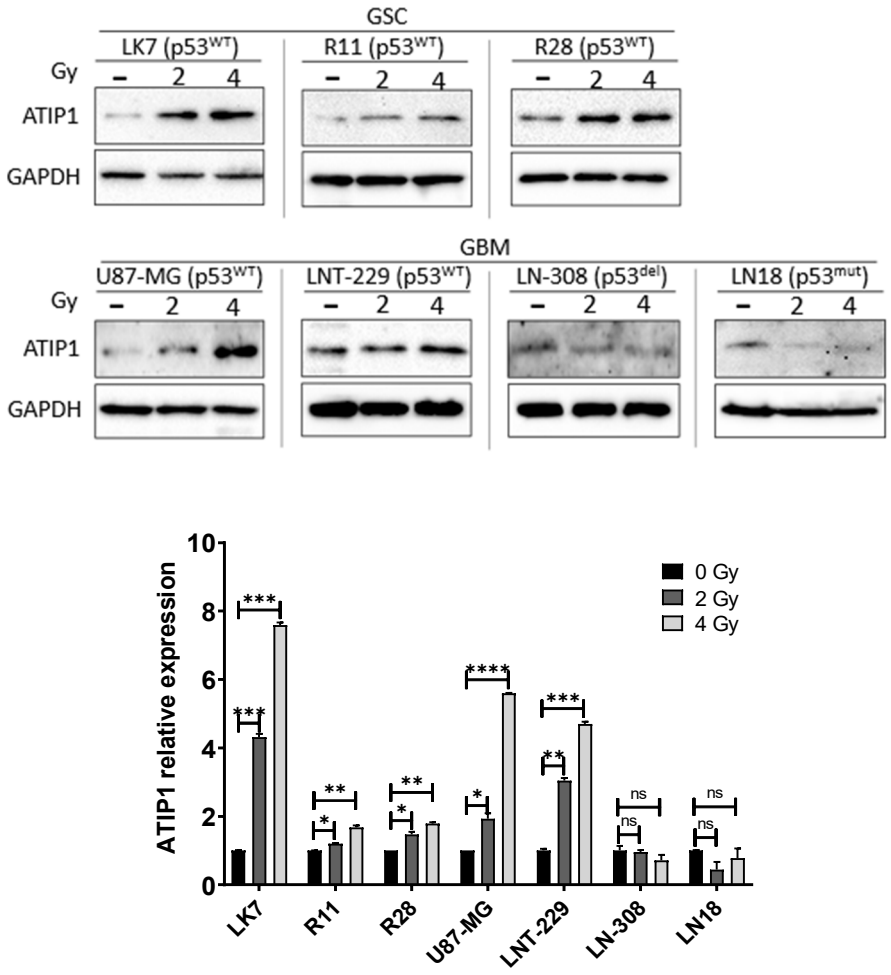

Figure 27. ATIP1 expression is modulated by irradiation. The cells were irradiated with 0 (-), 2 or 4 Gy. ATIP1 protein expression was analysed 24 h later. GAPDH serves as loading control. f. Quantification of ATIP1 expression in irradiated cells as indicated in (e) (n=3, SEM; non-significant: ns, * $P < 0.05$, ** $P < 0.01$, *** $P < 0.001$, **** $P < 0.0001$).

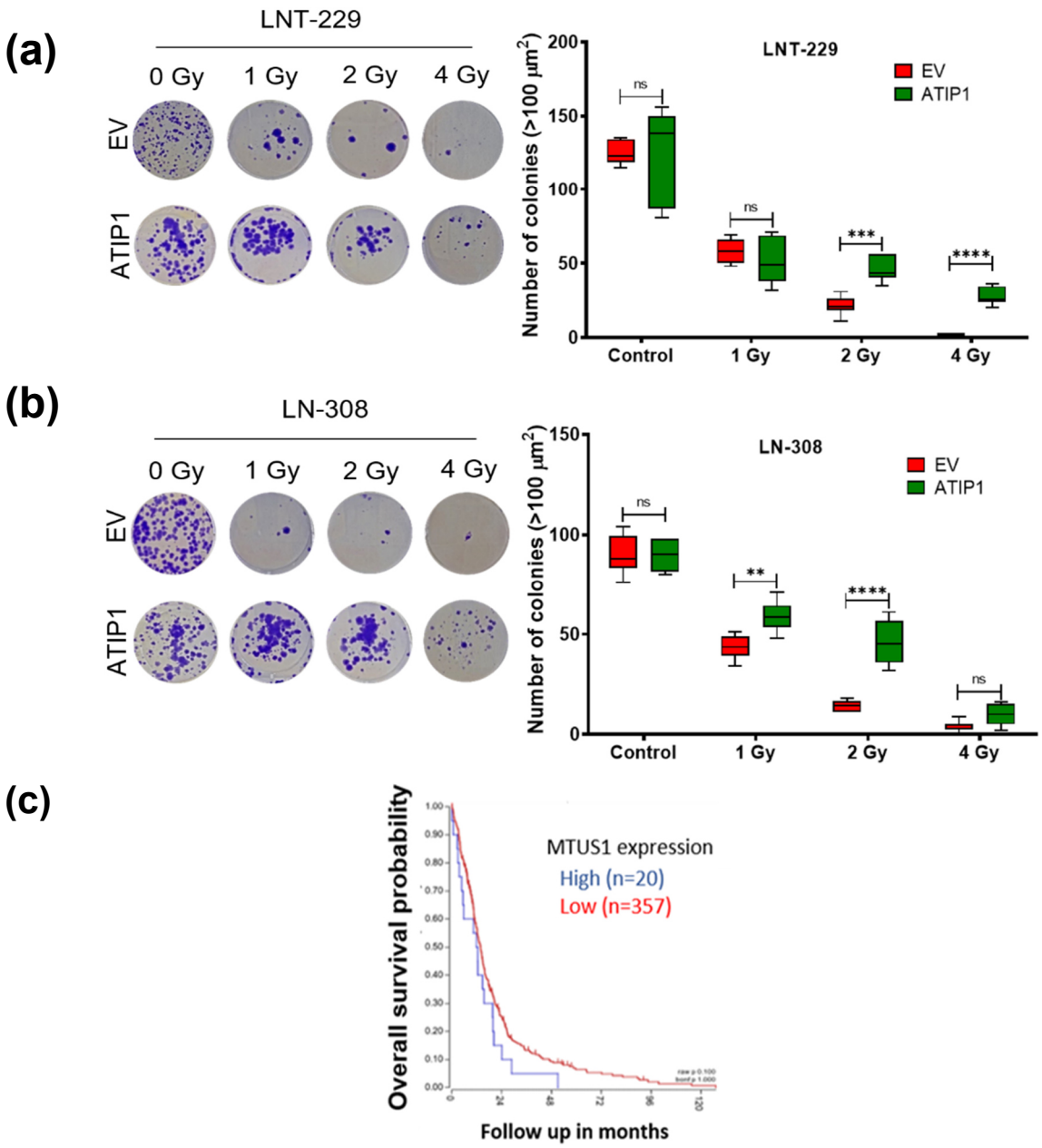

Figure 28. ATIP1 expression is modulated by irradiation. pcDNA3.1 (EV) or pcDNA3.1-ATIP1 (ATIP1) stably transfected LNT-229 (left panels) and LN-308 (right panels) were irradiated with 0, 1, 2 or 4 Gy and clonogenic survival was analysed. The first and third panels exemplarily show the outgrowth of cell clones, the graphs represent the total number of clones (n=3, SEM; non-significant: ns, ** $P < 0.01$, *** $P < 0.001$, **** $P < 0.0001$). Overall survival probability of glioma patients that received tumor irradiation. Patients with high *MTUS1* expression (n=20) showed worse overall survival compared to patients showing low *MTUS1* expression in the tumor (n=357).

5.3 Discussion

One of the major complications for glioma treatment is multidrug resistance (MDR) since the brain is protected by the blood-brain barrier (BBB) which restricts many anti-cancer drugs like vincristine, doxorubicin or erlotinib. The only drug approved by FDA which can cross the BBB for glioma treatment is Temozolomide (TMZ), a DNA alkylating agent. To understand the role of ATIP1 in glioma treatment, we treated GSC's and glioma cells with TMZ and ϒ- radiation (2Gy and 4Gy). Interestingly, the treatments significantly increased the ATIP1 expression in GSC's (LK-7, R11, and R28) and $p53^{WT}$ cells (LNT-229) but not in $p53^{-/-}$ cells (LN-308). This effect could be explained by increased ATIP1 expression in LNT-229 $p53^{V135A}$ transfected cells, where $p53^{WT}$ cells (32.5ºC) results in high expression as compared to the control and $p53^{mut/mut}$ cells (38.5ºC), suggesting that p53 might play a crucial role in the regulation of MTUS1. In order to validate these observations, TMZ treatment (10mg/kg) in an orthotopic intracranial rat model resulted in increased staining for ATIP1 protein in TMZ treated cohort as compared to the sham. TMZ treatment alone does not show any significant difference in the survival of ATIP1 overexpressed cells as compared to the control and EV cells. Major observations of this chapter are summarized in Figure 29.

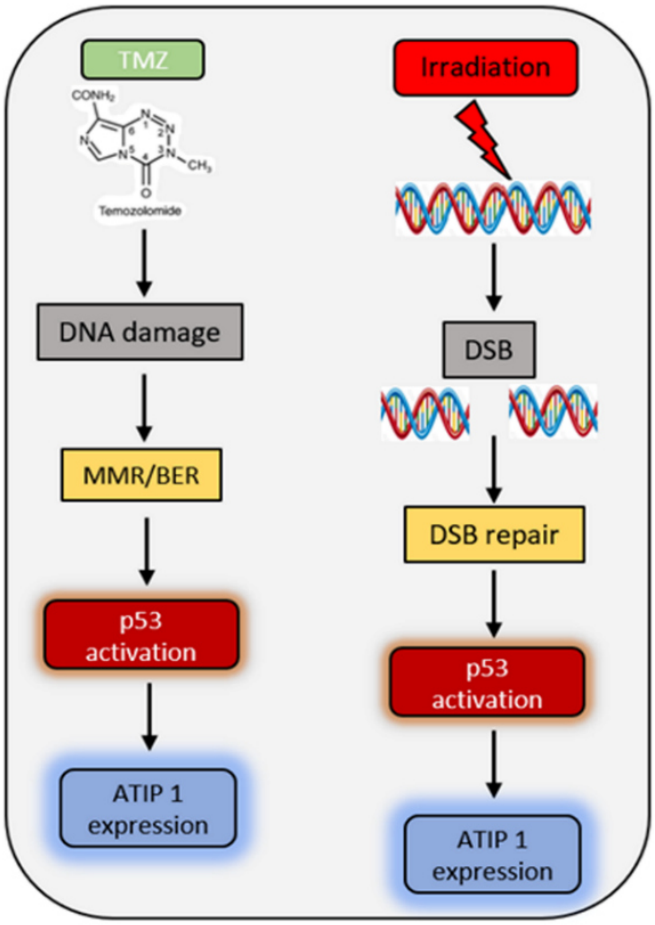

Figure 29. Effect of therapeutic treatments on ATIP1 expression. Representation of p53 mediated increased ATIP1 expression, post TMZ and radiation mediated therapeutic treatments on the established glioma cells and GSC.

Chapter 6

Role of *MTUS1*/ATIP1 in DNA repair

6.1 Introduction

Environmental aspects such as ultraviolet (UV) light, ionizing radiation (IR) and oxidative stress can lead to damage to the genome of cells. The presence of DNA damage leads to transcriptional deregulations and also in the post-transcriptional machinery, thereby leading to the alterations in gene products. The "guardian of the genome", p53 plays a crucial role in cancer development as it acts as and cells are not protected from mutations and genomic aberrations. As one of the most important functions of p53 is the response to DNA damage. Glioma cells which consist of mutated p53 undergo apoptosis through the intrinsic (mitochondrial) pathway.

6.1.1 DNA repair

DNA bases can be damaged through various mechanisms such as oxidative processes, alkylation of bases, base loss caused by the hydrolysis of bases, bulky adduct formation, DNA crosslinking, and DNA strand breaks, including single and double-stranded breaks (DSBs). Cells can repair most of the DNA lesions through a variety of well-evolved DNA repair mechanisms such as nucleotide excision repair (NER), base excision repair (BER), mismatch repair (MMR). Single stand breaks (SSBs) are the most commonly found and are a result of phosphodiester bond disruption between two deoxyribose residues in the backbone of DNA. DSBs are randomly generated in the genome by exogenous agents such as ionizing radiations (IR) and a compound that mimics ionizing radiations also known as radiomimetic drugs. IR interacts with biological compounds, energy gets deposited and the chemical bonds are disrupted which damages the basic components of proteins, lipids and nucleic acids. In the nucleus, direct damage occurs to DNA, producing a variety of lesions of which DSBs have a pivotal role to decide the cellular fate of survival post-radiation exposure. There are endogenous factors as well leading to accidental DSBs which include oxidative damage

replication fork degeneration and telomere erosion [184]. DNA DSBs are generally the most dangerous lesions in eukaryotic cells and are repaired through non-homologous end joining (NHEJ) or homologous recombination (HR). Several programmed events can cause DSBs such as during meiosis, V(D)J recombination and class switching recombination (CSR) necessary for immunoglobulin diversity and function. If the DSBs are left unrepaired or repaired in an inaccurate manner, results in adverse outcomes including mutations and chromosomal aberrations, which can cause cell death as well as genomic instability ultimately leading to the development of cancer. Methylating agents such as TMZ, procarbazine, dacarbazine, streptozotocin induce DNA lesions, which are repaired by repair mechanisms involving MGMT or BER. DNA damage signalling works through blocked replication forks and DSBs by activating the DNA damage response (DDR) kinases through the phosphatidyl-inositol-3-kinase-like protein kinase (PI3KK) family, ataxia telangiectasia mutated (ATM) and ATM and Rad3-related (ATR), respectively [185]. ATM is activated by DSBs and further phosphorylates the key proteins which lead to cell cycle checkpoint arrest or apoptosis. Although ATR also phosphorylates mostly the same proteins that ATM does but ATR, unlike ATM, responds to stalled replication forks and bulky lesions [186]. Histone H2AX is a target for ATM or ATR-mediated phosphorylation and is majorly involved in the transmission of DNA damage signals to downstream molecules Chk1 and Chk2. Phosphorylation of H2AX yields ϒH2AX and it is a marker for initial recognition of DNA damage [187].

6.1.2 Dynamics of ϒH2AX formation and elimination

DSBs lead to an array of damage responses, phosphorylation of the histone core variant H2AX at 139-serine in chromatin domains is one of them. This leads to the formation of discrete nuclear gamma-H2AX (ϒH2AX) foci around the DSB sites, leading to the recruitment of protein complexes to the site for DNA repair [188, 189]. ATM, DNA-PK and ATR are responsible for the induction of histone H2AX phosphorylation *in vivo*, the maximum induction

is observed about 30-60 min after IR [190, 191]. These phosphorylation are eliminated and kinetics of this elimination is correlated with DSB re-joining [192]. The elimination is phosphorylated H2AX from chromatin of irradiated cells is supposed to follow two mechanisms: direct dephosphorylation of ϒH2AX by phosphatases and dephosphorylation by replacement of ϒH2AX molecules with unmodified H2AX [192]. It was reported that the time required for half-elimination of ϒH2AX is correlated with radiosensitivity in vitro and mammalian tissues [193]. Studies have suggested a role of age in ϒH2AX foci formation and elimination, a slight tendency in the delay of ϒH2AX accumulation was observed in old patients [194], also, mammalian tissues differ in the dynamics of ϒH2AX after IR [195] [196] [197]. It has been discovered that IR is not only affecting those cells which are directly exposed but also to the surrounding cells. This phenomenon is known as the “bystander effect” (BE). BE represents that the cells located nearby to the area of irradiation implement the same response as those ones that were irradiated directly [198].

However, we still have to explore the dynamics of ϒH2AX in differentiated mammalian tissues which can be associated with different molecular mechanisms. In this objective, we tried to examine the dynamics of ϒH2AX formation with ectopically overexpressing ATIP1 cell lines after IR.

6.2 Results

6.2.1 ATIP1 promotes DNA double-strand break (DSB) repair

ATIP1-overexpression protected both LNT-229 and LN-308 cells from irradiation-induced cell death and growth inhibition but did not affect TMZ-mediated cytostatic effects (Figure 24a/ Figure 28). In contrast to TMZ that produces the O6-methylation of guanines, irradiation mainly produces DSB. To investigate the dynamics of DNA damage and ATIP1-expression, LNT-229 and LN-308 EV or ATIP1 cells were irradiated and were stained for phosho-γH2A.X, a biomarker for DSB. Phospho-γH2A.X-foci were detectable 15 minutes post-irradiation in both control and ATIP1 cells. As a control for DNA repair, we also irradiated LNT-229-$p53^{ts}$ cells at 32.5°C ($p53^{WT}$) or 38.5°C ($p53^{mut}$) and found a significant decrease in the number of foci 3 hours after irradiation when cultivating the cells at 32.5°C (Figure 30).

However, independent of p53, phospho-γH2A.X foci were nearly absent in ATIP1 cells 3 hours post-irradiation whilst being only slightly reduced in control cells (Figure 31), indicating that ATIP1 boosts DSB-repair. To evaluate if the reduction of phospho-γH2A.X-foci was linked to the p53-mediated induction of ATIP1, we irradiated LNT-229 cells and found that ATIP1-expression increases significantly 3 hours after irradiation (Figure 30) which is the time point we detected a reduction in the number of foci also in control cells (Figure 31). This indicates that ATIP1-expression drives DSB-repair, this way interfering with the irradiation-induced reduction of clonogenic outgrowth.

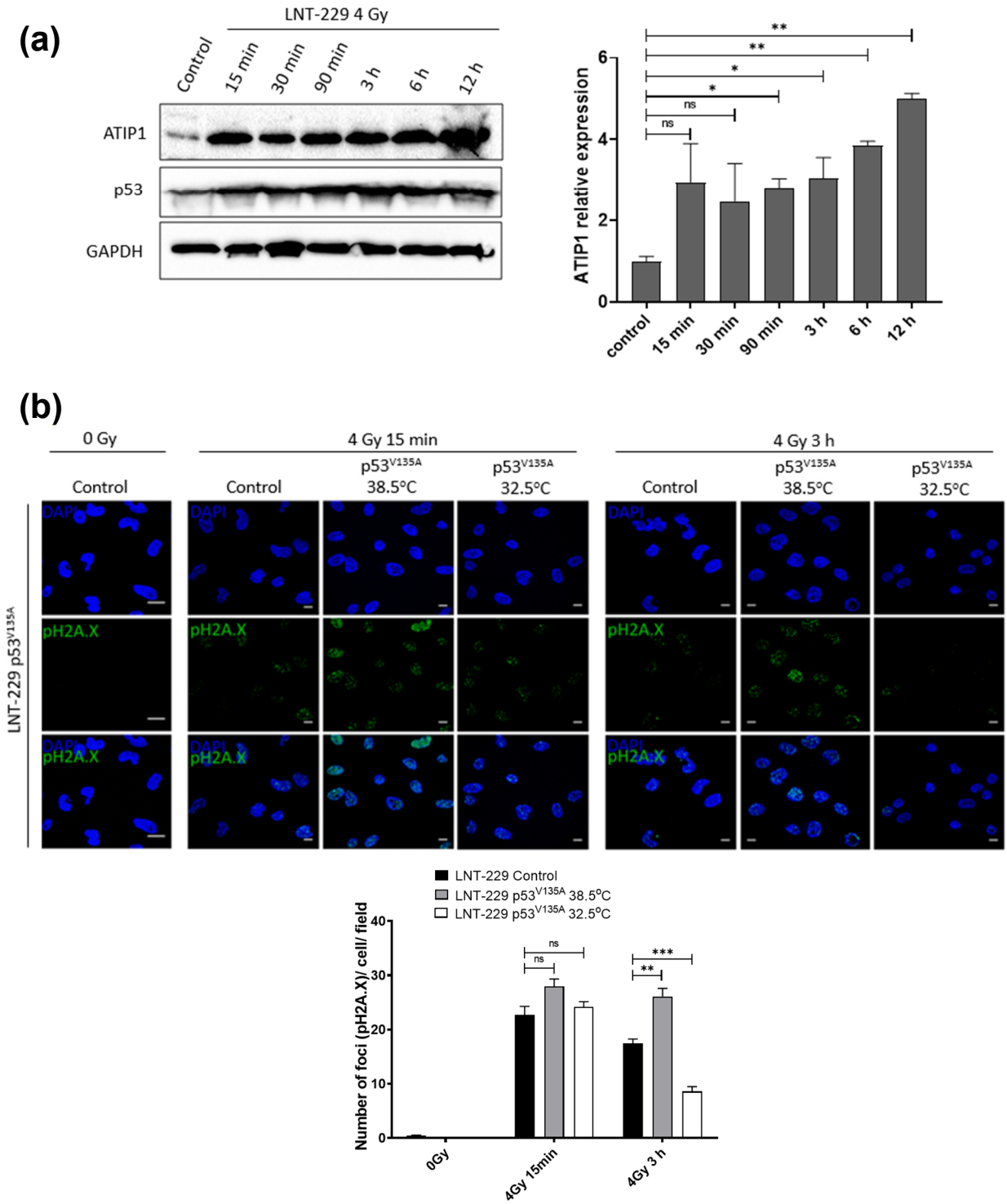

Figure 30. ATIP1 expression post-radiation and H2AX formation and elimination dynamics. In glioma cells, ATIP1 expression enhances the repair of irradiation-induced DNA damage. Immunoblot of ATIP1 and p53 in LNT-229 cells irradiated with 4 Gy. GAPDH serves as a loading control (n=3, one representative blot is shown). Quantification of ATIP1 expression in control or irradiated LNT-229 cells as indicated in a. (n=3, SEM; ns: not significant, * $P < 0.05$, ** $P < 0.01$).

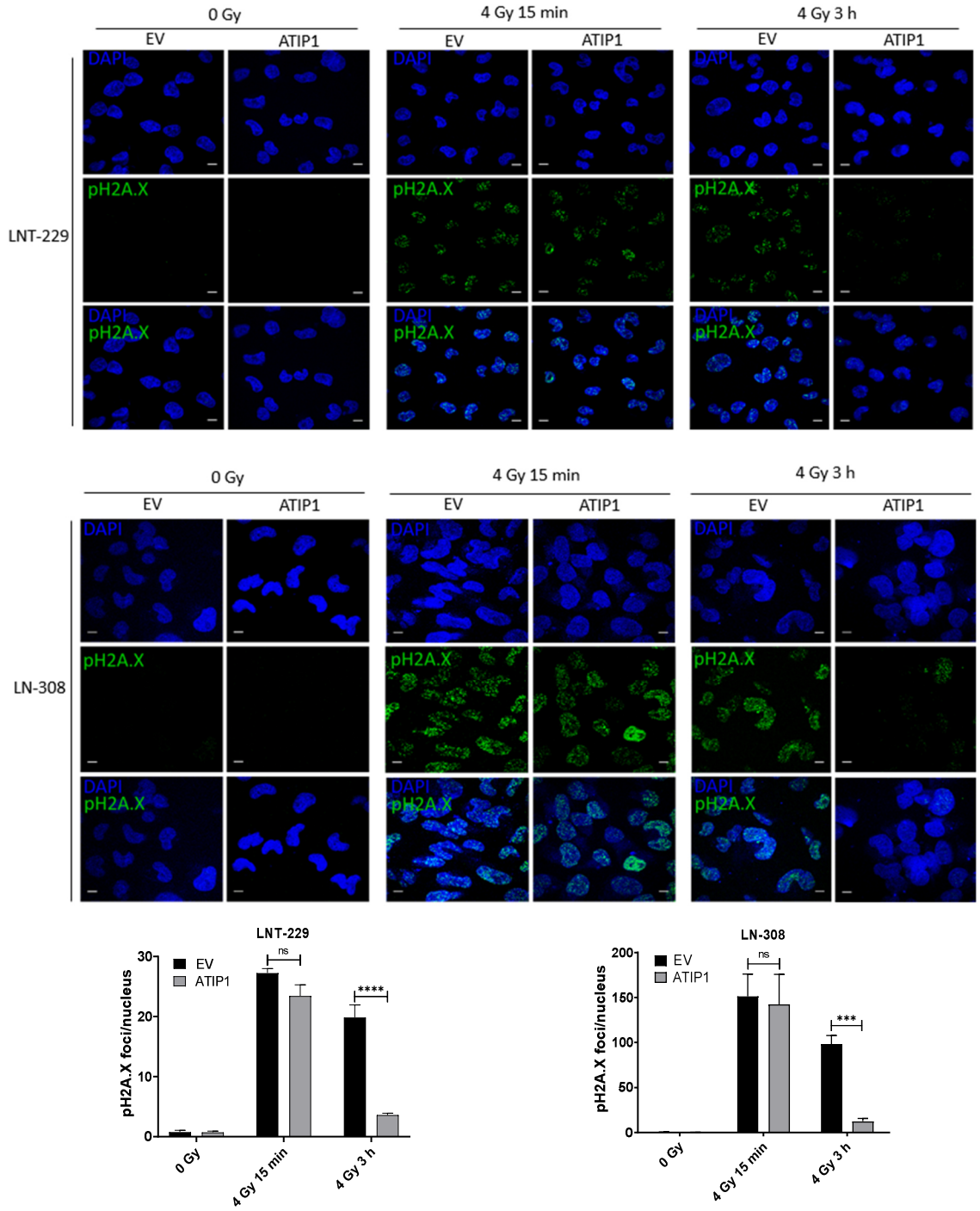

Figure 31. ATIP1 overexpression enhances DNA repair mechanism. In glioma cells ATIP1 expression enhances the repair of irradiation-induced DNA damage. γH2A.X foci formation in control (0 Gy) and irradiated (4 Gy) pcDNA3.1 (EV) and pcDNA3.1-ATIP1 (ATIP1) stably transfected LNT-229 and LN-308 cells at the illustrated time points (scale = 100µm). b. Quantification of γH2A.X foci per nucleus (n=9, SEM; ns: not significant, * $P < 0.05$, ** $P < 0.01$, *** $P < 0.001$, **** $P < 0.0001$). c. A simplified model of the role of ATIP1 in tumor progression.

6.3 Discussion

We also investigated the effect of ϒ- radiation, responsible for causing DSB's. Gliomagenesis also involves errors in DNA replication, DNA repair, and modulation of several signalling cascades associated with genomic mutations. The collection of these alterations gives rise to the "mutator phenotype" in glioma cells and DNA repair mechanisms play a central role in this [199]. Phosphorylation of H2AX at Ser139, a biomarker of DSB's is a critical event in the series of early responses [200, 201]. In order to discover the role of ATIP1 in DNA repair, the LNT-229-EV and LNT-229-ATIP1 stably expressing cells were irradiated with ϒ- rays, responsible for inducing DSB's. Interestingly, we found that with more ATIP1 expression the cells were able to repair the DNA DSB's resulting in fewer H2A.X foci as compared to the EV cells which also results in the survival of the glioma cells. Validation of these results was done by irradiating the LNT-229 $p53^{V135A}$ transfected cells, where the $p53^{WT}$ cells contain a fewer number of foci as compared to the control cells. This clearly explains that ATIP1 assists in DNA repair resulting in fewer foci as compared to the control cells. Although the exact mechanism remains unclear, our results represent that induces p53 expression and hence support the fact that p53 is associated with ATIP1 expression. Also, TMZ is mainly inducing the MMR pathway and hence does not have any significant effect on the survival of the cells. Major observations of this chapter is summarizedin Figure 29.

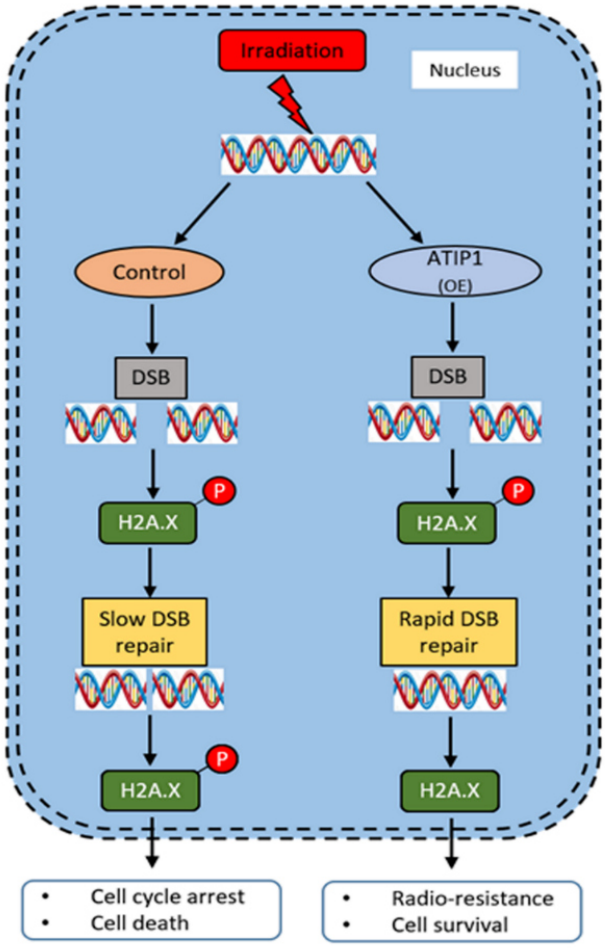

Figure 32. Dynamics of H2AX appearance and elimination. Role of ATIP1 overexpression in DNA repair mechanism, understood through H2A.X dynamics. ATIP1 results in H2A.X dephosphorylation through enhanced DSB repair, ultimately resulting in radio-resistance and cell survival.

Conclusion

7. Conclusion

In our study, we demonstrated that the *MTUS1*/ATIP1 serves as a TSG in glioma. ATIP1 provides multiple tumor-suppressive functions like mitigating proliferation, cell motility and clonogenic survival. Additionally, in glioma *MTUS1*/ATIP1 is a prognostic marker since its expression correlated well with glioma malignancy and survival [87, 202, 203]. However, ATIP1 is an important player in DNA repair processes and this might interfere with DNA damaging tumor therapies and future studies are also needed to explore the molecular mechanisms and epigenetic modifications which will uncover further details of *MTUS1*/ATIP1 regulation.

Nevertheless, ATIP1 has shown promising results to inhibit glioma progression and invasion with a survival benefit in our study. In glioma cells, elevated ATIP1 levels push DNA repair and protect the cells from irradiation-induced DNA damage. Therefore, it should be kept in mind that in HGG patients that possess highly ATIP1 positive tumors, even being ATIP1 correlated with a better basal outcome, the elevated expression of ATIP1 might interfere with the anti-tumoral effects of irradiation. However, ATIP1 down-regulation can be used as a promising biomarker for glioma onset and progression. Although we have not explored the involvement of the complete RAS with glioma progression, but our study demonstrates that targeting this pathway can help us to understand the gliomagenesis.

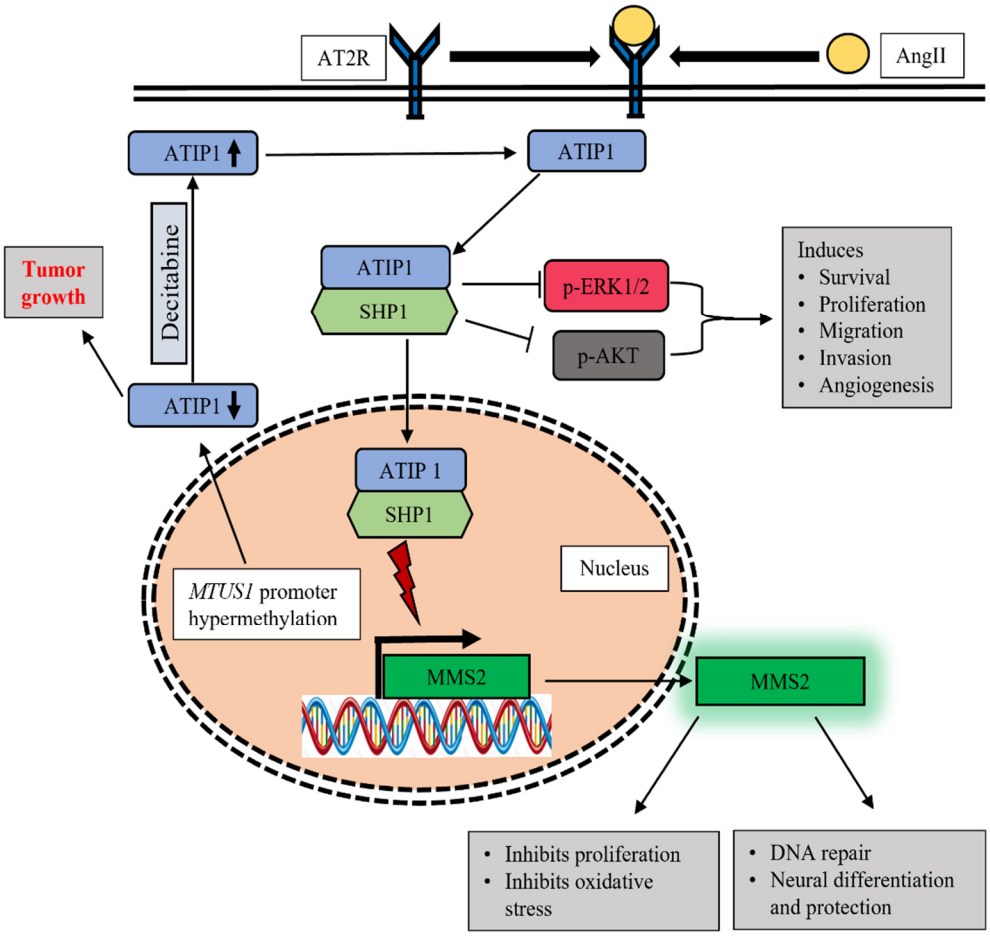

Figure 32. Role of ATIP1 in glioma. Representation of pathway followed by ATIP1, a transcript variant of *MTUS1*. ATIP1 interacts with SHP1 and this complex results in inhibition of ERK1/2, resulting in inhibition of proliferation and migration. Further ATIP1-SHP1 complex is translocated into the nucleus where it triggers the expression of MMS2 which plays a crucial role in DNA repair, neural differentiation and inhibits proliferation.

8. References

1. Stupp, R., et al., *Effect of Tumor-Treating Fields Plus Maintenance Temozolomide vs Maintenance Temozolomide Alone on Survival in Patients With Glioblastoma: A Randomized Clinical Trial.* JAMA, 2017. **318**(23): p. 2306-2316.
2. Chakrabarti, I., et al., *A population-based description of glioblastoma multiforme in Los Angeles County, 1974-1999.* Cancer, 2005. **104**(12): p. 2798-806.
3. Beier, D., et al., *CD133(+) and CD133(-) glioblastoma-derived cancer stem cells show differential growth characteristics and molecular profiles.* Cancer Res, 2007. **67**(9): p. 4010-5.
4. Adamson, C., et al., *Glioblastoma multiforme: a review of where we have been and where we are going.* Expert Opin. Investig. Drugs, 2009. **18**(8): p. 1061-1083.
5. Stupp, R., et al., *Effects of radiotherapy with concomitant and adjuvant temozolomide versus radiotherapy alone on survival in glioblastoma in a randomised phase III study: 5-year analysis of the EORTC-NCIC trial.* The Lancet Oncology, 2009. **10**(5): p. 459-466.
6. Zhang, J., M.F.G. Stevens, and T.D. Bradshaw, *Temozolomide: Mechanisms of Action, Repair and Resistance.* Current Molecular Pharmacology, 2012. **5**(1): p. 102-114.
7. Marosi, C. and M. Preusser, *Milestones of the last 10 years: CNS cancer.* Memo, 2017. **10**(1): p. 18-21.
8. Krex, D., et al., *Long-term survival with glioblastoma multiforme.* Brain, 2007. **130**(Pt 10): p. 2596-606.
9. Han, S., et al., *IDH mutation in glioma: molecular mechanisms and potential therapeutic targets.* Br J Cancer, 2020. **122**(11): p. 1580-1589.

10. Unruh, D., et al., *Methylation and transcription patterns are distinct in IDH mutant gliomas compared to other IDH mutant cancers.* Sci Rep, 2019. **9**(1): p. 8946.

11. Bledea, R., et al., *Functional and topographic effects on DNA methylation in IDH1/2 mutant cancers.* Sci Rep, 2019. **9**(1): p. 16830.

12. Zou, P., et al., *IDH1/IDH2 mutations define the prognosis and molecular profiles of patients with gliomas: a meta-analysis.* PLoS One, 2013. **8**(7): p. e68782.

13. SongTao, Q., et al., *IDH mutations predict longer survival and response to temozolomide in secondary glioblastoma.* Cancer Sci, 2012. **103**(2): p. 269-73.

14. Yan, H., et al., *IDH1 and IDH2 Mutations in Gliomas.* N Engl J Med, 2009. **360**: p. 765-73.

15. Badur, M.G., et al., *Oncogenic R132 IDH1 Mutations Limit NADPH for De Novo Lipogenesis through (D)2-Hydroxyglutarate Production in Fibrosarcoma Sells.* Cell Rep, 2018. **25**(4): p. 1018-1026 e4.

16. Mardis, E.R., et al., *Recurring Mutations Found by Sequencing an Acute Myeloid Leukemia Genome.* The new england journal of medicine, 2009. **361**(11): p. 1058-1066.

17. Bleeker, F.E., et al., *The prognostic IDH1(R132) mutation is associated with reduced NADP+-dependent IDH activity in glioblastoma.* Acta Neuropathol, 2010. **119**(4): p. 487-94.

18. Bleeker, F.E., et al., *IDH1 mutations at residue p.R132 (IDH1(R132)) occur frequently in high-grade gliomas but not in other solid tumors.* Hum Mutat, 2009. **30**(1): p. 7-11.

19. Ohgaki, H. and P. Kleihues, *The Definition of Primary and Secondary Glioblastoma.* Clinical Cancer Research, 2012: p. 764-773.

20. Louis, D.N., et al., *The 2016 World Health Organization Classification of Tumors of the Central Nervous System: a summary.* Acta Neuropathol, 2016. **131**: p. 803–820.

21. Almutrafi, A., et al., *The Epidemiology of Primary Central Nervous System Tumors at the National Neurologic Institute in Saudi Arabia: A Ten-Year Single-Institution Study.* Journal of Cancer Epidemiology, 2020. **2020**: p. 1429615.

22. Sanai, N., A. Alvarez-Buylla, and M.S. Berger, *Neural Stem Cells and the Origin of Gliomas.* N. Engl. J. Med., 2005. **353**: p. 811-822.

23. Eriksson, P.S., et al., *Neurogenesis in the adult human hippocampus.* Nature Medicine, 1998. **4**: p. 1313-1317.

24. Nunes, M.C., et al., *Identification and isolation of multipotential neural progenitor cells from the subcortical white matter of the adult human brain.* Nat Med, 2003. **9**(4): p. 439-47.

25. SHOSHAN, Y., et al., *Expression of oligodendrocyte progenitor cell antigens by gliomas: Implications for the histogenesis of brain tumors.* Proc. Natl. Acad. Sci., 1999. **96**: p. 10361–10366.

26. Roy, N.S., et al., *Identification, Isolation, and Promoter-Defined Separation of Mitotic Oligodendrocyte Progenitor Cells from the Adult Human Subcortical White Matter.* The Journal of Neuroscience, 1999. **19**: p. 9986–9995.

27. Kim, S.U., *Antigen Expression by Glial Cells Grown in Culture.* Journal of Neuroimmunology, 1985. **8**: p. 255-282.

28. Fidler, P.S., et al., *Comparing Astrocytic Cell Lines that Are Inhibitory or Permissive for Axon Growth: the Major Axon-Inhibitory Proteoglycan Is NG2.* The Journal of Neuroscience, 1999. **19**: p. 8778–8788.

29. Hou, L.C., et al., *Recurrent glioblastoma multiforme: a review of natural history and management options.* Neurosurg Focus, 2006. **20**(4).

30. LEE, S.W., et al., *Patterns of failure following high-dose 3-d conformal radiotherapy for high-grade astrocytomas: a quantitative dosimetric study.* int. j. radiation oncology biol. phys., 1999. **43**(1): p. 79–88.

31. Gaspar, L.E., et al., *Supratentorial Malignant Glioma: Patterns of Recurrence and Implications For External Beam Local Treatment.* int. J. Radiation Oncology Biol. Phys., 1992. **24**: p. 55-57.

32. Halperin, E.C., P.C. Burger, and D.E. Bullard, *The Fallacy of The Localized Supratentorial Malignant Glioma.* Int. J. Radiation Oncology Biol. Phys., 1988. **15**: p. 505-509.

33. Kim, H., et al., *Whole-genome and multisector exome sequencing of primary and post-treatment glioblastoma reveals patterns of tumor evolution.* Genome Res, 2015. **25**(3): p. 316-27.

34. Kim, J., et al., *Spatiotemporal Evolution of the Primary Glioblastoma Genome.* Cancer Cell, 2015. **28**(3): p. 318-28.

35. Zou, J.-P., et al., *Human Glioma-Induced Immunosuppression Involves Soluble Factor(s) That Alters Monocyte Cytokine Profile and Surface Markers.* J Immunol, 1999. **162**: p. 4882-4892.

36. Parsa, A.T., et al., *Loss of tumor suppressor PTEN function increases B7-H1 expression and immunoresistance in glioma.* Nat Med, 2007. **13**(1): p. 84-8.

37. Wainwright, D.A., et al., *IDO expression in brain tumors increases the recruitment of regulatory T cells and negatively impacts survival.* Clin Cancer Res., 2012. **18**: p. 6110–6121.

38. Zagzag, D., et al., *Downregulation of major histocompatibility complex antigens in invading glioma cells: stealth invasion of the brain.* Lab Invest, 2005. **85**(3): p. 328-41.

39. Wagner, S., et al., M*icroglial/Macrophage expression of interleukin 10 in human glioblastomas.* Int. J. Cancer, 1999. **82**: p. 12-16.

40. Kaminska, B., M. Kocyk, and M. Kijewska, *TGF beta signaling and its role in glioma pathogenesis.* Adv Exp Med Biol, 2013. **986**: p. 171-87.

41. Colombo, M.P. and S. Piconese, *Regulatory T-cell inhibition versus depletion: the right choice in cancer immunotherapy.* Nature Reviews, 2007. **7**.

42. Nduom, E.K., M. Weller, and A.B. Heimberger, *Immunosuppressive mechanisms in glioblastoma.* Neuro Oncol, 2015. **17 Suppl 7**: p. vii9-vii14.

43. Weller, M., et al., *CD95-Dependent T-Cell Killing by Glioma Cells Expressing CD95 Ligand: More on Tumor Immune Escape, the CD95 Counterattack, and the Immune Privilege of the Brain.* Cellular Physiology and Biochemistry, 1997. **7**: p. 282-288.

44. Lou, J., et al., *Brain microvascular endothelial cells and leukocytes derived from patients with multiple sclerosis exhibit increased adhesion capacity.* NeuroReport, 1997. **8**: p. 629–633.

45. Claudio, L., *Ultrastructural features of the blood-brain barrier in biopsy tissue from Alzheimer's disease patients.* Acta Neuropathol, 1996. **91**: p. 6–14.

46. Darvin, P., et al., *Immune checkpoint inhibitors: recent progress and potential biomarkers.* Experimental & Molecular Medicine, 2018. **50**: p. 1-11.

47. Lacroix, M., et al., *A multivariate analysis of 416 patients with glioblastoma multiforme: prognosis, extent of resection, and survival.* J. Neurosurg., 2001. **95**.

48. Stupp, R., et al., *Radiotherapy plus Concomitant and Adjuvant Temozolomide for Glioblastoma.* N Engl J Med, 2005. **352**: p. 987-96.

49. Wood, J.R., S.B. Green, and W.R. Shapiro, *The Prognostic Importance of Tumor Size in Malignant Gliomas: A Computed Tomographic Scan Study by the Brain Tumor Cooperative Group.* J Clin Oncol, 1988. **6**: p. 338-343.

50. Hau, P., et al., *Salvage therapy in patients with glioblastoma: is there any benefit?* Cancer, 2003. **98**(12): p. 2678-86.

51. Denny, B.J., et al., *NMR and Molecular Modeling Investigation of the Mechanism of Activation of the Antitumor Drug Temozolomide and Its Interaction with DNA.* Biochemistry, 1994. **33**: p. 9045-9051.

52. Jain, R.K., et al., *Angiogenesis in brain tumours.* Nat Rev Neurosci, 2007. **8**(8): p. 610-22.

53. Fidler, I.J. and L.M. Ellis, *The Implications of Angiogenesis for the-Biology and Therapy of Cancer Metastasis.* Cell 1994. **79**: p. 185-188.

54. D'amato, R.J., et al., *Thalidomide is an inhibitor of angiogenesis.* Proc. Nati. Acad. Sci. , 1994. **91**: p. 4082-4085.

55. Kerbel, R. and J. Folkman, *Clinical translation of angiogenesis inhibitors.* Nat Rev Cancer, 2002. **2**(10): p. 727-39.

56. Chan, L.S., J. Daruwalla, and C. Christophi, *Selective targeting of the tumour vasculature.* ANZ J Surg, 2008. **78**(11): p. 955-67.

57. Sadelain, M., *Chimeric antigen receptors: driving immunology towards synthetic biology.* Curr Opin Immunol., 2016. **41**: p. 68–76.

58. Bagley, S.J., et al., *CAR T-cell therapy for glioblastoma: recent clinical advances and future challenges.* Neuro-Oncology, 2018. **20**: p. 1429–1438.

59. Dagogo-Jack, I., et al., *Treatment of brain metastases in the modern genomic era.* Pharmacol Ther, 2017. **170**: p. 64-72.

60. Kirson, E.D., et al., *Alternating electric fields arrest cell proliferation in animal tumor models and human brain tumors.* PNAS, 2007. **104**: p. 10152–10157.

61. Giladi, M., et al., *Mitotic Spindle Disruption by Alternating Electric Fields Leads to Improper Chromosome Segregation and Mitotic Catastrophe in Cancer Cells.* Sci Rep, 2015. **5**: p. 18046.

62. Sadelain, M., R. Brentjens, and I. Riviere, *The basic principles of chimeric antigen receptor design.* Cancer Discov, 2013. **3**(4): p. 388-98.

63. Newick, K., et al., *CAR T Cell Therapy for Solid Tumors.* Annu Rev Med, 2017. **68**: p. 139-152.

64. Di Benedetto, M., et al., *Structural organization and expression of human MTUS1, a candidate 8p22 tumor suppressor gene encoding a family of angiotensin II AT2 receptor-interacting proteins, ATIP.* Gene, 2006. **380**(2): p. 127-36.

65. Pohl, U., et al., *p53 Enhances BAK and CD95 Expression in Human Malignant Glioma Cells but Does Not Enhance CD95L-Induced Apoptosis.* Cell Physiol Biochem, 1999. **9**: p. 29–37.

66. Meir, E.G.V., et al., *Analysis of the p53 Gene and Its Expression in Human Glioblastoma Cells1.* Cancer Research, 1994. **54**: p. 649-652.

67. Naumann, U., et al., *Chimeric Tumor Suppressor 1, a p53-derived Chimeric Tumor Suppressor Gene, Kills p53 Mutant and p53 Wild-type Glioma Cells in Synergy with Irradiation and CD95 Ligand.* Cancer Research, 2001(61): p. 5833–5842.

68. Wesseling, P. and D. Capper, *WHO 2016 Classification of gliomas.* Neuropathol Appl Neurobiol, 2018. **44**(2): p. 139-150.

69. Schindelin, J., et al., *Fiji: an open-source platform for biological-image analysis.* Nat Methods, 2012. **9**(7): p. 676-82.

70. Baumann, B.C., et al., *Stereotactic intracranial implantation and in vivo bioluminescent imaging of tumor xenografts in a mouse model system of glioblastoma multiforme.* J Vis Exp, 2012(67).

71. Pandey, V., et al., *Roscovitine effectively enhances antitumor activity of temozolomide in vitro and in vivo mediated by increased autophagy and Caspase-3 dependent apoptosis.* Sci Rep, 2019. **9**(1): p. 5012.

72. Zanotto-Filho, A., et al., *Autophagy inhibition improves the efficacy of curcumin/temozolomide combination therapy in glioblastomas.* Cancer Lett, 2015. **358**(2): p. 220-231.

73. McDuff, F.K. and S.D. Turner, *Jailbreak: oncogene-induced senescence and its evasion.* Cell Signal, 2011. **23**(1): p. 6-13.

74. Joyce, C., A. Rayi, and A. Kasi, *Tumor-Suppressor Genes*. 2020, NCBI Bookshelf.

75. Chow, A.Y., *Cell Cycle Control by Oncogenes and Tumor Suppressors: Driving the Transformation of Normal Cells into Cancerous Cells*. 2010, Nature Education.

76. Osada, H. and T. Takahashi, *Genetic alterations of multiple tumor suppressors and oncogenes in the carcinogenesis and progression of lung cancer.* Oncogene, 2002. **21**: p. 7421 – 7434.

77. Toss, A., et al., *Hereditary ovarian cancer: not only BRCA 1 and 2 genes.* Biomed Res Int, 2015. **2015**: p. 341723.

78. Krug, U., A. Ganser, and H.P. Koeffler, *Tumor suppressor genes in normal and malignant hematopoiesis.* Oncogene ,, 2002. **21**: p. 3475 - 3495.

79. Kotsopoulos, J., *BRCA Mutations and Breast Cancer Prevention.* Cancers (Basel), 2018. **10**(12).

80. Leiderman, Y.I., S. Kiss, and S. Mukai, *Molecular genetics of RB1--the retinoblastoma gene.* Semin Ophthalmol, 2007. **22**(4): p. 247-54.

81. Smith, A.L., T.P. Robin, and H.L. Ford, *Molecular pathways: targeting the TGF-beta pathway for cancer therapy.* Clin Cancer Res, 2012. **18**(17): p. 4514-21.

82. Savage, K.I. and D.P. Harkin, *BRCA1, a 'complex' protein involved in the maintenance of genomic stability.* FEBS J, 2015. **282**(4): p. 630-46.

83. Nayak, S.K., P.S. Panesar, and H. Kumar, *p53-Induced Apoptosis and Inhibitors of p53.* Current Medicinal Chemistry, 2009. **16**(21): p. 2627-2640.

84. Rahman, N. and R.H. Scott, *Cancer genes associated with phenotypes in monoallelic and biallelic mutation carriers: new lessons from old players.* Hum Mol Genet, 2007. 16 Spec No 1: p. R60-6.

85. Bozgeyik, I., O. Yumrutas, and E. Bozgeyik, *MTUS1, a gene encoding angiotensin-II type 2 (AT2) receptor-interacting proteins, in health and disease, with special emphasis on its role in carcinogenesis.* Gene, 2017. **626**: p. 54-63.

86. Ozcan, O., et al., *MTUS1 and its targeting miRNAs in colorectal carcinoma: significant associations.* Tumour Biol, 2016. **37**(5): p. 6637-45.

87. Ding, X., et al., *Down-regulation of tumor suppressor MTUS1/ATIP is associated with enhanced proliferation, poor differentiation and poor prognosis in oral tongue squamous cell carcinoma.* Mol Oncol, 2012. **6**(1): p. 73-80.

88. Seibold, S., et al., *Identification of a new tumor suppressor gene located at chromosome 8p21.3-22.* FASEB journal : official publication of the Federation of American Societies for Experimental Biology, 2003. **17**(9): p. 1180-1182.

89. Gallo-Payet, N., et al., *Angiotensin II, a Neuropeptide at the Frontier between Endocrinology and Neuroscience: Is There a Link between the Angiotensin II Type 2 Receptor and Alzheimer's Disease?* Front Endocrinol (Lausanne), 2011. **2**: p. 17.

90. Guimond, M.O. and N. Gallo-Payet, *The Angiotensin II Type 2 Receptor in Brain Functions: An Update.* Int J Hypertens, 2012. **2012**: p. 351758.

91. Pinter, M. and R.K. Jain, *Targeting the renin-angiotensin system to improve cancer treatment: Implications for immunotherapy.* Science Translational Mdeicine, 2017. **9**: p. 1-11.

92. Chen, Z., et al., *p53 regulates the expression of human angiotensin II AT(2) receptor interacting protein (ATIP1) gene.* Oncol Lett, 2011. **2**(5): p. 919-922.

93. Nouet, S., et al., *Trans-inactivation of receptor tyrosine kinases by novel angiotensin II AT2 receptor-interacting protein, ATIP.* J Biol Chem, 2004. **279**(28): p. 28989-97.

94. Fuchtbauer, L., et al., *Expression of astrocytic type 2 angiotensin receptor in central nervous system inflammation correlates with blood-brain barrier breakdown.* J Mol Neurosci, 2010. **42**(1): p. 89-98.

95. Rodrigues-Ferreira, S., et al., *AT2 Receptor-Interacting Proteins ATIPs in the Brain.* Int J Hypertens, 2013. **2013**: p. 513047.

96. Broomfield, S., B.L. Chow, and W. Xiao, *MMS2, encoding a ubiquitin-conjugating-enzyme-like protein, is a member of the yeast error-free postreplication repair pathway.* Proc. Natl. Acad. Sci. Genetics, 1998. **95**: p. 5678–5683.

97. Klutstein, M., et al., *DNA Methylation in Cancer and Aging.* Cancer Res, 2016. **76**(12): p. 3446-50.

98. Brien, G.L., D.G. Valerio, and S.A. Armstrong, *Exploiting the Epigenome to Control Cancer-Promoting Gene-Expression Programs.* Cancer Cell, 2016. **29**(4): p. 464-476.

99. Feinberg, A.P., R. Ohlsson, and S. Henikoff, *The epigenetic progenitor origin of human cancer.* Nat Rev Genet, 2006. **7**(1): p. 21-33.

100. Jones, P.A. and S.B. Baylin, *The fundamental role of epigenetic events in cancer.* Nat Rev Genet, 2002. **3**(6): p. 415-28.

101. Dabrowski, M.J. and B. Wojtas, *Global DNA Methylation Patterns in Human Gliomas and Their Interplay with Other Epigenetic Modifications.* Int J Mol Sci, 2019. **20**(14).

102. Feinberg, A.P. and B. Vogelstein, *Hypomethylation distinguishes genes of some human cancers from their normal counterparts.* Nature. **301**: p. 89-92.

103. Holliday, R. and J.E. Pugh, *DNA Modification Mechanisms and Gene Activity during Development.* Science, 1975. **187**: p. 226-232.

104. Kitange, G.J., et al., *Evaluation of MGMT promoter methylation status and correlation with temozolomide response in orthotopic glioblastoma xenograft model.* J Neurooncol, 2009. **92**(1): p. 23-31.

105. Bird, A., *DNA methylation patterns and epigenetic memory.* Genes Dev, 2002. **16**(1): p. 6-21.

106. Colot, V. and J.-L. Rossignol, *Eukaryotic DNA methylation as an evolutionary device.* BioEssays, 1999. **21**: p. 402–411.

107. Reik, W., G. Kelsey, and J. Walter, *Dissecting de novo methylation.* nature genetics, 1999. **23**: p. 380-382.

108. Li, E., T.H. Bestor, and R. Jaenisch, *Targeted Mutation of the DNA Methyltransferase Gene Results in Embryonic Lethality.* Cell, 1992. **69**: p. 915-926.

109. Gonzalo, S., et al., *DNA methyltransferases control telomere length and telomere recombination in mammalian cells.* Nat Cell Biol, 2006. **8**(4): p. 416-24.

110. Baylin, S.B., S.A. Belinsky, and J.G. Herman, *Aberrant Methylation of Gene Promoters in Cancer—Concepts, Misconcepts, and Promise.* Journal of the National Cancer Institute, 2000. **92**: p. 1460-1461.

111. Freitas, M.A., A.R. Sklenar, and M.R. Parthun, *Application of mass spectrometry to the identification and quantification of histone post-translational modifications.* J Cell Biochem, 2004. **92**(4): p. 691-700.

112. Luger, K., et al., *Crystal structureof thenucleosome core particle at 2.8A˚ resolution.* Nature, 1997. **389**: p. 251-260.

113. Vaissiere, T., C. Sawan, and Z. Herceg, *Epigenetic interplay between histone modifications and DNA methylation in gene silencing.* Mutat Res, 2008. **659**(1-2): p. 40-8.

114. Happold, C., et al., *Distinct molecular mechanisms of acquired resistance to temozolomide in glioblastoma cells.* J Neurochem, 2012. **122**(2): p. 444-55.

115. Mantwill, K., et al., *YB-1 dependent oncolytic adenovirus efficiently inhibits tumor growth of glioma cancer stem like cells.* Journal of Translational Medicine, 2013. **11**: p. 1-13.

116. Beier, C.P., et al., *Aberrant neuronal differentiation is common in glioma but is associated neither with epileptic seizures nor with better survival.* Sci Rep, 2018. **8**(1): p. 14965.

117. Ishii, N., et al., *Frequent Co-Alterations of TP53, p16/CDKN2A, p14ARF, PTEN Tumor Suppressor Genes in Human Glioma Cell Lines.* Brain Pathology, 1999. **9**: p. 469-479.

118. Hermisson, M., et al., *O6-methylguanine DNA methyltransferase and p53 status predict temozolomide sensitivity in human malignant glioma cells.* J Neurochem, 2006. **96**(3): p. 766-76.

119. Cancer Genome Atlas Research, N., *Comprehensive genomic characterization defines human glioblastoma genes and core pathways.* Nature, 2008. **455**(7216): p. 1061-8.

120. Parsons, D.W., et al., *An Integrated Genomic Analysis of Human Glioblastoma Multiforme.* SCIENCE, 2008. **321**: p. 1807-1812.

121. Zuern, C., et al., *Down-regulation of MTUS1 in human colon tumors.* Oncology Reports, 2009. **23**(1).

122. Rodrigues-Ferreira, S., et al., *8p22 MTUS1 gene product ATIP3 is a novel anti-mitotic protein underexpressed in invasive breast carcinoma of poor prognosis.* PLoS One, 2009. **4**(10): p. e7239.

123. Parbin, S., et al., *DNA methylation regulates Microtubule-associated tumor suppressor 1 in human non-small cell lung carcinoma.* Exp Cell Res, 2019. **374**(2): p. 323-332.

124. Kawaguchi, A., et al., *Gene expression signature-based prognostic risk score in patients with glioblastoma.* Cancer Sci, 2013. **104**(9): p. 1205-10.

125. Wong, A.J., et al., *Structural alterations of the epidermal growth factor receptor gene in human gliomas.* Proc. Nad. Acad. Sci. , 1992. **89**: p. 2965-2969.

126. Wong, A.J., et al., *Increased expression of the epidermal growth factor receptor gene in malignant gliomas is invariably associated with gene amplification.* Proc. Natl. Acad. Sci., 1987. **84**: p. 6899-6903.

127. Fleming, T.P., et al., *Amplification and/or Overexpression of Platelet-derived Growth Factor Receptors and Epidermal Growth Factor Receptor in Human Glial Tumors.* Cancer Research, 1992. **52**: p. 4550-4553.

128. Morrison, R.S., et al., *Basic fibroblast growth factor and fibroblast growth factor receptor I are implicated in the growth of human astrocytomas.* Journal of Neuro-Oncology, 1994. **18**: p. 207-216.

129. Ippen, F.M., et al., *Targeting the PI3K/Akt/mTOR pathway with the pan-Akt inhibitor GDC-0068 in PIK3CA-mutant breast cancer brain metastases.* Neuro Oncol, 2019. **21**(11): p. 1401-1411.

130. Keunen, O., et al., *Anti-VEGF treatment reduces blood supply and increases tumor cell invasion in glioblastoma.* Proc Natl Acad Sci U S A, 2011. **108**(9): p. 3749-54.

131. Parker, A.L., M. Kavallaris, and J.A. McCarroll, *Microtubules and their role in cellular stress in cancer.* Front Oncol, 2014. **4**: p. 153.

132. Yun, C.W. and S.H. Lee, *The Roles of Autophagy in Cancer.* Int J Mol Sci, 2018. **19**(11).

133. Curtin, J.C. and M.V. Lorenzi, *Drug Discovery Approaches to Target Wnt Signaling in Cancer Stem Cells.* Oncotarget, 2010. **1**(7).

134. Zhou, J., et al., *Neurotensin signaling regulates stem-like traits of glioblastoma stem cells through activation of IL-8/CXCR1/STAT3 pathway.* Cell Signal, 2014. **26**(12): p. 2896-902.

135. Anido, J., et al., *TGF-beta Receptor Inhibitors Target the CD44(high)/Id1(high) Glioma-Initiating Cell Population in Human Glioblastoma.* Cancer Cell, 2010. **18**(6): p. 655-68.

136. Li, H., J. Zeng, and K. Shen, *PI3K/AKT/mTOR signaling pathway as a therapeutic target for ovarian cancer.* Arch Gynecol Obstet, 2014. **290**(6): p. 1067-78.

137. Tapia, O., et al., *The PI3K/AKT/mTOR pathway is activated in gastric cancer with potential prognostic and predictive significance.* Virchows Arch, 2014. **465**(1): p. 25-33.

138. Honjo, S., et al., *Metformin sensitizes chemotherapy by targeting cancer stem cells and the mTOR pathway in esophageal cancer.* Int J Oncol, 2014. **45**(2): p. 567-74.

139. Mohammed, A., et al., *Antidiabetic Drug Metformin Prevents Progression of Pancreatic Cancer by Targeting in Part Cancer Stem Cells and mTOR Signaling.* Transl Oncol, 2013. **6**(6): p. 649-59.

140. Sunayama, J., et al., *Crosstalk between the PI3K/mTOR and MEK/ERK pathways involved in the maintenance of self-renewal and tumorigenicity of glioblastoma stem-like cells.* Stem Cells, 2010. **28**(11): p. 1930-9.

141. Yang, S.H., A.D. Sharrocks, and A.J. Whitmarsh, *MAP kinase signalling cascades and transcriptional regulation.* Gene, 2013. **513**(1): p. 1-13.

142. Robinson, M.J. and M.H. Cobb, *Mitogen-activated protein kinase pathways.* Current Opinion in Cell Biology, 1997. **9**: p. 180-186.

143. Pullikuth, A.K. and A.D. Catling, *Scaffold mediated regulation of MAPK signaling and cytoskeletal dynamics: a perspective.* Cell Signal, 2007. **19**(8): p. 1621-32.

144. Zassadowski, F., et al., *Regulation of the transcriptional activity of nuclear receptors by the MEK/ERK1/2 pathway.* Cell Signal, 2012. **24**(12): p. 2369-77.

145. Sigoillot, F.D., D.R. Evans, and H.I. Guy, *Growth-dependent regulation of mammalian pyrimidine biosynthesis by the protein kinase A and MAPK signaling cascades.* J Biol Chem, 2002. **277**(18): p. 15745-51.

146. Guo, Y.J., et al., *ERK/MAPK signalling pathway and tumorigenesis.* Exp Ther Med, 2020. **19**(3): p. 1997-2007.

147. Javan, M.R., A. Khosrojerdi, and S.M. Moazzeni, *New Insights Into Implementation of Mesenchymal Stem Cells in Cancer Therapy: Prospects for Anti-angiogenesis Treatment.* Front Oncol, 2019. **9**: p. 840.

148. Paw, I., et al., *Mechanisms regulating glioma invasion.* Cancer Lett, 2015. **362**(1): p. 1-7.

149. Tonn, J.C. and R. Goldbrunner. *Mechanisms of glioma cell invasion*. 2003. Vienna: Springer Vienna.

150. Reunanen, N. and V. Kähäri, *Matrix Metalloproteinases in Cancer Cell Invasion.* Madame Curie Bioscience Database - NCBI Bookshelf, 2019.

151. Koul, D., et al., *Suppression of matrix metalloproteinase-2 gene expression and invasion in human glioma cells by MMAC/PTEN.* Oncogene, 2001. **20**: p. 6669-6678.

152. Kubiatowski, T., et al., *Association of increased phosphatidylinositol 3-kinase signaling with increased invasiveness and gelatinase activity in malignant gliomas.* Journal of Neurosurgery, 2001. **95**: p. 480–488.

153. Kessenbrock, K., V. Plaks, and Z. Werb, *Matrix metalloproteinases: regulators of the tumor microenvironment.* Cell, 2010. **141**(1): p. 52-67.

154. Itoh, T., et al., *Reduced Angiogenesis and Tumor Progression in Gelatinase A-deficient Mice.* Cancer Research, 1998. **58**: p. 1048-1015.

155. Perego, C., et al., *Invasive behaviour of glioblastoma cell lines is associated with altered organisation of the cadherincatenin adhesion system.* Journal of Cell Science, 2002. **115**: p. 3331-3340.

156. Noh, M.G., et al., *Prognostic significance of E-cadherin and N-cadherin expression in Gliomas.* BMC Cancer, 2017. **17**(1): p. 583.

157. Hoogenraad, C.C. and F. Bradke, *Control of neuronal polarity and plasticity--a renaissance for microtubules?* Trends Cell Biol, 2009. **19**(12): p. 669-76.

158. Poulain, F.E. and A. Sobel, *The microtubule network and neuronal morphogenesis: Dynamic and coordinated orchestration through multiple players.* Mol Cell Neurosci, 2010. **43**(1): p. 15-32.

159. Katsetos, C.D., et al., *Emerging microtubule targets in glioma therapy.* Semin Pediatr Neurol, 2015. **22**(1): p. 49-72.

160. Mills, E., et al., *Roles for Rho/ROCK and vinculin in parietal endoderm migration.* Cell Commun Adhes, 2005. **12**(1-2): p. 9-22.

161. Ho¨ring, E., et al., *The "go or grow" potential of gliomas is linked to the neuropeptide processing enzyme carboxypeptidase E and mediated by metabolic stress.* Acta Neuropathol, 2012. **124**(1): p. 83-97.

162. Oliveira-Ferrer, L., et al., *Cilengitide induces cellular detachment and apoptosis in endothelial and glioma cells mediated by inhibition of FAK/src/AKT pathway.* J Exp Clin Cancer Res, 2008. **27**: p. 86.

163. Maziveyi, M. and a.S.K. Alahari, *Cell matrix adhesions in cancer: The proteins that form the glue.* Oncotarget, 2017. **8**(29): p. 17.

164. Goldmann, W.H., et al., *Vinculin, cell mechanics and tumour cell invasion.* Cell Biol Int, 2013. **37**(5): p. 397-405.

165. Laukaitis, C.M., et al., *Differential Dynamics of 5 Integrin, Paxillin, and -Actinin during Formation and Disassembly of Adhesions in Migrating Cells.* The Journal of Cell Biology, 2001. **153**(7): p. 1427–1440.

166. Alves, A., et al., *Small Molecules of Marine Origin as Potential Anti-Glioma Agents.* Molecules, 2021. **26**(9).

167. Reardon, D.A. and P.Y. Wen, *Therapeutic Advances in the Treatment of Glioblastoma: Rationale and Potential Role of Targeted Agents.* The Oncologist 2006. **11**: p. 152–164.

168. Moody, C.L. and R.T. Wheelhouse, *The medicinal chemistry of imidazotetrazine prodrugs.* Pharmaceuticals (Basel), 2014. **7**(7): p. 797-838.

169. Scott, J., et al., *Effectiveness of radiotherapy for elderly patients with glioblastoma.* Int J Radiat Oncol Biol Phys, 2011. **81**(1): p. 206-10.

170. Friedman, H.S., et al., *DNA Mismatch Repair and 0 6 -Alkylguanine-DNA Alkyltransferase Analysis and Response to Temodal in Newly Diagnosed Malignant Glioma.* Journal of Clinical Oncology, 1998. **16**(12): p. 3851-3857.

171. Keith, B. and M.C. Simon, *Hypoxia-inducible factors, stem cells, and cancer.* Cell, 2007. **129**(3): p. 465-72.

172. Singh, S.K., et al., *Identification of human brain tumour initiating cells.* Nature, 2004. **432**(7015): p. 396-400.

173. Schmalz, P.G., M.J. Shen, and J.K. Park, *Treatment resistance mechanisms of malignant glioma tumor stem cells.* Cancers (Basel), 2011. **3**(1): p. 621-35.

174. Capela, A. and S. Temple, *LeX/ssea-1 Is Expressed by Adult Mouse CNS Stem Cells, Identifying Them as Nonependymal.* Neuron, 2002. **35**: p. 865-875.

175. Hemmati, H.D., et al., *Cancerous stem cells can arise from pediatric brain tumors.* PNAS, 2003. **100**: p. 15178-15183.

176. Lendahl, U., L.B. Zimmerman, and R.D.G. McKay, *CNS Stem Cells Express a New Class of Intermediate Filament Protein.* Cell 1990. **60**: p. 585-595.

177. Liang, B.C., *Effects of hypoxia on drug resistance phenotype and genotype in human glioma cell lines.* Journal of Neuro-Oncology, 1996. **29**: p. 149-155.

178. Haar, C.P., et al., *Drug resistance in glioblastoma: a mini review.* Neurochem Res, 2012. **37**(6): p. 1192-200.

179. Amberger-Murphy, V., *Hypoxia Helps Glioma to Fight Therapy.* Current Cancer Drug Targets, 2009. **9**: p. 381-390.

180. Moeller, B.J., et al., *Radiation activates HIF-1 to regulate vascular radiosensitivity in tumors: Role of reoxygenation, free radicals, and stress granules.* Cancer Cell, 2004. **5**: p. 429-441.

181. Banelli, B., et al., *The histone demethylase KDM5A is a key factor for the resistance to temozolomide in glioblastoma.* Cell Cycle, 2015. **14**(21): p. 3418-29.

182. Chai, R.C., et al., *A Novel DNA Methylation-Based Signature Can Predict the Responses of MGMT Promoter Unmethylated Glioblastomas to Temozolomide.* Front Genet, 2019. **10**: p. 910.

183. Brusky, J., Y. Zhu, and W. Xiao, *UBC13, a DNA-damage-inducible gene, is a member of the error-free postreplication repair pathway in Saccharomyces cerevisiae.* Curr Genet, 2000. **37**: p. 168-174.

184. Dueva, R. and G. Iliakis, *Alternative pathways of non-homologous end joining (NHEJ) in genomic instability and cancer.* Transl Cancer Res):, 2013. **2**(3): p. 163-177.

185. Kaina, B. and M. Christmann, *DNA repair in personalized brain cancer therapy with temozolomide and nitrosoureas.* DNA Repair (Amst), 2019. **78**: p. 128-141.

186. O'Driscoll, M., et al., *A splicing mutation affecting expression of ataxia-telangiectasia and Rad3-related protein (ATR) results in Seckel syndrome.* Nat Genet, 2003. **33**(4): p. 497-501.

187. KUO, L.J. and L.-X. YANG, *γ-H2AX – A Novel Biomarker for DNA Double-strand Breaks.* in vivo, 2008. **22**: p. 305-310.

188. Rogakou, E.P., et al., *DNA double-stranded breaks induce histone H2AX phosphorylation on serine 139.* J Biol Chem, 1998. **273**(10): p. 5858-68.

189. Tomilin, N.V., et al., *Visualization of Focal Nuclear Sites of DNA Repair Synthesis Induced by Bleomycin in Human Cells.* Radiation Research, 2001. **156**: p. 347-354.

190. Motoyama, N. and K. Naka, *DNA damage tumor suppressor genes and genomic instability.* Curr Opin Genet Dev, 2004. **14**(1): p. 11-6.

191. Stiff, T., et al., *ATM and DNA-PK Function Redundantly to Phosphorylate H2AX after Exposure to Ionizing Radiation.* Cancer Research , , 2004. **64**: p. 2390–2396.

192. Svetlova, M., et al., *Elimination of radiation-induced gamma-H2AX foci in mammalian nucleus can occur by histone exchange.* Biochem Biophys Res Commun, 2007. **358**(2): p. 650-4.

193. Olive, P.L. and J.P. Banath, *Phosphorylation of histone H2AX as a measure of radiosensitivity.* Int J Radiat Oncol Biol Phys, 2004. **58**(2): p. 331-5.

194. Firsanov, D., A. Kropotov, and N. Tomilin, *Phosphorylation of histone H2AX in human lymphocytes as a possible marker of effective cellular response to ionizing radiation.* Cell and Tissue Biology, 2011. **5**(6): p. 531-535.

195. Yoshida, K., et al., *Expression and Radiation-induced Phosphorylation of Histone H2AX inMammalian Cells.* J. Radiat. Res., 2003. **44**: p. 47–51.

196. Gavrilov, B., et al., *Slow elimination of phosphorylated histone gamma-H2AX from DNA of terminally differentiated mouse heart cells in situ.* Biochem Biophys Res Commun, 2006. **347**(4): p. 1048-52.

197. Koike, M., et al., *Histone H2AX phosphorylation independent of ATM after X-irradiation in mouse liver and kidney in situ.* J Radiat Res, 2008. **49**(4): p. 445-9.

198. Prise, K.M. and J.M. O'Sullivan, *Radiation-induced bystander signalling in cancer therapy.* Nat Rev Cancer, 2009. **9**(5): p. 351-60.

199. Loeb, L.A., *Mutator Phenotype May Be Required for Multistage Carcinogenesis.* Cancer Research, 1991. **51**: p. 3075-3079.

200. Firsanov, D., et al., *Dynamics of gammaH2AX formation and elimination in mammalian cells after X-irradiation.* Biochimie, 2012. **94**(11): p. 2416-22.

201. Tu, W.Z., et al., *gammaH2AX foci formation in the absence of DNA damage: mitotic H2AX phosphorylation is mediated by the DNA-PKcs/CHK2 pathway.* FEBS Lett, 2013. **587**(21): p. 3437-43.

202. Zhao, T., et al., *MTUS1/ATIP3a down-regulation is associated with enhanced migration, invasion and poor prognosis in salivary adenoid cystic carcinoma.* BMC Cancer, 2015. **15**: p. 203.

203. Louis, S.N.S., et al., *The Expression of MTUS1/ATIP and Its Major Isoforms, ATIP1 and ATIP3, in Human Prostate Cancer.* Cancers, 2011. **3**(4): p. 3824-3837.

Publications

1. Ranjan, N.; Pandey, V.; Panigrahi, M.K.; Klumpp, L.; Naumann, U.; Babu, P.P. The Tumor Suppressor MTUS1/ATIP1 Modulates Tumor Promotion in Glioma: Association with Epigenetics and DNA Repair. **Cancers**, March 2021, 13, 1245. https://doi.org/10.3390/cancers13061245

2. Pandey V*., **Ranjan N*.,** Narne P., Babu P. P., Roscovitine effectively enhances antitumor activity of temozolomide *in vitro* and *in vivo* mediated by increased autophagy and Caspase-3 dependent apoptosis. **Scientific Reports**. March 23, 2019. PMID:30899038
**** Authors contributed equally.***

3. Allam M. Bhavani, A. K. D., Mudiraj A., **Ranjan N.,** Thippana, M., Babu P. P. Synthesis of pyrazolo[3,4-d] pyrimidin-4(5H)-ones tethered to 1,2,3-triazoles and their evaluation as potential anticancer agents. **European Journal of Medicinal Chemistry**. September 15, 2018. PMID:30006173

4. **Ranjan N.**, Yadav D., Pandey V., P. B. Kirti and Babu P. P., Overexpression of AnnAt8, Arabidopsis thaliana annexin protein constrain gliomagenesis and enhances autophagy in established human glioblastoma cell lines.

****Manuscript in preparation.***

5. Design and synthesis of fused bicyclic 1,2,4 triazolothiazoles using multicomponent strategy:Potential anticancer activity and docking studies.

****Manuscript in preparation.***

University of Hyderabad
Hyderabad- 500 046, India

PLAGIARISM FREE CERTIFICATE

This is to certify that the similarity index of this thesis as checked by the Library of University of Hyderabad excluding bibliographic content 39%. Out of this 32% similarity is identified from the candidate's own publication (Nikhil Ranjan) which has been certified by Indira Gandhi Memorial Library (IGML), University of Hyderabad and forms the adequate part of the thesis. The details of the student's publication are as follows:

Ranjan, N., Pandey, V., Panigrahi, M.K., Klumpp, L., Naumann, U., Babu, P.P., *The Tumor Suppressor MTUS1/ATIP1 Modulates Tumor Promotion in Glioma: Association with Epigenetics and DNA Repair.* **Cancers**, March 2021, 13, 1245. DOI: https://doi.org/10.3390/ cancers13061245

Similarity index – 32%

About 7% similarity was identified from external sources in the present thesis which is according to prescribed regulations of the University. All the publications related to this thesis have been appended at the end of the thesis. Hence the present thesis is considered to be plagiarism-free.

31/12/2021

Prof. P. Prakash Babu

Supervisor

Prof. P. Prakash Babu
Department of Biotechnology & Bioinformatics
School of Life Sciences
University of Hyderabad
Hyderabad-500 046. (T.S.)

Role of tumor suppressor MTUS1/ATIP1 in gliomagenesis: association with epigenetics and DNA repair

by Nikhil Ranjan

Submission date: 24-Dec-2021 03:51PM (UTC+0530)
Submission ID: 1735473419
File name: Nikhil_Ranjan.docx (3.73M)
Word count: 11577
Character count: 68068

Role of tumor suppressor MTUS1/ATIP1 in gliomagenesis: association with epigenetics and DNA repair

ORIGINALITY REPORT

39%	37%	9%	1%
SIMILARITY INDEX	INTERNET SOURCES	PUBLICATIONS	STUDENT PAPERS

PRIMARY SOURCES

1	www.ncbi.nlm.nih.gov Internet Source	32%
2	d-nb.info Internet Source	2%
3	www.mdpi.com Internet Source	<1%
4	nenaconference.files.wordpress.com Internet Source	<1%
5	www.karger.com Internet Source	<1%
6	Vimal Pandey, Nikhil Ranjan, Parimala Narne, Phanithi Prakash Babu. "Roscovitine effectively enhances antitumor activity of temozolomide in vitro and in vivo mediated by increased autophagy and Caspase-3 dependent apoptosis", Scientific Reports, 2019 Publication	<1%

pericles.pericles-prod.literatumonline.com

7	Internet Source	<1%
8	www.nature.com Internet Source	<1%
9	medvetande.dk Internet Source	<1%
10	Denis Firsanov, Anastasia Vasilishina, Andrey Kropotov, Vyacheslav Mikhailov. "Dynamics of γH2AX formation and elimination in mammalian cells after X-irradiation", Biochimie, 2012 Publication	<1%
11	Submitted to Nottingham Trent University Student Paper	<1%
12	"Toxicology and Epigenetics", Wiley, 2012 Publication	<1%
13	WWW.MDPI.COM Internet Source	<1%
14	Richard L. Momparler. "Preclinical and Clinical Studies on 5-Aza-2'-Deoxycytidine, a Potent Inhibitor of DNA Methylation, in Cancer Therapy", Medical Intelligence Unit, 2005 Publication	<1%
15	Shengchao Xu, Lu Tang, Xizhe Li, Fan Fan, Zhixiong Liu. "Immunotherapy for glioma:	<1%

	Current management and future application", Cancer Letters, 2020 Publication	
16	archiv.ub.uni-heidelberg.de Internet Source	<1 %
17	cancerci.biomedcentral.com Internet Source	<1 %
18	Isabelle M. Germano, Mateo Ziu, patrick wen, david ryan ormond, jeff olson. "Congress of Neurological Surgeons Systematic Review and Evidence-Based Guidelines Update on the Role of Cytotoxic Chemotherapy and Other Cytotoxic Therapies in the Management of Progressive Glioblastoma in Adults", Research Square Platform LLC, 2021 Publication	<1 %
19	Submitted to University of Exeter Student Paper	<1 %
20	Submitted to University of Sydney Student Paper	<1 %
21	Zhao-xia Chen. "Maintenance and regulation of DNA methylation patterns in mammals", Biochemistry and Cell Biology, 08/2005 Publication	<1 %
22	dokumen.pub Internet Source	<1 %

23	worldwidescience.org Internet Source	<1%
24	Submitted to The College of Health Care Professions Student Paper	<1%
25	V. Bazan. "Molecular detection of TP53, Ki-Ras and p16INK4A promoter methylation in plasma of patients with colorectal cancer and its association with prognosis. Results of a 3-year GOIM (Gruppo Oncologico dell'Italia Meridionale) prospective study", Annals of Oncology, 06/01/2006 Publication	<1%
26	theses.gla.ac.uk Internet Source	<1%
27	Jamila H. Siamwala, Francesco S. Pagano, Patrycja M Dubielecka, Alexander Zhao et al. " Identification of CD4 Sub-population of Resident Cardiac Fibroblasts Linked to Myocardial Fibrosis ", Cold Spring Harbor Laboratory, 2021 Publication	<1%

Exclude quotes	On	Exclude matches	< 14 words
Exclude bibliography	On		